ENERGY, HEAT TRANSFER AND ECONOMIC ANALYSIS OF FLAT-PLATE SOLAR COLLECTOR UTILIZING SiO$_2$ NANOFLUID

MOHD FAIZAL FAUZAN

FACULTY OF ENGINEERING
UNIVERSITY OF MALAYA
KUALA LUMPUR

2015

ENERGY, HEAT TRANSFER AND ECONOMIC ANALYSIS OF FLAT-PLATE SOLAR COLLECTOR UTILIZING SiO$_2$ NANOFLUID

MOHD FAIZAL FAUZAN

THESIS SUBMITTED IN FULFILMENT OF THE REQUIREMENTS FOR THE DEGREE OF DOCTOR OF PHILOSOPHY

FACULTY OF ENGINEERING
UNIVERSITY OF MALAYA
KUALA LUMPUR

2015

<div align="center">

UNIVERSITY OF MALAYA

ORIGINAL LITERARY WORK DECLARATION

</div>

Name of Candidate: Mohd Faizal Fauzan   (I.C/Passport No:

Registration/Matric No: KHA110066

Name of Degree: PhD Engineering

Title of Project Paper/Research Report/Dissertation/Thesis ("this Work"):

ENERGY, HEAT TRANSFER AND ECONOMIC ANALYSIS OF FLAT-PLATE SOLAR COLLECTOR UTILIZING SiO_2 NANOFLUID

Field of Study: Energy

I do solemnly and sincerely declare that:

(1)   I am the sole author/writer of this Work;

(2)   This Work is original;

(3)   Any use of any work in which copyright exists was done by way of fair dealing and for permitted purposes and any excerpt or extract from, or reference to or reproduction of any copyright work has been disclosed expressly and sufficiently and the title of the Work and its authorship have been acknowledged in this Work;

(4)   I do not have any actual knowledge nor do I ought reasonably to know that the making of this work constitutes an infringement of any copyright work;

(5)   I hereby assign all and every rights in the copyright to this Work to the University of Malaya ("UM"), who henceforth shall be owner of the copyright in this Work and that any reproduction or use in any form or by any means whatsoever is prohibited without the written consent of UM having been first had and obtained;

(6)   I am fully aware that if in the course of making this Work I have infringed any copyright whether intentionally or otherwise, I may be subject to legal action or any other action as may be determined by UM.

Candidate's Signature   Date:

Subscribed and solemnly declared before,

Witness's Signature   Date:

Name:

Designation:

ABSTRACT

Solar thermal energy can be a good replacement for fossil fuel because it is clean and sustainable. However, the current solar technology is still not efficient and expensive. The effective way to increase the efficiency of solar collector is to use nanofluid. This study is carried out to analyze the impact on thermal performance, heat transfer and economic of a flat-plate solar collector when SiO_2 nanofluid utilized as working fluid. The analysis is based on different volume flow rates and varying nanoparticles volume fractions. From the numerical study, it can be revealed that CuO have the highest thermal efficiency enhancement of up to 38.46% compared to water where else SiO_2, TiO_2 and Al_2O_3 performed almost similarly. However, SiO_2 nanofluid is the cheapest and the most abundance materials on earth. Therefore, it is more suitable option. The experimental study has indicated that up to 27.2% increase in the thermal efficiency and 34.2% increase in exergy efficiency were achieved by using 0.2% concentration SiO_2 nanofluid on solar collector compared to water as working fluid. The drawback of adding nanoparticles in the base fluids is the increase in viscosity of the working fluid that has led to increase in pumping power of the system and pressure drop in pipes. However, for low concentration nanofluids, only negligible effect in the pumping power and pressure drop is noticed. Using nanofluid could also improve the heat transfer coefficient by 28.26%, saving 280 MJ more embodied energy, offsetting 170 kg less CO_2 emissions and having a faster payback period of 0.12 years compared to conventional water based solar collectors. Applying SiO_2 nanofluid could improve the thermal efficiency, heat transfer and economic performance of a flat-plate solar collector.

ABSTRAK

Tenaga haba solar adalah bersih dan tak terbatas dan boleh menjadi pengganti yang baik untuk bahan bakar fosil. Walau bagaimanapun , teknologi solar semasa masih mahal dan rendah kecekapan. Salah satu cara yang efektif dalam meningkatkan kecekapan adalah dengan menggunakan nanofluid. Kajian ini dilakukan untuk menganalisis kesan ke atas prestasi haba, pemindahan haba dan ekonomi kolektor haba matahari dengan menggunakan SiO_2 nanofluid sebagai media penyerap haba. Analisis ini berdasarkan kadar aliran yang berbeza dan berbeza-beza konsentrasi nanopartikel. Dari kajian berangka, ia boleh mendedahkan bahawa CuO mempunyai prestasi yang tertinggi sehingga 38.46% berbanding dengan air. Walau bagaimanapun, SiO_2 nanofluid adalah yang termurah dan bahan-bahan yang paling banyak dan pentingnya ia dalam hal kesinambungan adalah lebih tinggi. Kajian eksperimen telah menunjukkan bahawa sehingga 27.2% peningkatan dalam kecekapan tenaga haba dan peningkatan 34.2% dalam kecekapan exergy telah dicapai dengan menggunakan kepekatan 0.2% SiO_2 nanofluid pada kolektor suria dibandingkan dengan air. Kesan negatif menambahkan nanopartikel dalam cairan asas adalah peningkatan kelikatan bendalir kerja yang telah menyebabkan peningkatan mengepam kuasa dan penurunan tekanan. Walau bagaimanapun, bagi nanofluid kepekatan rendah, hanya kesan kecil pada penigkatan kuasa pam dan penurunan tekanan di tunjukkan. Menggunakan nanofluid juga boleh meningkatkan pemindahan haba sebanyak 28.26%, menjimatkan 280 MJ tenaga, mengimbangi 170 kg kurang emisi CO_2 dan mempunyai tempoh bayaran balik yang lebih cepat sebanyak 0.12 tahun berbanding pengumpul konvensional suria berasaskan air. Menerapkan SiO_2 nanofluid dapat meningkatkan kecekapan haba, pemindahan haba dan prestasi ekonomi dalam pengumpul suria plat datar .

ACKNOWLEDGEMENTS

TABLE OF CONTENTS

LIST OF FIGURES

this study with theoretical calculation

LIST OF TABLES

LIST OF SYMBOLS AND ABBREVIATIONS

β : Surface tilt angle from the horizontal

α : Solar altitude

δ : Solar declination angle

Φ : Solar zenith angle

φ_n : Volume fraction of nanoparticles in nanofluid (%),

m_n : Mass of nanoparticle (kg)

m_w : Mass of water (kg)

ρ_n : Density of nanoparticle (kg/m^3)

ρ_w : Density of water (kg/m^3)

$\dot{E}_{in}$: Inlet exergy rate

$\dot{E}_s$: Stored exergy rate

$\dot{E}_{out}$: Outlet exergy rate

$\dot{E}_l$: Leakage exergy rate

$\dot{E}_d$: Destroyed exergy rate

ΔP_{in} : Pressure difference of the fluid with the surroundings at entrance

ρ : Fluid density

T_s : Apparent sun temperature

$\dot{S}_{gen}$: Overall rate of entropy generation

$\dot{Q}_S$: Solar energy absorbed by the collector surface

$\dot{Q}_O$: Heat loss to the environment

μ : Viscosity

T_b	:	Bulk temperature
q	:	Heat flux
Pr	:	Prandtl
f	:	Friction factor
K	:	Loss coefficient
Al_2O_3	:	Aluminum Dioxide
AST	:	Apparent Solar Time
CPC	:	Compound parabolic collector
CTC	:	Cylindrical trough collector
CuO	:	Copper Oxide
D	:	Diameter of the pipe
DASC	:	Direct absorption solar collector
DS	:	Daylight saving (it is either 0 or 60 min)
ET	:	Equation of time
ETC	:	Evacuated tube collector
FPC	:	Flat-plate collector
H	:	Solar hour angle
h	:	Heat transfer coefficient
HFC	:	Heliostat field collector
LFR	:	Linear Fresnel reflector
LL	:	Local longitude
LST	:	Local standard time
MWCNT	:	Multi-Walled Carbon Nanotubes
N	:	The day of the year
Nu	:	Nusselt number
PDR	:	Parabolic dish reflector

PTC   :   Parabolic trough collector

Re   :   Reynolds number

SH   :   Shape factor

SiO_2 :   Silicon Dioxide

SL   :   Standard longitude

SWCNH   :   Single-wall carbon nanohorn

TiO_2 :   Titanium Oxide

U   :   Overall heat loss coefficient

V   :   Velocity of working fluid

z   :   Solar azimuth

Zs   :   Surface azimuth angle, equals to 0° for south facing tilted surface

CHAPTER 1: INTRODUCTION

1.1 Background

World energy demand is increasing and expected to accelerate more in the future due to developments and rise in human population. However, the sources and production of fossil oil are depleting. Climate change and environmental pollution are now becoming huge global problems (IPCC 2014). Human population are increasing rapidly (UNPF 2014). Global temperature is rising. Pollution level is high. Energy resources are becoming more scarce and costly. Valero et al. (2010) pointed out that there might not be sufficient petroleum available to fulfill the future predicted energy demand. For the last 150 years, more than 800 billion barrels of petroleum have been utilized from the estimated reserves of 2.2 trillion barrels. Based from the present consumption of 90 million barrels a day worldwide, the remaining 1.4 trillion barrels of oil can only last for the next 40 years. Because of the high pollution level, the regulations of environmental laws have become stricter than ever. The lack or decrease of resources had increase the price of oil. Renewable energies are becoming more important in the world economy today because they are sustainable, safe and clean. Therefore, there is a large effort in using solar thermal energy as solutions to replace oil as a source of heat energy.

Currently, there are two main ways of utilizing solar energy: photovoltaic (PV) and solar thermal or heat energy from the sun. Photovoltaic works by converting the light energy from the sun directly to electrical energy. Solar thermal energy is in the form of heat energy from the sun for the purpose of heating, drying and also electric power production. Flat plates are generally used for heating. For high temperature requirements, sunlight is concentrated using mirrors or lenses for electric power

generation. The principle is more or less the same as burning coal or oil in boiler power plant except that the source of heat energy to boil water is from the sun which is clean and renewable. Concentrating sunlight as a heat energy source to produce electricity is the best options as a replacement of burning fuel in boiler power plants. However, the peak efficiencies of current combined cycle power plants have reach to more than 50% (Langston 2009) compared to the efficiency of concentrated solar thermal power plants that are still below 20% (Pacheco 2001; Romero et al. 2002).

In household energy usage, a large portion of energy consumption is used to heat water for shower, cooking or washing. In Malaysia, the average energy demand for water heating is around 11.03% as shown in Figure 1.1. Most of this heat energy demand is supplied by electrical energy or burning of petroleum gas that will contribute to a lot of environmental problems. Solar thermal energy is free and unlimited source of energy that can meet the world's future energy needs without harming the earth. Therefore, a lot of studies had been made to address this issue. Tora and El-Halwagi (2009) had developed an optimal design to integrate solar systems and fossil fuel for stable and sustainable power generation. Nemet et al. (2012) continued the work further by developing CSEC (captured solar energy curve) and MCTC (minimal capture temperature curve) to maximize the solar heat energy delivered to the process. Ranjan and Kaushik (2013) performed a thermodynamics analysis of active solar distillation system integrated with solar pond that can contribute to water security and sustainability. Sanchez-Bautista et al. (2014) presented an optimization model for the optimal design of water-heating system for homes in Mexico. In the model, location, solar radiation, inhabitants and time-based consumption pattern were accounted to determine the optimal design of integrated solar and boilers water heating systems

2

aimed to minimized cost and greenhouse gas emissions. All these are part of the effort to make the solar thermal energy system more efficient.
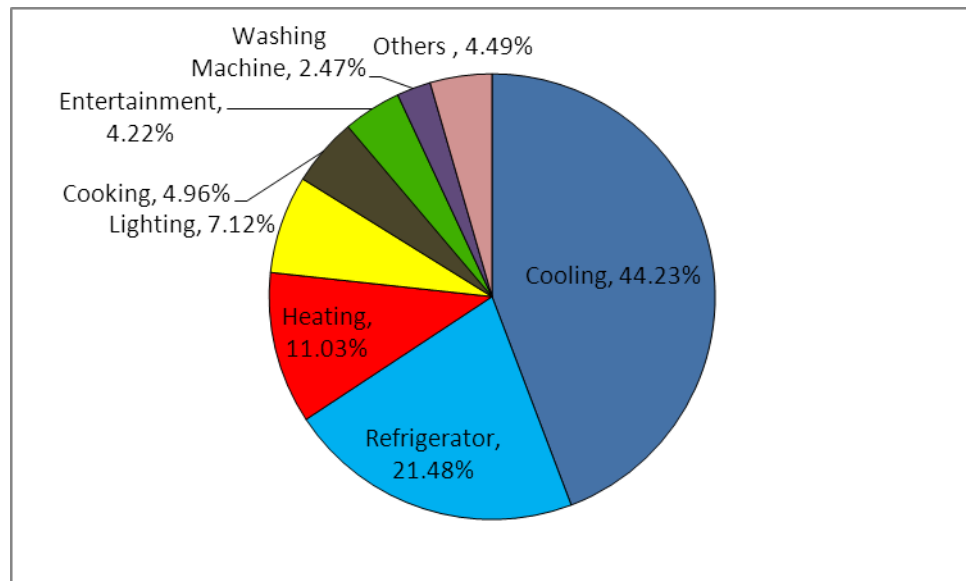
Figure 1.1: Average electricity consumption breakdown (%) in Malaysia

(Lalchand 2012)

Because of the low efficiency of solar thermal energy, a lot of effort is taken to raise their efficiency to decrease the cost per watt of power production. The effective way to increase the efficiency of solar collector is to use nanofluid. Nanofluid is a base fluid with suspended nanometer-sized particles. After carbon nanotubes have been discovered in 1991, carbon-based nano particles have been of high interest to researchers because of their superior thermal, mechanical, and electrical properties (Haddon 2002; Saidur et al. 2011).

Researches on enhanced thermal efficiency of solar collector by applying nanofluids have been made in the past few years by numerous researchers such as Yousefi (2012), Lenert and Wang (2012), Otanicar (2010) and Taylor et al. (2011). An

experimental investigation conducted by Yousefi et al. (2012c) on the effect of Al_2O_3 based nanofluid showed an efficiency increase of 28.3% for flat-plate solar collectors. Lenert and Wang (2012) presented a model and performed an experimental study of concentrated solar power application using carbon-coated cobalt (C-Co) nanoparticles and Therminol VP-1 base fluid. They concluded that the efficiency was more than 35% with nanofluid and the efficiency would increase with increasing nanofluid concentration. Lu et al. (2011) showed that the application of Copper Oxide (CuO) nanoparticles in evacuated tube solar collectors would significantly enhance the thermal performance of evaporator and evaporating heat transfer coefficient by 30% compared to water as working fluid. 5% improvement in the efficiency was found out by Otanicar et al. (2010) using variety of nanoparticles with water as base fluid for micro-solar-thermal collector. Shin and Banerjee (2011) applied novel nanomaterials in molten salts base fluid to concentrated solar power coupled with thermal storage and experienced an enhancement in operational efficiencies. Taylor et al. (2011) used graphite base nanofluids in high flux solar collectors that resulted in 10% increase in the efficiency. Zamzamian et al. (2014) performed an experimental study to investigate the effect of Cu nanoparticle on the efficiency of a flat-plate solar collector in different volume flow rates and weight fractions of the nanoparticles and found that the optimum point for solar collector efficiency can be reach up to 0.3 wt% Cu nanofluid at 1.5 L/min.

Because of higher thermal conductivity and efficiency of nanofluids, smaller and compact design of solar thermal collectors has become possible without affecting the output desired. Smaller size collector can reduce the material usage, cost and energy required in manufacturing (Leong et al. 2012). Studies were made on the potential of

size reduction of various engineering applications by using nanofluids. These studies were based on vehicle's weight reduction (Saidur and Lai 2011), building heat exchanger's heat transfer area (Kulkarni et al. 2009), the reduction of air frontal area of a car radiator (Leong et al. 2010) and the size reduction of shell and tube recovery exchanger (Leong et al. 2012). Applying nanofluid in solar collectors is also expected to produce similar potential.

Another important issue to address in solar energy system is the cost of the system (Kalogirou 2008). Solar technology is commonly perceived by many as very expensive. Therefore, economic analysis is a very important aspect to consider when dealing with a renewable energy technology especially the life cycle analysis and payback period. Some studies had been made to evaluate the economic and environmental impact of solar hot water system (Ardente et al. 2005; Kalogirou 2004a; Kalogirou 2008; Tsillingiridis et al. 2004), where one particular study focused on the environmental and economical analysis of direct absorption micro solar thermal collector utilizing graphite nanofluid (Otanicar 2009).

Nanofluids have been proven to improve the performance and heat transfer characteristics for solar collector's application. However, there are still some issue with nanofluid including the raised of viscosity of the fluid that will lead to increase in pumping power load and the major issue of nanofluids for long term engineering applications is the stability (Liu and Liao 2008). Nanoparticles in the base fluid naturally will aggregate and sediment. In theory, there are both attractive force and repulsive force between particles (Ise and Sogami 2005). The attractive force is the van der Waals force and the repulsive force is the electrostatic repulsion that will occur

when particles get too close together. If the repulsive force is stronger than the attractive force, nanoparticles in the base fluid can remain stable or otherwise it will aggregate and serious aggregation will lead to sedimentation. Adding surfactants to the nanofluid can enhance the electrostatic repulsion of nanoparticles. Surfactants such as sodium dodecyl benzene sulfonate, sodium dodecyl sulfate or Triton X-100 had been tested and proven to stabilize nanofluid (Wang 2009). However, the effect might be broken down when the Brownian motion of nanoparticles is too strong or when the nanofluid is heated. Another way to stabilize nanofluid is by changing the pH value of the solution (Yousefi et al. 2012a). The pH of isoelectric point for nanoparticles carries no electrical charge and therefore causes no interparticle repulsion force which in turn causing more aggregated solution. The more differences between the pH of nanofluid and pH of isoelectric point will cause less aggregation and better dispersion. A better way to stabilize nanofluid as was proposed by Yang and Liu (2010) is to graft polymers onto the surface of nanoparticles and also known as surface functionalization. Silanes were grafted on silica nanoparticles making "Si-O-Si" covalent bonding and resulting in steric stabilization effect even when heated. Functionalized SiO_2 nanoparticles have been reported to keep dispersing well after 12 months and no sedimentation was observed (Chen et al. 2013).

Thermodynamics analysis is one of the preferred methods to analyze the performance of a solar collector. In thermodynamics analysis, the energy equation alone is insufficient to evaluate the flat-plate solar collector efficiency. The second law or exergy analysis is more effective to determine the source and magnitude of irreversibilities, and can be used to improve the efficiency of the system. Exergy is the maximum output that can be achieved relative to the environment temperature (Cengel and Boles 2010). Some exergy analysis studies have been conducted by (Saidur et al.

2012) on various solar energy applications and Farahat et al. (2009) on flat-plate solar collectors. Mahian et al. (2013) also comprehensively reviewed the entropy generation in nanofluid flow while Alim et al. (2013) made an analytical analysis of entropy generation in a flat plate solar collector by using different types of metal oxide nanofluids. However, to the best of the author's knowledge, experimental studies on solar collector using SiO_2 nanofluid have not appeared in the open literature even though a lot of simulation works have been done and all the studies on the exergy analysis on flat-plate solar thermal collectors are either simulation or theoretical. Therefore, this thesis will focus on the thermodynamics performance, heat transfer characteristic and economic analysis of flat-plate solar collectors when applying SiO_2 nanofluid to fill up those gaps.

1.2 Objectives of study

Because of the low efficiency of solar thermal energy devices, a lot of effort is taken to raise their efficiency that will decrease the cost per watt of power production. One of the effective methods to increase the efficiency is to replace the working fluid with nanofluids. Therefore in order to design and analyse a solar thermal collector effectively, it is necessary to address the following objectives:

1. To analyse the thermodynamics performance of flat-plate solar thermal collector utilizing SiO_2 nanofluid

2. To measure the effect of heat transfer enhancement in nanofluid solar collector

3. To estimate the economic advantage of applying nanofluid in solar collector

1.3 Scope of this study

Solar collectors are bulky, low in efficiency and mostly expensive. Applying nanofluid in solar collector can address all these issues. The present investigation is an attempt to provide the efficiency, heat transfer and economic analysis of solar collector when applying nanofluid as working fluid. The thermo physical properties, rheological behaviour and stability of proposed silane coated SiO_2 nanofluid were considered. The prepared nanofluid was applied in a conventional flat-plate solar collector where parameters such as solar radiations, inlet temperatures, outlet temperatures, absorber surface temperatures, ambient temperatures and wind velocities were recorded. All these data were then used to perform efficiency, heat transfer and economic analysis of nanofluid solar collectors and comparison was made with distilled water solar collectors.

1.4 Organization of the thesis

This thesis consists of five (5) chapters and organized as follows:

Chapter 1 introduce about the background and motivation of this studies including issues in fossil energy sources and the importance of switching to renewable energy sources such as solar thermal energy. Objectives are listed and scope of the study is presented in this chapter.

Chapter 2 provides a literature review for the study. Views on the potential of solar energy are shared. Different types of solar collectors are listed in this chapter. Development of flat-plate collectors is also described. Recent studies of the application of nanofluids in solar collectors are reviewed and some of the important properties of nanofluids are taken and tabled.

Chapter 3 explains the methodology for this project. In this chapter, an explanation of preparation of SiO_2 nanofluids, apparatus, experimental set up and experimental procedure of flat-plate solar collector applying SiO_2 nanofluid are presented. Analytical methods that are applied to calculate efficiency, exergy, pumping power, heat transfer, embodied energy analysis, economic analysis and environmental analysis are also provided.

Chapter 4 presented all the results that have been obtained from the experiments, calculations and analysis on tables and graphs followed by detailed discussion explaining, reasoning, justifying, commenting upon and comparing with literature reviews.

Chapter 5 concludes the study and recommends some further works that can be taken in the future.

CHAPTER 2: LITERATURE REVIEW

2.1 Introduction

Solar Energy is fee and unlimited source of energy that can meet the world's future energy needs without harming the earth. Solar energy actually has the potential to cover all energy needs including electrical, thermal, chemical and even transportation. The National Science Foundation USA in testimony before the Senate Interior Committee in 1972 stated that "Solar Energy is an essentially inexhaustible source potentially capable of meeting a significant portion of the nation's future energy needs with a minimum of adverse environmental consequences. The indications are that solar energy is the most promising of the unconventional energy sources"(Goswami et al. 2000).

Solar energy comes from the sun. The sun is the star of our solar system. The earth and other planets in our solar system orbit the sun. About 74% of the sun's mass is hydrogen, 25% is helium, and another 1% is traces of heavier elements. The sun's temperature is approximately 5500K. The sun is a sphere that generates massive amount of energy consistently and continuously by thermonuclear fusion reactions from hydrogen atom into helium atom. Very small fractions of this massive amount of energy reach the earth. Continuously, 1.7×10^{17} W of radiations from the sun reach the earth. 10 billion world population with a total power needed per person of 10 kWh would require about 10^{11} kW of energy. If solar radiation of only 1% of the earth surface could be converted into useful energy with 10% efficiency, the total energy generated per year would be 11.2×10^{14} kWh; more than enough to fulfil the energy needs of the entire population (Singal 2008).

Basically all forms of energy in the world come from solar. Plants convert the energy of solar radiation to chemical form by photosynthesis. Photosynthesis is the synthesis of glucose from sunlight, carbon dioxide and water with oxygen as a waste product (Kalogirou 2009). Oil, coal, natural gas and wood were produced by photosynthesis, drying, and decaying vegetation and complex chemical reaction over a long period of time. Even the energy from wind are caused by solar that affected the temperature and pressure in different regions of the earth.

Historically, the sun has been use to dry and preserve food as the first utilization of solar energy. The sun has evaporated sea water so that we have salt. Since humans began to think in reason, they believed the sun as a power behind every phenomenon. Some nations like Persions considered the sun as god. One of greatest engineering achievements, the Great Pyramid, was built as a stairway to the sun (Anderson et al. 2010).

From prehistoric times, people had benefited from the good use of solar energy. Table 2.1 below summarize the history of application of solar energy.

Table 2.1: History of Application of Solar Energy (U. S. Department of Energy, 2013)

Year	Event
7th Century B.C.	Magnifying glass to make fire and to burn ants
3rd Century B.C.	Mirrors to light prayer torches by Greeks and Romans
2nd Century B.C.	Stories about reflective bronze shields used by the Greek scientist, Archimedes to set fire to wooden Roman Empire's ship. Greek Navy recreated the experiment in 1973 and successfully set fire to a wooden boat at 50m distance.
20 A.D.	Mirrors to light religious torches in Chinese documents
1st to 4th Century A.D.	The famous Roman Bathhouses built with large windows facing south
6th Century A.D.	Justinian code "sun rights" ensure individual access to sunlight.
1200s A.D.	Anasazi, ancestors' of Pueblo people in North America live in cliff dwellings facing south
1767	Hot box made of glass with two boxes inside invented by Horace de Saussere, the Swiss scientist. The design used by Sir John Herschel to cook food during his 4th Africa expedition in 1830s
1816	The sterling engine system patented by Robert Sterling used by Lord Kelvin using concentrated solar thermal energy to produce electricity
1839	Photovoltaic effect discovered first time by Edmond Becquerel, French when he found out that electricity generation increased when exposed to sunlight
1860s	Solar-powered steam engines proposed by French August Mouchet and the first solar powered engines constructed in two decades with Abel Pifre using parabolic dish collector
1873	Photoconductivity of selenium discovered by Willoughby Smith

Year	Event
1876	Discovery of electrical current produced when selenium exposed to light by William Grylls Adam but not enough to power electrical equipment at that time
1880	Bolometer, used to measure light from the faintest stars and the sun's heat rays invented by Samuel P. Langley
1883	The 1st selenium wafers solar cells designed by American Charles Fritts
1891	The 1st commercial solar water heater patented by Clarence Kemp
1904	Discovery of copper and cuprous oxide combined is photosensitive by Wilhelm Hallwachs as the beginning of the new development of pv
1905	Theory of relativity and photoelectric effect published by Albert Einstein
1908	Solar collector with copper coils and insulated box invented by William J. Bailey of the Carnegie Steel company
1914	Barrier layer in photovoltaic devices was recognized
1916	Einstein theory of photovoltaic effect proved experimentally by Robert Milikan
1918	Development of single-crystal silicon by Jan Czochralski, Polish Scientist
1920s	Discovery of natural gas that stops solar thermal industry
1921	Albert Einstein wins the Nobel Prize for his theory of photoelectric effect
1932	Discovery of photovoltaic effect of Cadmium Sulfide (Cds) by Audobert and Stora
1947	Passive solar buildings built in the US after the prolonged world war II
1953	The 1st theoretical calculations on the efficiency of various materials of different band gap widths based on the spectrum of the sun made by Dr. Dan Trivich from Wayne State University
1954	The 1st silicon PV cell with 4% efficiency developed by Daryl Chapin, Calvin Fuller, and Gerald Pearson at Bell Labs
1955	Western Electric began to sell commercial licenses for silicon PV
Mid 1950s	World's 1st commercial office building using solar water heater and passive design by architect Frank Bridgers
1956	Development of PV cells for satellites initiated by William Cherry, U.S. Signal Corps Laboratories by approaching Joseph Loferski from RCA Labs

Year	Event
1957	8% efficient PV cells was achieved by Hoffman Electronics
1958	Fabrication of n-on-p silicon PV cells that has higher resistant to radiation by T. Mandelkom, U.S. Signal Corps Laboratories.
	The Vanguard 1 space satellite used a small, less than 1 watt array for radios. Other satellites including Explorer III, Vanguard II and Sputnik -3 were using PV-powered systems
1959	10% efficient PV cells were achieved by Hoffman Electronics. Commercialized and used grid contact that can significantly reduce the series resistance
	The Explorer VI satellite is launched on August 7 with PV array of 9600 cells of 1 cm x 2 cm each. Explorer VII launched on October 13
1960	14% efficient PV cells was achieved by Hoffman Electronics
	Production of selenium and silicon PV cells by newly founded Silicon Sensors, Inc.
1962	The Telstar with initial power of 14 W was launched by Bell Telephone Laboratories as the first telecommunication satellite
1963	Sharp successfully produced practical silicon PV modules
	Japan installs a 242 W PV array on a lighthouse as the world's largest at that time
1964	The 1st Nimbus spacecraft launched by NASA.
1965	Solar Power Satellites proposed by Peter Glaser
1966	The 1st Orbiting Astronomical Observatory powered by 1 kW PV array was launched by NASA
1969	An 8-storey parabolic mirror called Odeillo Solar Furnace was constructed in Odeillo, France
1970	A significantly lower cost solar cell, reduced cost from $100 a Watt to $20 a Watt by Dr. Elliot Berman and funded by Exxon Corp. Powered navigation warning lights and horns on offshore gas and oil rigs, lighthouses, railroad crossings and also in remote area.
1972	Educational television installed by the French at a village school using a cadmium sulphide (Cds) PV system
	World's 1st lab specific for PV R & D established as The Institute of Energy Conversion at the University of Delaware.
1973	"Solar One", the world's 1st PV powered residences was built by University of Delaware.

Year	Event
1976	83 PV power systems were installed by NASA Lewis Research Center on every continent except Australia. 1st amorphous silicon PV cells was fabricated by David Carlson and Christopher Wronski in RCA Lab
1977	Solar Energy Research Institute was launched by U.S. Department of Energy The total production of photovoltaic had exceeds 500 kW
1978	World's 1st village PV system with 3.5 kW was installed by NASA's Lewis Research Centre on the Papago Indiana Reservation located in southern Arizona.
1980	The 1st company successfully produced more than 1 MW of PV modules in a year is ARCO Solar More than 10% efficiency achieved by the 1st thin-film solar cell developed at the University of Delaware using copper sulphide/cadmium sulphide
1981	The 1st solar-powered aircraft, the Solar Challenger, was built by Paul Mac Gready and flew across the English Channel from France to England. Over 16,000 solar cells mounted on the wings producing 3,000 W of power
1982	The 1st megawatt scale PV power station built by ARCO Solar in Hisperia, California that consist of modules on 108 dual-axis trackers with 1 MW power capacity The 1st solar-powered car, the Quiet Achiever was driven by Australian Hans Tholstrup in almost 2,800 miles between Sydney and Perth in 20days. The achievements is 10 days faster than the 1st gasoline-powered car Solar One, a 10 MW central receiver was developed by the U.S. Department of Energy. It uses power tower system for concentrated solar thermal energy to produce electricity Volkswagen begins testing 160 W roof mounted PV arrays on Dasher Station Wagons for the ignition system. PV production exceeds 9.3 MW worldwide

Year	Event
1983	6 MW PV substations were built by ARCO Solar in Central California. The facility covered 120-acre of land that supplies electricity to the Pacific Gas & Electric Company's utility grid.
	A stand-alone, 4 kW powered solar system was completed by Solar Design Associates in the Hudson River Valley
	PV production exceeds 21.3 MW with sales of more than $250 million worldwide
1984	1 MW PV electricity generating facility was commissioned by Sacramento Municipal Utility District
1985	20% efficiency barrier for silicon solar cells was broken by the University of South Wales under 1-sun conditions
1986	The world's largest solar thermal facility was commissioned in Kramer Junction, California. The system used concentrating mirrors arranged in rows to supply heat for steam turbine power generator
	The world's first commercial thin-film power module, the G-4000 was released by ARCO solar.
1988	Lepcon and Lumeloid, two newly developed solar power technology were patented by Dr. Alvin Marks.
1991	The U.S. Department of Energy's Solar Energy Research Institute is changed to the National Renewable Energy Laboratory by President George Bush
1992	15.9% efficient thin-film PV cell made of cadmium telluride was developed by University of South Florida
	Functioning 7.5 kW prototype dish system was developed using an advanced stretched-membrane concentrator
1993	The 1st grid supported 500 kW PV system was completely installed by Pacific Gas & Electric in Kerman, California.
1994	The most energy efficient of all U.S. government buildings worldwide, the Solar Energy Research Facility construction was completed by the National Renewable Energy Laboratory.
	The 1st free-piston Stirling engine powered by solar dish tied to utility grid
	The 1st solar cell to exceed 30% conversion efficiency was developed by the National Renewable Energy Laboratory and made from gallium iridium phosphate and gallium arsenite

Year	Event
1996	Icare, the world's most advances solar-powered airplane, was successfully flown over Germany. 3,000 super-efficient solar cells covered 21 m^2 areas of the wings and tail surface.
	Solar Two, an upgraded Solar One solar power tower project begins to operate.
1998	An altitude record of 80,000 feet was achieved by "Pathfinder" the remote-controlled solar power aircraft on its 39th consecutive flight on August 6, in Monrovia, California
	The invention of flexible solar shingles, was led by Subhendu Guha, a noted scientist for his pioneering work in amorphous silicon
1999	4 Time Square constructions were completed as the tallest skyscraper built in the 1990s in New York City. It includes building-integrated photovoltaic (BIPV) panels on the 37th through 43rd floors on the south and west facing facades.
	32.3% conversion efficiency was achieved by Spectrolab, Inc. and the National Renewable Energy Laboratory by combining 3 layers of PV materials into a single solar cell. The cell performed efficiently with concentrated sunlight
	18.8% efficiency achieved by the National Renewable Energy Laboratory for thin-film PV solar cells
	1000 MW PV capacity was reached cumulatively worldwide
2000	Production begins by First Solar in Perrysburg, Ohio, the world's largest PV manufacturing plant.
	The largest solar power array began to be installed and used in space by the International Space Station consisting of 32,800 solar cells for each wing of the array
	A new inverter for solar electric system was developed by Sandra National Laboratories increasing the safety of the systems from power failure
	10.8% and 10.6% conversion efficiency of 0.5 m^2 and 0.9 m^2 thin-film solar modules was achieved by BP Solarex as the highest efficiency in the world.
	The largest solar electric system installed on a family home in Morrison, Colorado U.S.

Year	Event
2001	3 of Home Depot stores in San Diego, California began selling residential solar power system. It expands to 61 stores nationwide a year later
	A new world record, at more than 30 m high made by NASA's solar-powered aircraft named Helios
	NASDA announced to develop satellite based solar power system that would beam energy to earth
	Holographic films were developed by TerraSun LLC to concentrate selective, only sunlight needed for power production onto a solar cell.
	The world's largest hybrid system (wind and solar) was developed by PowerLight Corporation in Hawaii. It is a grid-connected system. Solar energy capacity = 175kW. Wind energy capacity = 50kW
	A service station that features a solar-electric canopy announced to be opened by British Petroleum (BP) and BP Solar in Indianapolis
2002	Pathfinder Plus, a solar-powered, remote-controlled aircraft were successfully tested by NASA for high altitude platform for telecommunications technologies and aerial imaging system for coffee growers
	The largest rail yard in the U.S. was installed with 350 blue signal rail yard lanterns, using solar cells to power the LED light by Union Pacific Railroad at its North Platt, Nebraska, rail yard.

Over the past hundreds of years, fossil fuel is the major source of energy, because of the cheaper price and the more convenience of it than any other energy sources. Pollution has also been of little concern before. Oil demand increased rapidly because of increasing production of low cost oil from the Middle East and North Africa during the 1950s and 1960s. However, after the Egyptian army stormed across the Suez Canal on October 12, 1973, the economics of fuel changed. An international crisis was created. Six Gulf members of the Organization of Petroleum Exporting Countries (OPEC) met in Kuwait and announced that they were raising the price of crude oil by 70% and will not consult any more prices with the oil companies (Kalogirou 2009).

World oil reserves are proven to be 1200 billion barrels in 2005 and natural gas at 180 trillion m^3 in 2004. Current production rate is 80 million barrels per day for oil and 7.36 billion m^3 daily for natural gas, which can only last for only another 41 to 67 years respectively (Goswami 2007). On the other hand, reserves for coal can last for at least the next 230 years. This will result in acceleration of fuels price as the reserves decreased continuously. Also, concerns about the pollution caused by burning of fuels are growing nowadays.

2.2 The Sun

The sun is a hot sphere gaseous matter with a diameter of 1.39×10^9 m. The distance from the sun to the earth is about 1.5×10^8 km. After leaving the sun thermal radiation travels with the speed of 300,000 km/s and reach the earth in 8 min and 20 s. The sun disk forms an angle of 32 min of a degree as observed from the earth. Surface temperature of the sun is 5760 K and continuously turns hydrogen into helium through fusion reaction. Total energy output of the sun is 3.8×10^{20} MW and equal to 63 MW/m^2. This energy radiates in all directions and only a fraction of about 1.7×10^{14} kW reach the earth. However, this small fraction of energy in 84 min can meet the need of the world energy demand for a year (Kalogirou 2009).

Diameter = 1.39×10^9 m

Diameter = 1.27×10^7 m

Sun

Angle = 32'

Earth

Distance = 1.496×10^{11} m
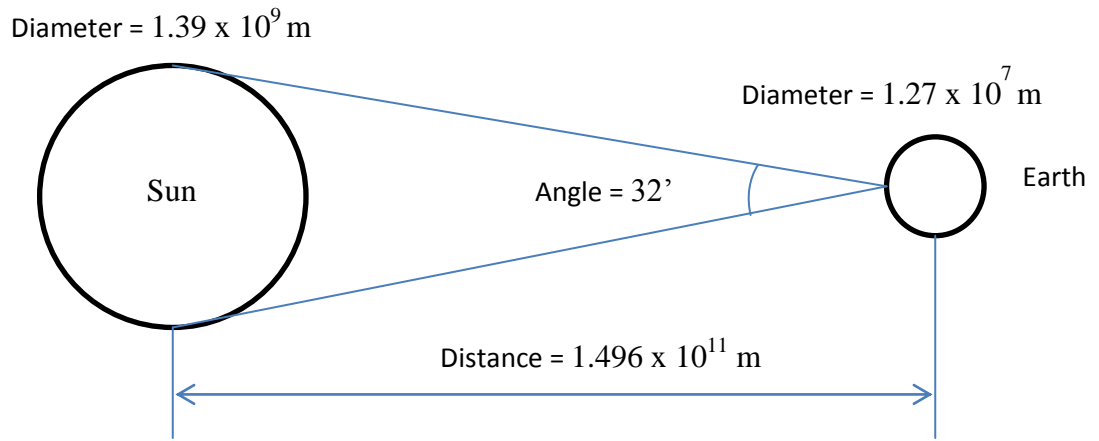
Figure 2.1: The distance between the sun and the earth

The path of the sun as seen from the earth varies throughout the year. Knowing the sun path is important to determine the solar radiation falling on a surface so that proper orientation and placement of solar collectors can be made to avoid shading (Kalogirou 2009).

2.2.1 Solar Time

The earth's orbital velocity around the sun throughout the year varies. So, the solar time is not the same as the uniform rate of time on a clock. The variation is called the equation of time (ET). The length of a day is the time for the earth to complete one revolution about its axis and it is not uniform throughout the year. The average length of a day can be taken as 24 hours. The length of a day varies due to the elliptical orbit and the tilt of the earth's axis from the normal plane of its orbit. The earth is closer to the sun on January and furthest on July. The earth's orbiting speed is faster from about October to March and slower from April through September.

2.2.2   Apparent Solar Time

Standard clock time is taken from the Greenwich. Greenwich is at longitude of 0°. Sun takes 4 min to transverse 1° of a longitude. Clock time will be added if the location is east and subtracted if it is west of the Greenwich.

2.3 Solar Angle

One rotation of the earth about its axis takes 24h and one revolution around the sun is about 365.25 days. The revolution follows an ellipse. The shortest distance from the sun is around January and it is called perihelion and longest at July is aphelion. The longest distance is 152.1×10^6 km and the shortest is 147.1×10^6 km. The earth rotation about its axis is tilted at an angle of 23.45° to the plane of elliptic. The sun position observed from the earth can be calculated by solar altitude (α) and solar azimuth (z) with calculated value of solar declination angle (δ) and solar hour angle (h) first (Kalogirou 2009). The declination angle (δ) for any day in a year (N) can be calculated by ASHRAE (2007). The hour angle can be obtained by using apparent solar time (AST). Solar zenith angle, (Φ) is the angle between the sun's rays and the vertical. The solar altitude angle is the angle between the sun's rays and a horizontal plane. The solar incidence angle (θ) is the angle between the sun's rays and a surface. Surface azimuth angle, equals to 0° for south facing tilted surface in the Northern Hemisphere and equals to 180° for north facing Southern Hemisphere.

For solar energy system design, possibility of the shading of solar collectors needs to be estimated. Mathematical model or graphical method can be used to determine the shading. The objective is to determine the suitability of a position suggested for the collectors. Collectors are usually installed facing true south (Kalogirou 2009).

2.4 Solar Energy Resources in Malaysia

Geographically Malaysia is situated at the equatorial region with an average solar radiation of 400 – 600 MJ/m^2 per month (Mekhilef et al. 2012b). The annual average solar radiation in Malaysia is portrayed in Figure 2.2 and Table 2.2. Malaysia lies on the South China Sea between 1° and 7° in North latitude and 100° and 120° in East longitude (Nugroho 2010). Twice a year, the monsoon winds occur. Between November and March, Northeast monsoon occurs where the wind blow from central Asia to South China Sea through Malaysia to Australia. Between May and September, the Southwest monsoon occurs when the wind blows from Australia to the Strait of Malacca. Rainfall in West Malaysia is measured as 2500 mm per year and East Malaysia is approximated of 5080 mm per year with the load mainly on October to February (Nugroho 2010).
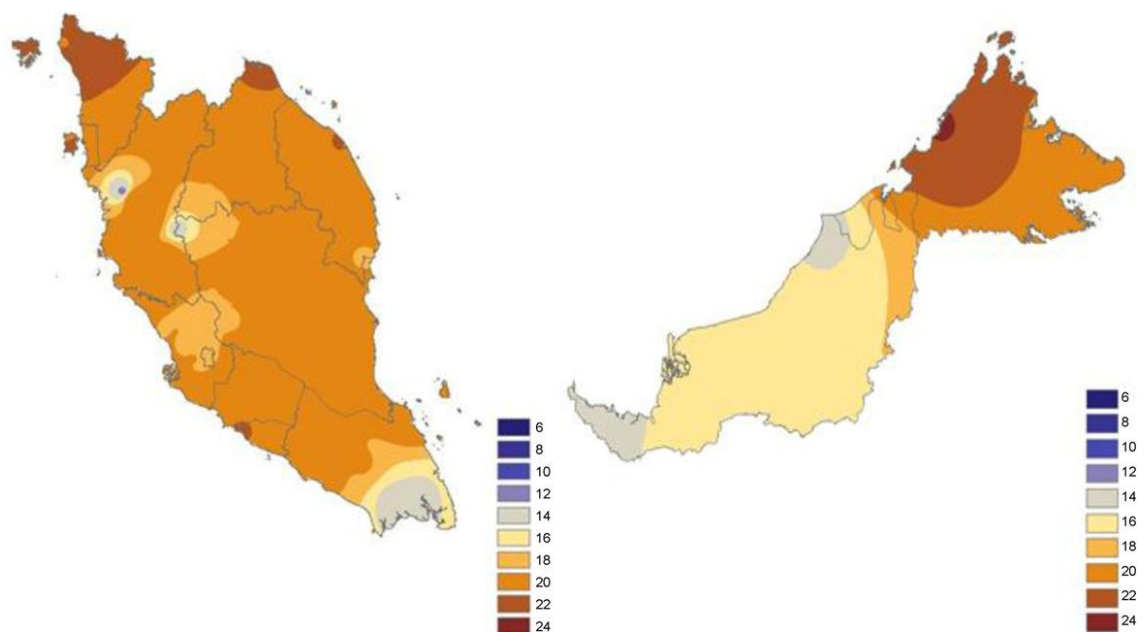
Figure 2.2: Annual average solar radiation (MJ/m^2/day) (Mekhilef et al. 2012b)

Table 2.2: Solar radiation in Malaysia (average value throughout the year)
(Mekhilef et al. 2012a)

Irradiance	Yearly average value (kWh/m2)
Kuching	1470
Bandar Baru Bangi	1487
Kuala Lumpur	1571
Petaling Jaya	1571
Seremban	1572
Kuantan	1601
Johor Bahru	1625
Senai	1629
Kota Baru	1705
Kuala Terengganu	1714
Ipoh	1739
Taiping	1768
George Town	1785
Bayan Lepas	1809
Kota Kinabalu	1900

2.5 Solar Collectors

Solar collector is the major component, most important part of a solar energy system (Kalogirou 2009). Solar collector is a device to absorb solar radiation and heat the fluid that flows through the collector. The heat can be used directly or be stored for night time or on cloudy days. Solar collectors are classified into low temperature, medium temperature and high temperature heat exchangers. Mainly, there are three types of collectors which are flat plate, evacuated tube, and concentrating (Foster et al. 2009). Kalogirou (2009), divide solar collectors into non-concentrating or stationary and

concentrating. Table 2.3 shows a list of collectors available (Kalogirou 2004b). Images of other types of solar collectors can be found in Appendix A.

Table 2.3: Solar Energy Collectors

Motion	Collector type	Absorber type	Concentration ratio	Indicative temperature range (°C)
Stationary	Flat-plate collector (FPC)	Flat	1	30-80
	Evacuated tube collector (ETC)	Flat	1	50-200
	Compound parabolic collector (CPC)	Tubular	1-5	60-240
Single-axis tracking	Linear Fresnel reflector (LFR)	Tubular	10-40	60-250
	Cylindrical trough collector (CTC)	Tubular	15-50	60-300
	Parabolic trough collector	Tubular	10-85	60-400
Two-axis tracking	Parabolic dish reflector (PDR)	Point	600-2000	100-1500
	Heliostat field collector (HFC)	Point	300-1500	150-2000

2.5.1　Flat-Plate Collectors

This study focus is on the application of nanofluids in flat-plate solar collector. A flat-plate solar collector is shown in figure 2.3. Solar radiation will pass through the transparent cover and will be absorbed by the absorber plate and be transported to the fluid in the tube and carried for use. The transparent cover purpose is to reduce convection losses from the plate and radiation losses from the collector. Flat-plate collector is cheap, fixed, without sun tracking, and oriented directly toward the equator which is facing south in the Northern Hemisphere and facing north in the Southern Hemisphere. In Malaysia, the optimum tilt angle should be around 10° to 15° (Kalogirou 2009).

The performance of a flat plate solar collector can be influenced by several factors such as material, shape, coating of absorber plate, type of glazes, number of tubes, distance between tubes, and collector's insulation material. The collector's performance can also be affected by operating condition such as flow rate, ambient temperature, wind speed and solar radiation. Lots of researches focus on these parameters for improving flat plate solar collectors.
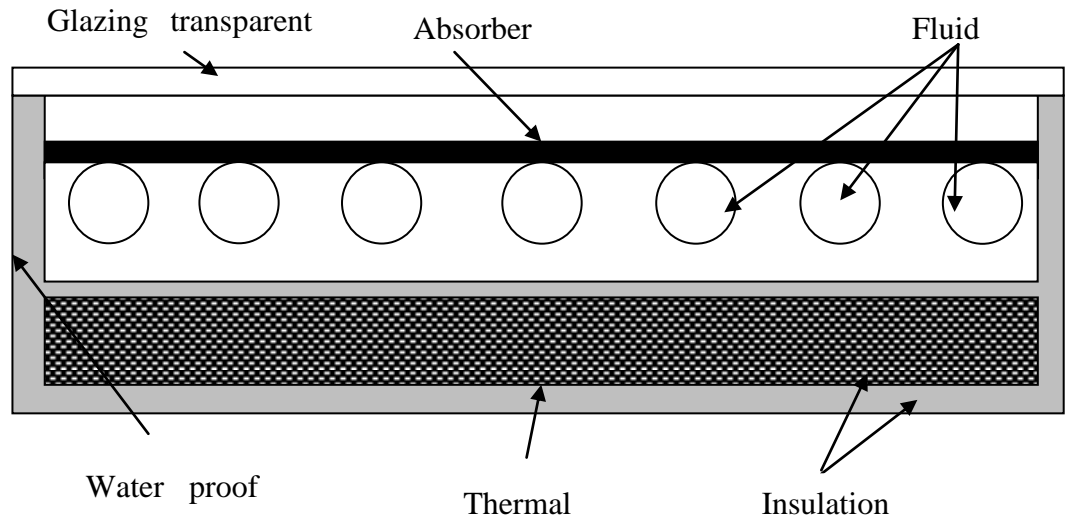
Figure 2.3: Flat Plate Collectors

During the early development of flat-plate collectors, Hottel and Woertz (1942) were the pioneered in the analysis of flat-plate solar thermal collectors. The fundamental quantitative relations among basic parameters including flow rate, inlet and ambient temperature, wind speed and solar radiation were established from their experimental and theoretical work. All those parameters are very crucial in the performance of a flat-plate collector. The importance of economic balance in comparison with the performance of flat-plate collectors were also stressed by them.

A mathematical model for efficiency factors that are applicable to flat-plate solar collectors was derived by Bliss Jr (1959). The appropriate use of the efficiency factors suggested could eliminate the empiricism and lead to a more accurate design of the solar collectors. The efficiency factors include the collector efficiency factor, F', which is the ratio of the actual useful heat collection rate to the theoretical useful heat collection rate with collectors overall surface at average fluid temperature and another factor is F_R,

which is the ratio of the actual useful heat collection rate to the theoretical useful heat collection rate with collectors overall surface at inlet fluid temperature.

Liu and Jordan (1963) argued that in designing a flat-plate solar collector, the average long term performance is more important than the instantaneous rate of energy collection. A simple procedure was reported to predict the long-term performance of a flat-plate collector at any tilt angle and at any location. The proposed method can simplified the calculation of collector's performance without undergoing a detailed analysis. Only two parameters are needed for the proposed method which is the monthly average clearness index and the difference between inlet water temperature to the collector and ambient air temperature.

San Martin and Fjeld (1975) performed an experimental investigation to compare the performance on three different configurations of flat-plate solar collector. The three different configurations include a double glaze ordinary tube-in-sheet flat-plate collector, a water trickle sandwich construction with a corrugated aluminium sheet on top and a thermal trap flat-plate collector. In the result, they found out that thermal trap flat-plate collectors can achieve higher temperatures and was twice more efficient than the sandwich-construction collector. However, the thermal trap materials must be highly transparent to the short wavelength radiation but poorly transparent to the long wavelength radiation. They also indicated that compared to the other two collector configurations, the thermal trap collectors operates longer with higher solar thermal collection rate. Kenna (1983) later performed a specific study on thermal traps solar collectors by applying acrylic materials. However, using acrylic will add cost to the system and have temperature limitations. Therefore, it is preferred to add cover to the system and reduce the trap thickness.

Siebers and Viskanta (1977) did a comparison of predicted performance of flat-plate collectors of constant outlet temperature with variable mass flow rate and flat-plate collectors of constant mass flow rate. They indicate that a flat-plate solar collector operating at constant outlet temperature is better economically. They also added that the additional cost for the collector's control system could be compensated by the advantages that it have. The efficiency of the proposed constant outlet temperature collector is higher at noon and lower at other time compared to the conventional constant mass flow rate collector but in the overall efficiency of both systems, there is no significant difference.

Cooper (1981) studied the effect of inclination angle on the heat loss from flat-plate solar collectors. The top heat loss coefficient of flat-plate collectors are generally caused by wind speed, plate and ambient temperatures, plate emittance, inclination angle and the sky temperature. In the result, he showed that for solar collector inclination angle below 60°, the plate and ambient temperatures will not affected the top heat loss coefficient.

Chiou (1982) analyse the effect of nonuniform fluid flow distribution on the thermal performance of a flat-plate solar collector. A numerical method was developed to determine the variation of the performance of a collector influenced by non-uniform distribution of the flow and the results showed that the deterioration of efficiency could be up to more than 20%. He concluded that when designing or analysing a flat-plate solar collector, the non-uniformity of the flow should not be overlooked.

Hahne (1985) investigated the various parameter effects on design and performance of flat plate solar collectors. The various parameters under steady and transient conditions were numerically investigated for the efficiency and warm-up time

of flat-plate collectors. He concluded that any simple method is sufficient in providing reasonable design of the collector for suitable weather conditions such as high values of ambient temperature and solar radiation. However, a more sophisticated design method is required including accounting for the inclination angle and pipe spacing for unfavourable weather condition.

Hollands and Lightstone (1989) perform study to investigate the influence of flow rate on the thermal performance of solar collector. The result showed that the low flow rate system have 17% higher delivered solar energy than the high flow rate. They also indicated that the low flow rate system is more cost effective and 38% improvement in performance was achieved by using the low flow rates collector incorporated with a stratified tank compared to a high flow rate collector with fully mixed tank.

Studies on laminar flow distribution of working fluid inside solar collectors had been made by a number of researchers. Kikas (1995) studied analytically the distribution of laminar flow of water in solar collector with two equal sized manifolds and pointed out that the efficiency of the collector can be improved with uniform flow through parallel tubes. He also found that in reverse return circuit where the flow enters from one side of the collector and exits from the opposite side, the flow in the system is more uniform. Weitbrecht et al. (2002) tested the theoretical studies by Kikas (1995) by conducting experiment to explore laminar flow distribution in solar collector. The effect of various parameters including pressure drop and energy loss caused by friction on the flow distribution were also being measured.

Groenhout et al. (2002) experimentally studied the heat loss characteristics of a flat-plate collector heating system design with double-side flat absorber plate, covered

with a low iron antireflective glaze. This set up showed a significant reduction of conductive and radiative heat loss indicating overall measured heat loss is about 30-70% less than conventional system. Chen et al. (2012) studied the effect of the volume flow rate on the efficiency of a solar collector and found out that if the volume flow rate of solar collector fluid is increasing, the efficiency, the start efficiency and the incidence angle modifier are increasing and the heat loss coefficient is decreasing. Roberts and Forbes (2012) did an analytical study of the influence of absorber plate absorptance and emittance for the instantaneous efficiency of a flat plate solar collector and showed that changing parameters such as reducing heat loss coefficients could give direct impact on the efficiency. The absorptance must be kept as high as possible for hot water heaters. Excessive heat loss from the base or inadequate shielding of the cover plate from wind causing high forced convection losses are also found out to be the main reason for poor efficiency of flat-plate solar collectors.

Application of nanofluids in solar collectors has been made in the past few years by numerous researchers. An experimental investigation conducted by (Yousefi et al. 2012c) on the effect of Al_2O_3 based nanofluid showed an efficiency increase of 28.3% of flat-plate solar collectors. (Lenert and Wang 2012) presented a model and performed an experimental study of concentrated solar power application using carbon-coated cobalt (C-Co) nanoparticles and Therminol VP-1 base fluid. They concluded that the efficiency was more than 35% with nanofluid and the efficiency would increase with increasing nanofluid height. (Lu et al. 2011) showed that the application of Copper Oxide (CuO) nanoparticles in evacuated tube solar collectors would significantly enhance the thermal performance of evaporator and evaporating heat transfer coefficient increased by 30% compared to water as working fluid. 5% improvement in the efficiency was found out by (Otanicar et al. 2010) using variety of nanoparticles with

water as base fluid for micro-solar-thermal collector. (Shin and Banerjee 2011) applied novel nanomaterials in molten salts base fluid to concentrated solar power coupled with thermal storage and experienced an enhancement in operational efficiencies. (Taylor et al. 2011) used graphite base nanofluids in high flux solar collectors that resulted in 10% increase in the efficiency. Zamzamian et al. (2014) performed an experimental study to investigate the effect of Cu nanoparticle on the efficiency of a flat-plate solar collector in different volume flow rates and weight fractions of the nanoparticles and found that the optimum point for solar collector efficiency can be reach up to 0.3 wt% Cu nanofluid at 1.5 L/min.

2.5.2 Other types of solar collectors

2.5.2.1 Evacuated tube collector (ETC)

Evacuated tube collectors consist of a heat pipe inside a vacuum-sealed tube. The vacuum will reduce convection and conduction heat loss. The efficiency is higher than flat-plate collectors but the cost is relatively expensive (Kalogirou 2009).
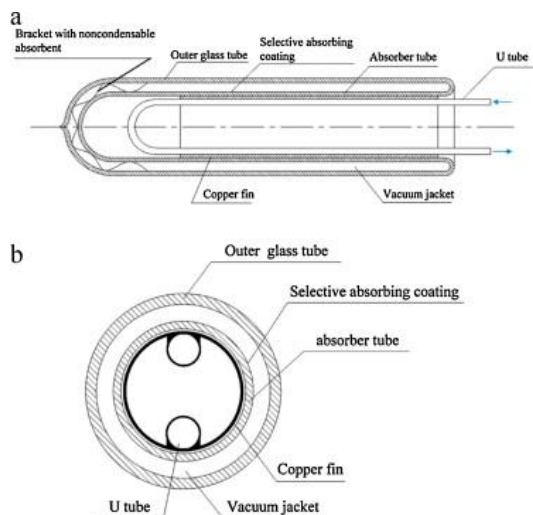
Figure 2.4: Glass evacuated tube solar collector with U-tube. (a) Illustration of the glass evacuated tube and (b) cross section (Ma et al. 2010)

2.5.2.2 Linear Fresnel reflector (LFR)

A linear Fresnel Reflector collector is made from an array of linear mirror strips that concentrate light onto a linear receiver.
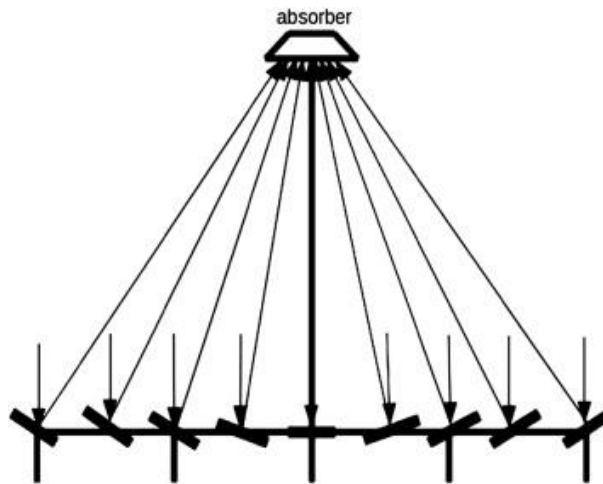
Figure 2.5: Linear Fresnel reflectors (Larsen et al. 2012)

2.5.2.3 Parabolic trough collector

Parabolic trough collectors parabolic shape reflector is made by bending a sheet of reflective materials where a black metal tube that is covered with a glass tube to reduce losses is used as the receiver. The system consists of low cost, light structure; single axis tracking and can effectively obtained heat up to 400°C (Kalogirou 2009).
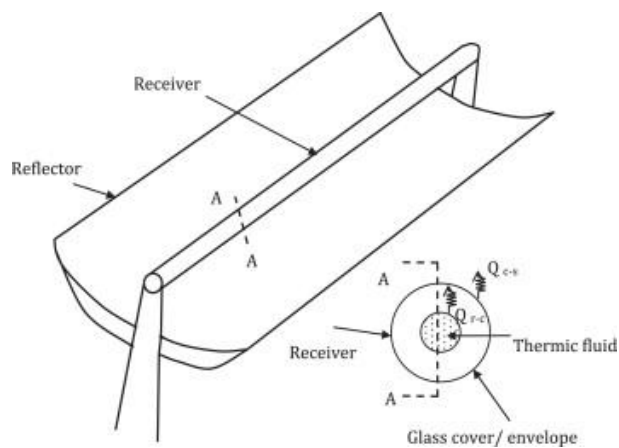
Figure 2.6: Parabolic trough collectors (Reddy et al. 2012)

2.5.2.4 Parabolic dish reflector (PDR)

A parabolic dish reflector will concentrate solar energy at focal point receiver and tracks the sun in two axes. Parabolic dish reflector can be used for electricity generation using parabolic dish engine system with temperature generated can be more than 1500°C. Advantages of parabolic dishes are (Laquil et al. 1993):

- The most efficient collectors because it always pointing at the sun
- Highly efficient at thermal energy absorption and power generation because of very high concentration ratios of 600 to 2000
- Can function either independently or as part of a larger system
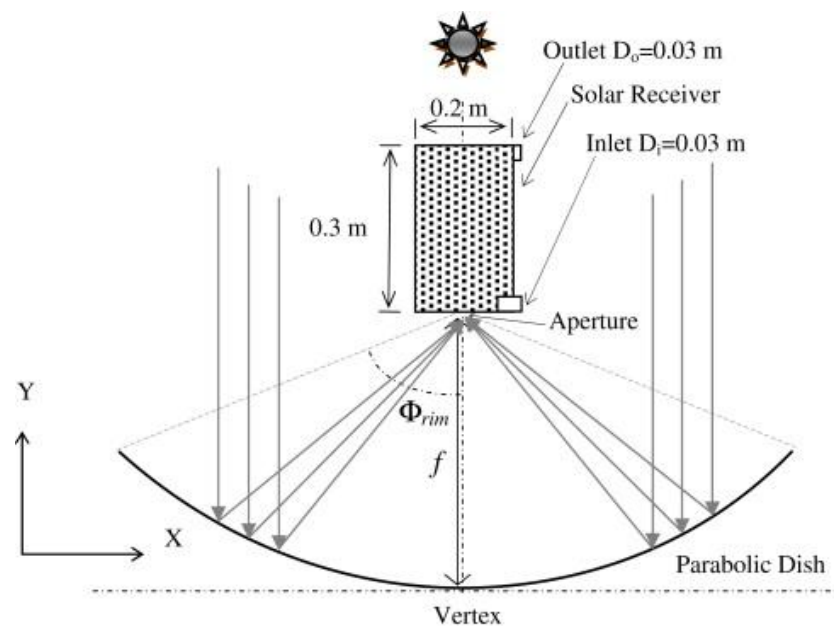
Figure 2.7: Parabolic dish reflectors (Wang et al. 2010)

2.5.2.5 Heliostat field collector (HFC)

Heliostat collector use slightly concave segment, multiple flat mirrors that direct large amount of heat energy into the cavity of a steam generator to produce electricity. They have single receiver, with concentration ratios of 300 to 1500, can store thermal energy and quite large in size generally more than 10 MW (Laquil et al. 1993). Energy collected by the system will be converted to electricity using a steam turbine generator that is similar with the conventional fossil-fuelled thermal power plants (Romero et al. 2002).
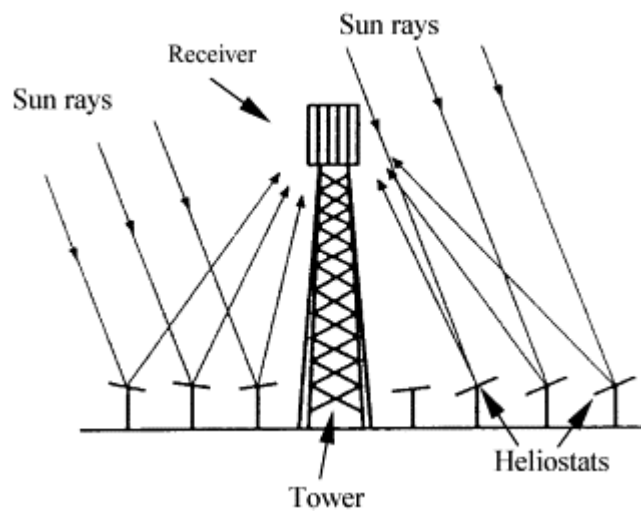
Figure 2.8: Heliostat field collectors (Kalogirou 2004b)

2.6 Heat transfer in flat-plate solar collectors

The major drawback of the flat-plate solar collectors is high heat losses from the absorber plate to surroundings and reducing the useful energy gain of the system. The enhancement of heat transfer rate in solar collectors could improve the overall performance of the heating system. Enhancement of heat transfer rate can be achieved

by increasing the heat transfer coefficient by disrupting boundary layer, increasing the Reynolds number or increasing the temperature gradient.

In the effort of raising the efficiency of solar collector, the values of the convective and radiative heat transfer coefficients are often of interest to many researchers. For a flat-plate solar collector, solar radiation incident on the aperture of a solar collector is transmitted through the glass covers to the absorber plate. The glass covers will absorb a fraction of the solar radiation. Absorption of solar radiation in a glass cover will increase its temperature and consequently affected the values of heat transfer coefficients. Nagar et al. (1984) has presented an experimental method to obtain the emittance of a selective coating by calculating the top heat loss coefficient, U_t using an empirical relation. They theoretically analyzed variation of stagnation temperature of various coatings kept in an insulated one glass cover box and shown that it is possible to make an approximate estimate of thermal emittance of the coating of known absorptance from the knowledge of parameters such as stagnation temperature, ambient temperature and solar radiation. Similar work had been done by Francey and Paraioannou (1985). They experimentally measured the heat loss from a flat-plate solar collector over a range of inlet temperatures, tilt angles and wind velocities while operating in a wind tunnel and obtained the wind heat transfer coefficient, h_w by calculating it from U_t using an empirical relation for Ut. However, large errors were figured out later by Mullick and Samdarshi (1988) for using the empirical relation of U_t for heat transfer coefficient. Similar findings were also reported by Samdarshi and Mullick (1991). They developed a more accurate analytical equation for the top heat loss factor of a flat-plate collector with double glazing and argued that the maximum computational errors resulting from the use of their equation are plus or minus three percent compared to numerical solution of the heat balance equations. Akhtar and

Mullick (2007) agreed with their statement. They analyze a wide range of variables and compared the results with those obtained by numerical solutions of heat-balance equations and found that the values of top heat loss coefficient, *Ut* computed are very close to those obtained by numerical solutions of heat-balance equations with maximum absolute error is only around 1.0% indicating that numerical solutions of heat-balance equations for the computation of *Ut* are not required.

2.7 Nanofluid

The interest in nanoparticles research is increasing due to its unique properties such as increased electrical and thermal conductivity. This section discusses about some researches that had been done for various nanoparticles in the area of solar thermal collectors.

2.7.1 Multi-Walled Carbon Nanotubes (MWCNT)
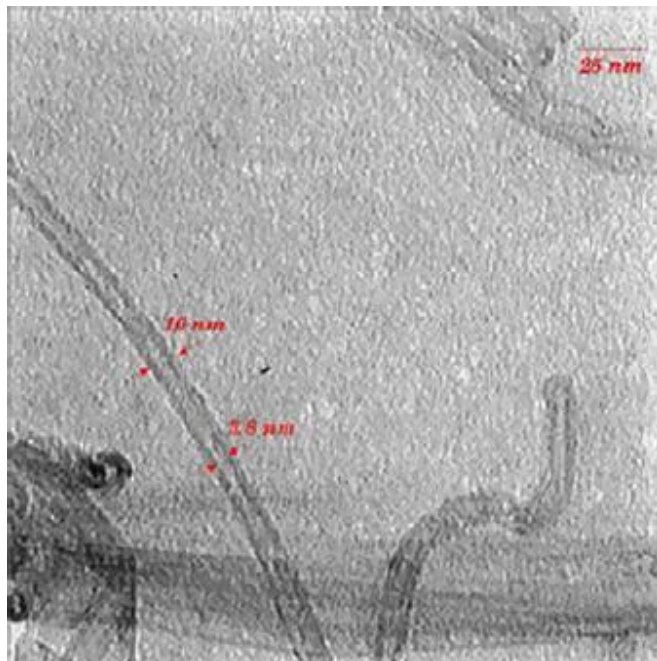
Figure 2.9: TEM image of MWCNT (Yousefi et al. (2012b)

A carbon nanotube is a family of nanomaterials made up of only carbon. Multi-walled carbon nanotubes (MWCNTs) are structurally having multiple layer of graphite forming a tubular shape. Carbon nanotubes have very high properties and very close to theoretical limits. Three exceptional qualities in the properties of MWCNTs includes the electrical conductivity that is as conductive as copper, the mechanical strength that is stronger and lighter than steel and the thermal conductivity that is more than five times that of copper. In an experimental investigation, Yousefi et al. (2012b) applied MWCNT water based nanofluid in a flat-plate solar collector. From the test results it was concluded that the efficiency for nanofluid is higher than water and the efficiency 0.4 wt% nanoparticles in the nanofluid is greater than 0.2 wt%. Yousefi et al. (2012a) also experimentally investigate the effect of pH values of MWCNT nanofluid and shown that changing the pH values with respect to the pH of isoelectric point will increase the efficiency of the system. Natarajan and Sathish (2009a) had tested MWCNT nanofluid in solar water heater. According to the results, the thermal conductivity was increased by 41% by using the volume fraction of 1% MWCNT nanofluid. Viscosity and thermal conductivity of MWCNT nanofluid prepared by using gum Arabic as dispersant were measured experimentally by Indhuja et al. (2013) in the effort of finding better ways of making a stable nanofluid solution. In the experiment, the temperature had been varied between 28 - 60°C and nanofluid concentration of 0.14 – 0.24 vol% had been used to measure the viscosity and effective thermal conductivity. It has been concluded that increasing temperature will increase the thermal conductivity ratios and relative viscosities especially at temperature above 45°C potentially because of the role of Brownian motion.

2.7.2 Silicon Dioxide (SiO$_2$)

Silicon dioxide or also known as silica is one of the most abundant materials on earth. Azmi et al. (2013) experimentally investigated the heat transfer coefficients and friction factor of SiO$_2$ nanofluid up to 4% volume fraction in a circular tube under constant heat flux boundary condition by varying Reynolds number of 5000 to 27,000 at 30°C. It had been concluded that the heat transfer coefficient increased by increasing nanoparticles concentration up to 3% but decreased thereafter. Chen et al. (2013) tried new water-based SiO$_2$ functionalized nanofluid in a loop thermosyphon as the working fluid and found out that functionalized nanofluid, even with unique dispersing ability, making the evaporating heat transfer coefficient and the maximum heat flux of the loop thyermosyphon became worse. It had been concluded that the deterioration in heat transfer might be because of the changes in the thermal properties of functionalized nanofluid. Experimental result from Fazeli et al. (2012) showed that dispersing SiO$_2$ nanoparticles in water in a miniature heat sink significantly increased the overall heat transfer coefficient and decreasing of thermal resistance of heat sink up to 10%.

2.7.3 Titanium Dioxide (TiO$_2$)

Titanium dioxide is also known as titania and is widely applied as white pigment in paints, coatings, plastics, papers, inks, foods, medicines and toothpastes due to its very high refractive index. Fedele et al. (2012) measured the viscosity and thermal conductivity of TiO$_2$ nanofluid at concentration of 1 wt%, 10 wt%, 20 wt% and 35 wt%. From their study, it was concluded that nanofluids exhibit a Newtonian rheological behavior and increasing mass concentration and temperature increased the thermal

conductivity. Abbasian Arani and Amani (2012) performed experimental investigation in a horizontal double tube counter-flow heat exchanger to study the effect of TiO_2 nanofluid volume fraction on the convective heat transfer characteristics and pressure drop. It had been concluded from their investigation that by increasing the Reynolds number of nanofluid volume fraction, the Nusselt number increases. Abbasian Arani and Amani (2013) also investigated the effect of diameter size of TiO_2 nanoparticle on Nusselt number and pressure drop. The diameter of nanoparticles is in between $10 - 50$ nm size. It had been concluded that the 20nm particle size diameter for TiO_2 has highest thermal performance than other diameter. Sajadi and Kazemi (2011) experimentally investigated the turbulent heat transfer of TiO_2 nanofluid in circular pipe by using volume fraction of less than 0.25%. Their results showed that by adding small amount of nanoparticles to the base fluid remarkably increased the heat transfer but there was not much effect on heat transfer enhancement by increasing the volume fraction even more. Their findings also showed that pressure drop was slightly higher for nanofluid than base fluid.

2.7.4 Copper (II) Oxide (CuO)

Copper (II) oxide is a brownish-black colored solid particle. Pastoriza-Gallego et al. (2011) experimentally determined the viscosity of CuO nanofluid and found out that particle size of nanoparticle subtly influence the density of nanofluid but there are very large differences in viscosity. Naraki et al. (2013) experimentally measured overall heat transfer coefficient in the car radiator by using CuO nanofluid under laminar flow regime ($100 \leq Re \leq 1000$) and concluded that CuO nanofluid shown greater heat transfer performance compared to water.

2.7.5 Aluminum Oxide (Al$_2$O$_3$)

An aluminum oxide or alumina nanoparticle is spherical and commonly seen as white powder. Yousefi et al. (2012c) experimentally investigated the effect of using Al$_2$O$_3$ nanofluid in a flat-plate solar collector with varying weight fraction of 0.2% and 0.4% and mass flow rate from 1 to 3 Lit/min. It was concluded that the efficiency of 0.2 wt% nanofluid is higher than 0.4 wt% and heat transfer can also be enhanced by adding surfactant. Experimental investigation on the thermophysical properties of ethylene glycol/water mixture and water based Al$_2$O$_3$ nanofluids had been carried out by Said et al. (2013). Nanofluids were found out to increase the thermal conductivities with increasing concentration and increasing nanofluid temperature leads to exponential decrease of viscosity. Albadr et al. (2013) did an experimental study on the forced convective heat transfer and flow characteristics of Al$_2$O$_3$ nanofluid in a horizontal shell and tube counter flow heat exchanger under turbulent flow condition by using different volume concentrations (0.3 – 2%). The results indicates that using Al$_2$O$_3$ nanofluid increased the convective heat transfer coefficient and it increases with an increase in the mass flow rate and also with the increase of the volume concentration but it also leads to increase in the viscosity and friction factor in the nanofluid. Sokhansefat et al. (2014) did a numerical study of Al$_2$O$_3$/synthetic oil nanofluid for parabolic through collector tube investigating the effect of Al$_2$O$_3$ particle concentration and operational temperature on the rate of heat transfer from the absorber plate. In the results it was shown that the volumetric concentration of nanoparticles increases the convective heat transfer coefficient and increasing the absorber operational temperature leads to reduce in the heat transfer enhancement. Ghanbarpour et al. (2014) did an experiment and theoretical study on thermal properties and rheological behavior of Al$_2$O$_3$ nanofluid as a heat

transfer fluid. It was found that the thermal conductivity and viscosity of Al_2O_3 nanofluid increases with increasing concentration.

2.8 Efficiency enhancement of solar collector when using nanofluid

Experimental investigation conducted by Yousefi et al. (2012c) on the effect of Al_2O_3 based nanofluid shown that the increase of 28.3% efficiency of flat-plate solar collectors. Lenert and Wang (2012) presented a modeling and experimental study of concentrated solar power application using carbon-coated cobalt (C-Co) nanoparticles and Therminol VP-1 base fluid and concluded that the efficiency is more than 35% with nanofluid and the efficiency will increase with increasing nanofluid height. Lu et al. (2011) shown that the application of Copper Oxide (CuO) nanoparticles in evacuated tubular solar collector will significantly enhance the thermal performance of evaporator and evaporating heat transfer coefficient increased by 30% compared to water as working fluid. 5% improvement in efficiency was found out by Otanicar et al. (2010) by using diversity of nanoparticles with water as base fluid for micro-solar-thermal collector. Shin and Banerjee (2011) applied novel nanomaterials in molten salts base fluid for concentrated solar power coupled with thermal storage and experienced an enhancement in operational efficiencies. They also concluded that the cost of electricity will be reduced. (Taylor et al. 2011) used graphite based nanofluid in high flux solar collectors resulting with 10% increase in efficiency. Zamzamian et al. (2014) performed an experimental study to investigate the effect of Cu nanoparticle on the efficiency of a flat-plate solar collector in different volume flow rates of the nanofluid from 0.016 to 0.050 kg/s. The weight fractions of the nanoparticles tested in the study 0.2% and 0.3% and have average diameter of 10 nm. The Cu nanoparticles were suspended in ethylene

glycol as the solvent. From their study, it was found that the optimum point for solar collector efficiency can be reached for 0.3 wt% Cu nanofluid at 1.5 L/min.

2.9 Nanofluid as sunlight absorber

Black surface or fluid is commonly used as light absorber in any heating application. Sani et al. (2011) had conducted an experiment on black fluid direct sunlight absorber using single-wall carbon nanohorn (SWCNHs) nanoparticles and ethylene glycol base fluid. They concluded that energy absorption capability of SWCNH is more than conventional carbon black suspensions to absorb heat from sunlight with ethylene glycol as a better base fluid than water. Tyagi et al. (2009) theoretically studied the comparison of performance of non-concentrating direct absorption solar collector (DAC) to conventional flat-plate solar collector with aluminium nanoparticles with water based fluid and found out that the efficiency of DAC is 10% more than flat-plate collector. Han et al. (2011) concluded that the thermal conductivity of carbon black nanofluid increased with the increase of volume fraction of the nanoparticles after applying it to a solar absorption device.

2.10   Properties of nanofluids

The key thermo-physical properties of heat transfer fluids for thermal system include density, specific heat capacity, thermal conductivity and viscosity. Various researchers have published the properties of nanoparticles and thermal properties of nanofluids as the basis of research on nanofluids applications. Table 2.4 shows the published specific heat, thermal conductivity and density of different nanoparticles.

Table 2.4: Properties of different nanomaterial and base fluid (Kamyar et al. 2012a; Namburu et al. 2007a)

Material	Specific heat, C_p (J/kg K)	Thermal conductivity, k (W/m K)	Density, ρ (kg/m^3)
Alumina (Al_2O_3)	773	40	3960
Copper oxide (CuO)	551	33	6000
Titanium oxide (TiO_2)	692	8.4	4230
Silicon dioxide (SiO_2)	765	36	2330
Water (H_2O), base fluid	4182	0.60	1000

Improvement in thermal properties of nanofluids such as thermal conductivity and convective heat transfer that have been described in previous section had a few mechanism contributing to it as listed by Keblinski et al. (2002) such as Brownian motion, particle and liquid interface nanolayer and heat transfer in nanoparticles. However, all this special characteristics cannot be achieved unless the nanoparticles are properly dispersed and stable. Surfactants can play a major role in achieving better dispersion and stability of nanofluids (Ghadimi et al. 2011; Murshed et al. 2011). However, some researchers did not add any surfactants or dispersants in the fluid because the addition of it could influence the thermal conductivity of the fluid and can deteriorate the thermal conductivity enhancement (Trisaksri and Wongwises 2007).

2.11   Thermal conductivity of nanofluids

To increase heat transfer of a fluid, thermal conductivity must be increased. Solid metals have higher thermal conductivity than fluids. Suspending metal particles in

fluid can increase the thermal conductivity and heat transfer performance of it. Experimental investigation on the thermal conductivity of nanofluids has been reported by many researchers. Measuring thermal conductivity of nanofluids had been done by using methods such as transient hot wire method, temperature oscillation and steady-state parallel plate method. The most popular method used by most researchers was the transient hot wire technique. In this method, the temperature over time response to an abrupt electrical pulse of the wire was measured. The thermal conductivity was calculated from the temperature data and Fourier's law. All the studies indicates that nanofluid have higher thermal conductivity than base fluids. Lee et al. (1999) shown that more than 20% enhancement of thermal conductivity achieved by using 4% volume fraction of CuO nanoparticles in ethylene glycol. Eastman et al. (2001) observed that up to 40% increase in thermal conductivity of ethylene glycol containing 0.3% volume fraction of Cu nanoparticles with mean diameter less than 10 nm compared to pure ethylene glycol. Xie et al. (2002) investigated experimentally the thermal conductivity of Al_2O_3 nanoparticles suspended in deionized water, ethylene glycol and pump oil and found out that small amount of Al_2O_3 in the solution have higher thermal conductivity than the base fluid and the enhancement increased by increasing the volume fraction of nanoparticles. Das et al. (2003) shown that 1% of volume concentration of CuO nanoparticles suspended in water have increased the thermal conductivity ratio from 6.5% to 29%. Murshed et al. (2005) reported that the thermal conductivity of TiO_2/water nanofluid increased remarkably with increasing volume fraction of nanoparticles. Mintsa et al. (2009) presented in his experimental data of Al_2O_3/water and CuO/water nanofluids that the effective thermal conductivity increased with increasing volume fraction, decreasing particle size and at higher temperatures. From all the reports in many publications it have been confirmed that adding nanoparticles in

fluid can increase the thermal conductivity of the base fluid and the enhancement in thermal conductivity of nanofluids influenced by some factors including temperature, size and volume concentration of nanoparticles.

2.12   Convective heat transfer of nanofluids

The forced convective heat transfer of working fluids is a very important mechanism in solar collectors. Nanofluids, with enhanced thermal conductivity are very attractive in this area. By adding a very small amount of nanoparticles in a base fluid, the convective heat transfer are expected to be enhanced while making little or no undesired effect in pressure drop that had been the major problem for micro-sized particles before. Xuan and Li (2003a) investigated experimentally the convective heat transfer of Cu nanofluids in a 10mm straight tube and showed that heat transfer rate had been enhanced by using nanofluids and low concentration nanofluids friction bring no significant penalty in pumping power. Wen and Ding (2004) tested the convective heat transfer of Al_2O_3 nanofluids in a copper tube under laminar flow regime and found an enhancement in heat transfer is quite significant in the entrance region. They suggested that enhancement in thermal conductivity might not be the only reason for increase in convective heat transfer but particle migration that result in non-uniform distribution of thermal conductivity and viscosity that will then reducing the thickness of thermal boundary layer might be the caused as well. Similarly, Kim et al. (2009) tested the amorphous carbonic-water nanofluid that have almost the same thermal conductivity with water but managed to increase the convective heat transfer coefficient by 8% under laminar flow. Ding et al. (2007) experimentally investigated forced convective heat transfer is using aqueous and ethylene glycol-based spherical titania nanofluids, and aqueous-based titanate nanotubes, carbon nanotubes and nano-diamond nanofluids and

found out that all the tested nanofluids shown a higher effective thermal conductivity than the one predicted by theories. However, at low Reynolds numbers, the convective heat transfer for TiO_2/ethylene glycol nanofluid and nano-diamond/water nanofluid was observed to be deteriorated due to the competing effects of particle migration on the thermal boundary layer thickness and the effective thermal conductivity might be the caused for it. Hwang et al. (2009) tested the convective heat transfer coefficient and pressure drop of Al_2O_3/water nanofluids and shown that the convective heat transfer coefficient for 0.3% nanofluid concentration increased by 8% compared to pure water. Duangthongsuk and Wongwises (2010) tested and presented the values for the heat transfer coefficient and friction factor of TiO_2/water nanofluids in the turbulent flow condition and concluded that the heat transfer coefficient of nanofluids at 1% concentration has 26% greater than pure water whereas increasing the concentration to 2% reduces the heat transfer coefficient to 14% lower than the base fluid under the same condition. At lower particle volume fraction, the pressure drop only incurred very slightly however, the pressure drop in nanofluids increased by increasing concentration due to increase in viscosity of the fluid. Fotukian and Nasr Esfahany (2010) experimentally investigated the turbulent convective heat transfer coefficient and pressure drop for a very low concentration of less than 0.24% CuO/water nanofluid in a circular tube and observed that the increase in heat transfer coefficient was to be on average of 25% with 20% reduction in pressure drop. Haghighi et al. (2014) investigated independently the turbulent convective heat transfer coefficients of 9 wt% Al_2O_3/water and TiO_2/water nanofluids inside a circular tube. In the investigation, the heat transfer coefficients of nanofluids were compared with those of the base fluids at the same Reynolds number or at the same pumping power. The same Reynolds number requires higher flow rate of nanofluids therefore such comparison shows up to 15%

increase in heat transfer coefficient but at equal pumping power, the heat transfer coefficient of Al_2O_3 nanofluid was practically the same with water while was about 10% lower for TiO_2. It had been concluded that comparing performance at equal Reynolds number is clearly misleading since the heat transfer coefficient can always be increased by increased pumping power and so, the comparison between the fluids should be done at equal pumping power.

2.13   Viscosity of nanofluid

Viscosity of nanofluids is a property as important as thermal conductivity for investigation of solar collector's performance although less attention was given for viscosity than thermal conductivity over the past few years (Mahbubul et al. 2012). Adding nanoparticles additive in fluid will increase the viscosity of the fluid and lead to increase in pumping power required. Nguyen et al. (2007) have investigated experimentally the influence of both the temperature and the particle size on the dynamic viscosities Al_2O_3 and CuO nanofluids. Dynamic viscosities was measured using a 'piston-type' calibrated viscometer based on the Couette flow inside a cylindrical measurement chamber and the results shown that viscosity of nanofluid increases with increasing of particle volume concentrations but it decreases with the increase in temperature. Namburu et al. (2007b) presented an experimental investigation of rheological properties of nanofluid containing CuO nanoparticles. The nanofluids tested have volume percentage ranging from 0% to 6.12% in temperatures ranging from −35 °C to 50 °C to demonstrate their applicability in cold regions. The test results indicate that the viscosity increased with increasing concentration and exponentially decreased with temperature. Phuoc and Massoudi (2009) displayed experimental observations on the effects of the shear rates and particle volume fractions on the shear

stress and the viscosity of Fe_2O_3 nanofluids using Polyvinylpyrrolidone (PVP) or Polyethylene oxide (PEO) as a dispersant. At volume fractions beyond 0.02, a non-Newtonian law exhibiting shear-thinning was observed indicating that shear viscosity depend on the shear rate and concentration of nanofluids. Other researchers, such as Lee et al. (2011) on SiC nanofluids for high temperature heat transfer applications, Aladag et al. (2012) on CNTs and Al_2O_3 nanofluids at low temperatures application and Elias et al. (2014) on the thermo-physical properties of Al_2O_3 nanofluids in car radiator application also indicated that nanofluid viscosity increases with increasing volume fraction.

Table 2.5: Summary of literature review

Nano particle	Solar thermal system	Remark	Reference
Aluminium (Al)	non concentrating DAC and flat plate	direct absorption collector (DAC) has 10% higher efficiency than flat plate solar collector using aluminium nanoparticles nanofluid	(Tyagi et al. 2009)
Diversity of nanoparticles	micro-solar-thermal collector	5% efficiency improvement	(Otanicar 2009)
Multi-walled carbon nanotubes (MWCNT)	solar water heater	thermal conductivity enhancement	(Natarajan and Sathish 2009b)
Single-wall carbon nanohorn (SWCNHs)	black fluid direct sunlight absorber	1) ethylene glycol is better based fluid than water 2) Energy absorption capability of SWCNH is more than carbon-black suspensions	(Sani et al. 2011) et al.
Graphite	high flux solar collectors	10% increase in efficiency	(Taylor et al. 2011)
Novel nanomaterials	concentrated solar power (CPS) with Thermal energy storage (TES)	enhance operational efficiencies and reduced cost of electricity	(Shin and Banerjee 2011)
Carbon black	solar absorption	thermal conductivity increased with the increase of volume fraction of nanofluid	(Han et al. 2011)
Copper Oxide (CuO)	evacuated tubular solar collector	Enhanced thermal performance of evaporator and evaporating heat transfer coefficient by 30% compared to water	(Lu et al. 2011)
Carbon coated cobalt (C-Co)	concentrated solar power (CPS)	1) 35% increase in efficiency with nanofluid 2) efficiency increase with increasing nanofluid height	(Lenert and Wang 2012)
Multi-walled carbon nanotubes (MWCNT)	flat-plate solar collector	efficiency increase by increasing or decreasing the pH value	(Yousefi et al. 2012a)
Multi-walled carbon nanotubes (MWCNT)	flat-plate solar collector	efficiency for 0.4 wt% nanoparticle is greater than 0.2 wt%	(Yousefi et al. 2012b)
Aluminium (III) Oxide (Al_2O_3)	flat-plate solar collector	efficiency increase by 28.3% with nanofluid	(Yousefi et al. 2012c)
Copper (Cu)	flat-plate solar collector	The optimum point for solar collector efficiency can be reached for 0.3 wt% Cu/EG nanofluid at 1.5 L/min	(Zamzamian et al. 2014)

2.14   Summary of literature review

Works on application of nanofluids in solar collectors is shown in Table 2.5. Based on the literature review, it can be seen that solar thermal application is improving and can solve lot of energy and environmental problems. It has also been concluded from numerous studies that nanofluids can increase the efficiency of flat-plate solar thermal collector. However, there are some gaps that have not yet been addressed in the area of nanofluid flat-plate solar thermal collector such as the effect of nanofluid on the conduit walls of the collector. Only Alumina, Copper and MWCNT nanofluid have been tested in flat-plate solar thermal collector. Lot of other nanoparticles has not been tested yet. In the reported articles only temperature and improved thermal efficiency have been reported. Pressure drops and exergy analysis has not been covered. No work has been done on the potential of size reduction of flat-plate collector by using nanofluids that can lead to costs and energy savings to manufacturers of the solar collector.

CHAPTER 3: METHODOLOGY

3.1 The thermodynamics performance of flat-plate solar thermal collector utilizing SiO$_2$ nanofluid

3.1.1 Efficiency Calculation of Nanofluids Flat-Plate Solar Collectors

This section explained the method used to calculate the efficiency of flat-plate solar thermal collectors by using nanofluids as working fluids. The study started by theoretical calculation and then followed by experimental method.

3.1.1.1 Analytical approach

Before the experimental investigation were being conducted, calculations were made analytically to find out the theoretical value of energy and exergy efficiency of various types of metal oxides nanofluids including SiO$_2$, Al$_2$O$_3$, TiO$_2$ and CuO.

3.1.1.1.1 First Law of Thermodynamics

First law of thermodynamics is about energy balance. It states that energy is a conservative property; which means that the energy entering into the system is equal to the energy leaving the system at steady-state. Overall amount of conserved energy is the same, although different forms of energy, for example thermal, mechanical, internal, potential, kinetic experience quantitative changes. Depending on this law, (for a stationary process observed through a control volume) an energy balance can be written as follows (Orsay Cedex 2010):

$$\dot{Q} - P = \sum_{outlet} \dot{m}_k \left(h + gz + \frac{w^2}{2} \right)_k - \sum_{inlet} \dot{m}_k \left(h + gz + \frac{w^2}{2} \right)_k \tag{3.1}$$

Where $\dot{Q}$, P, $\dot{m}$, z, w and h are the passing thermal energy through the system boundaries, mechanical power crossing the system boundaries, entering / leaving mass flow rate to and from the system, system height from reference level, mass flow velocity ($\dot{m}/\rho A$) and specific enthalpy measured at the system inlet and outlet respectively.

In the application of solar thermal collector, possible heat gain (Q_u) by absorbing medium is given by;

$$Q_u = \dot{m}C_p\left(T_{f,out} - T_{f,in}\right)$$
(3.2)

Where, $T_{f,in}$, $T_{f,out}$ and C_p symbolize the fluid inlet temperature, outlet temperature and specific heat of the absorbing medium, respectively. Nanofluids have different value for specific heat and density depending on the type and amout of nanoparticles being suspended inside the solution. The heat capacity and density of nanofluid are calculated as follow (Xuan and Roetzel 2000; Zhou and Ni 2008b)

$$C_{p,nf} = \varphi C_{p,np} + C_{p,bf}\left(1 - \varphi\right)$$
(3.3)

$$\rho_{nf} = \left(1 - \varphi\right)\rho_{bf} + \varphi\rho_{np}$$
(3.4)

Where, φ and ρ indicate the volume fraction of nanoparticles and density of absorbing medium. Another equation exists for possible heat gain (Q_u) of a flat plate solar collector, and is known as Hottel–Whillier equation. Equation considers the heat losses between atmosphere and solar collector, as shown by (Struckmann 2008)

$$Q_u = A_p F_R\left[S - U_1\left(T_{f,in} - T_a\right)\right]$$
(3.5)

Where, T_a and (F_R) represent ambient/atmospheric temperature and heat removal factor. F_R is prescribed as,

$$F_R = \frac{\dot{m}C_p}{U_1 A_p}\left[1-\exp\left\{-\frac{F'U_1 A_p}{\dot{m}C_p}\right\}\right]$$

(3.6)

Where, F' stands for the collector efficiency factor. For a steady state condition, An energy balance equation on the absorber plate can be expressed as, (Sukhatme and Sukhatme 1996),

$$Q_u = A_p S - U_1 A_p \left(T_c - T_a\right)$$

(3.7)

In eq. (3.4) - (3.6), T_c, S and A_p are the absorber plate temperature (average), absorbed irradiation flux by unit area of the absorber plate and absorber plate area, respectively. U_1 is the overall loss. These parameters are assumed as a constant factor or a variable with little effect. The instantaneous collector efficiency relates the useful energy to the total radiation incident on the collector surface by Eq. (3.7) or (3.8).

$$\eta_{En} = \frac{Q_u}{A_p I_T} = \frac{\dot{m}C_p\left(T_{f,out}-T_{f,in}\right)}{I_T}$$

(3.8)

$$\eta_{En} = F_R\left(\tau\alpha\right) - F_R U_1 \frac{T_{f,in}-T_a}{I_T}$$

(3.9)

The analysis is performed with considering the normal incidence condition, hence, the $F_R(\tau\alpha)$, F_R, and U_1 are constant within the range of tested temperatures for the analytical analysis (Yousefi et al. 2011).

But, in fact, several forms of energy have several probabilities to originate possible work. Hence efficiency definition is only a comparison between quantities which are metrically homogeneous but not conceptually equivalent.

Another parameter is the optical properties of a fluid. The optical properties of a base fluid can be significantly altered by adding and suspending a small amount of nanoparticle in the fluid (Taylor et al. 2011). To analyse this, absorbed irradiation per unit area of solar collector absorber plate (S) in eq. (3.5) can be determined by,

$$S = I_T(\tau\alpha)$$

(3.10)

Where $(\tau\alpha)$ is known as optical efficiency (η_o) or product of transmittance – absorptance of the solar collector (Sukhatme and Sukhatme 1996).

3.1.1.1.2 The Second Law of Thermodynamics

Second law of thermodynamics is used to overcome the drawbacks of the 1st law. It started by considering that real processes are not reversible and it will gain entropy through the processes. Some of the common irreversible processes are molecular diffusion, friction, hysteresis etc. According to clausius statement, second law can be written as (Orsay Cedex 2010),

$$\sum_{outlet}(\dot{m}.s)_k - \sum_{inlet}(\dot{m}.s)_k = \sum_j \left(\frac{\dot{Q}}{T}\right)_j + \sigma$$

(3.11)

Where, s, T and σ represent entropy generation per unit mass, ambient temperature and overall entropy production due to irreversibility respectively. During first law analysis,

there is a term for work, but no consideration for irreversibility, besides, second law discusses irreversibility but avoids the term work. To gather more information, first law and second law are combined together. By combining equations (3.1) and (3.11), one can obtain the Gouy-Stodola equation (Sarhaddi et al. 2010):

$$P = \sum_n \dot{Q}_n \left(1 - \frac{T_a}{T_n} \right) + \sum_{Inlet} \dot{m}_k \left(h - T_a s + \frac{w^2}{2} + gz \right)_k - \sum_{Outlet} \dot{m}_k \left(h - T_a s + \frac{w^2}{2} + gz \right)_k - T_a \sigma$$

(3.12)

Exergy can be expressed as the obstruction of any work proportion to its dead state. There is no further work, when the environment becomes equilibrium with the system. At this state, the system is defined as dead state. Therefore for a control volume, eq. (3.11) may be rewritten in terms of exergy, as follows:

$$\left(E_P \right)_{out} - \left(E_P \right)_{in} = \left(E_Q \right)_{in} - \left(E_Q \right)_{out} + \left(E_m \right)_{in} - \left(E_m \right)_{out} - \sigma T_a$$
$$\left(E_P + E_Q + E_{\dot{m}} \right)_{in} = \left(E_P + E_Q + E_{\dot{m}} \right)_{out} + \sigma T_a$$
$$\textit{Therefore},$$

$$\sigma T_a = \sum_{in} E_j - \sum_{out} E_k$$

(3.13)

Where, exergy of work E_P, exergy of heat Q available at temperature T, E_Q and exergy of a mass flow, $E_{\dot{m}}$ are defined as follow;

$$E_P = P;$$
$$E_Q = Q \left(1 - \frac{T_a}{T} \right); and$$
$$E_{\dot{m}} = \dot{m} \left[\left(h - h_o \right) - T_a \left(s - s_o \right) + \frac{w^2 - w_o^2}{2} + g \left(z - z_o \right) \right]$$

The irreversibility can then be quantified as the difference in exergy measured at the inlet and outlet sections of the control volume. The simplest exergy balance equation per unit interception area of a solar collector can be expressed in steady state as shown below (Suzuki 1988a):

$$\dot{E}_g = \eta_o \dot{E}_{sun} - \dot{E}_{loss}$$

(3.14)

Where, η_o symbolizes the optical efficiency, $\dot{E}_g$, $\dot{E}_{sun}$, and $\dot{E}_{loss}$ represent exergy gain per collector interception area, exergy flow from the sun, exergy loss per collector interception area, respectively and the exergy loss due to the fluid pressure drop is assumed to be negligibly small. Eq. (3.13) can also be written as (Jafarkazemi and Ahmadifard 2012),

$$\sum \dot{E}_{in} - \sum \dot{E}_{out} = \sum \dot{E}_{dest}$$

(3.15)

Where $\dot{E}_{in}$, $\dot{E}_{out}$ and $\dot{E}_{dest}$ are the inlet, outlet and destructed exergy rate, respectively. The exergy collection rate in steady state is exergy gained by heat transfer fluid while the fluid temperature increases from $T_{f,\ in}$ at the inlet to $T_{f,\ out}$ at the outlet. The expression of the exergy collection rate, assuming that the fluid is incompressible, can be obtained by using of the following equation without considering mechanical exergy,

$$\dot{E}_g = \dot{m} C_p \left(T_{f,out} - T_{f,in} - T_a \ln \frac{T_{f,out}}{T_{f,in}} \right)$$

(3.16)

There are two important points that should be noted in considering the exergy available ratio for solar radiation. One is that the solar flux radiating on earth can be assumed as always being in a steady state but never in equilibrium state. The other is

that the radiation of the sun is a kind of an open system which means banishment of photons cannot be recovered unlike equilibrium closed system. From these facts the Carnot's expression of (1 - T_a/T_s) is appropriate for the solar radiation exergy which has the same form as Jeter's result (Jeter and Stephens 2012). From the above mentioned, the exergy flux from the sun is defined here as:

$$\dot{E}_{sun} = I_T \left(1 - \frac{T_a}{T_s} \right)$$

(3.17)

Where, T_a and T_s stand for ambient temperature and apparent sun temperature, respectively. The heat transfer process from the sun to the collector's working fluid consists of two main parts, absorbing the solar radiation by absorber plate and heat transfer from absorber plate to working fluid. The exergy destructions occur during these two processes including flowing parts (Suzuki 1988a):

1. Absorption exergy loss (radiation → plate): an exergy annihilation process when the solar radiation at T_s, is absorbed by the absorber at T_c.

2. Leakage exergy loss (plate → ambient): an exergy loss process accompanied with heat leakage from the absorber out into its surroundings.

3. Conduction exergy loss (plate → fluid): an exergy annihilation process caused by heat conduction between the absorber and the heat transfer fluid.

The above three kinds of exergy loss processes are closely related with the corresponding entropy generation rates through Gouy-Stodola's theorem (Bejan and Kestin 1983). These three entropy generation rates can be stated from the thermodynamically considerations as follows:

$$\Delta \dot{s}_{rp} = \int_0^1 k I_T \left(\frac{1}{T_1} - \frac{1}{T_s} \right) d\sigma$$

(3.18)

$$\Delta \dot{s}_{pa} = \int_0^1 U_1(T_1 - T_a)\left(\frac{1}{T_a} - \frac{1}{T_1}\right)d\sigma, and$$

(3.19)

$$\Delta \dot{s}_{pf} = \int_0^1 k(T_1 - T_f)\left(\frac{1}{T_f} - \frac{1}{T_1}\right)d\sigma$$

(3.20)

Where, k is heat conductivity between the absorber and the fluid, although equations (3.18)-(3.20) cannot be integrated unless a distribution of the local absorber temperature (T_1) and the heat transfer coefficient are known, these equations still can be approximated by using of the mean absorber temperature as follows:

$$\Delta \dot{s}_{rp} = kI_T\left(\frac{1}{T_c} - \frac{1}{T_s}\right)$$

(3.21)

$$\Delta \dot{s}_{pa} = U_1(T_c - T_a)\left(\frac{1}{T_a} - \frac{1}{T_c}\right), and$$

(3.22)

$$\Delta \dot{s}_{pf} = \int_{T_{f,in}}^{T_{f,out}} \frac{\dot{m}C_p dT}{T} - \frac{\dot{m}C_p(T_{f,out} - T_{f,in})}{T_{f,out}}$$

(3.23)

In equation (3.23), the first term on the right-hand side is an entropy flow received by the fluid from the absorber and the second term represents entropy of the collected energy as it has been in the absorber. The difference of both terms becomes the entropy generation rate while heat transfers from the absorber to the fluid. The exergy loss term in equation (3.13) can be seen from equations (3.20) - (3.23) using Gouy-Stodola's theorem as,

$$\dot{E}_{loss} = T_a(\Delta \dot{s}_{rp} + \Delta \dot{s}_{pa} + \Delta \dot{s}_{pf})$$

(3.24)

Hence, the exergy-balance-equation of a solar collector in steady state can be derived by substituting equations (3.18), (3.19), and (3.24) into equation (3.13). After a few arrangements, it becomes:

$$\dot{m}C_p\left(T_{f,out} - T_{f,in} - T_a \ln \frac{T_{f,out}}{T_{f,in}}\right) = I_T\left(1 - \frac{T_a}{T_s}\right)$$

$$-\left[(1-\eta_o)I_T\left(1 - \frac{T_a}{T_c}\right) + I_T T_a\left(\frac{1}{T_c} - \frac{1}{T_s}\right) + U_1(T_c - T_a)\left(1 - \frac{T_a}{T_c}\right) + \dot{m}C_p T_a\left(\ln \frac{T_{f,out}}{T_{f,in}} - \frac{T_{f,out} - T_{f,in}}{T_c}\right)\right]$$

(3.25)

By rearranging this equation, the following energy-balance equation of a solar collector can be easily obtained:

$$\dot{m}C_p(T_{f,out} - T_{f,in}) = \eta_o I_T - U_1(T_c - T_a)$$

(3.26)

The exergetic efficiency is defined here and is expressed using equation (3.25) as follows:

$$\eta_{Ex} = \frac{\dot{E}_g}{\dot{E}_{sun}}$$

$$= 1 - \left[(1-\eta_o)\frac{1 - T_a/T_c}{1 - T_a/T_s} + \frac{1/T_c - 1/T_s}{1/T_a - 1/T_s} + \frac{U_1(T_c - T_a)}{I_T}\frac{1 - T_a/T_c}{1 - T_a/T_s} + \frac{\dot{m}C_p T_a}{I_T(1 - T_a/T_s)}\left(\ln \frac{T_{f,out}}{T_{f,in}} - \frac{T_{f,out} - T_{f,in}}{T_c}\right)\right]$$

(3.27)

$$\eta_{Ex} = 1 - \left[e_{opt} + e_{rp} + e_{pa} + e_{pf}\right]$$

(3.28)

All terms in brackets in equations (3.27) and (3.28) represent exergy losses and their physical meanings are given as follows:

1. e_{opt}: optical loss fraction of the absorbed solar radiation due to transmissivity of glazing and absorptance of the absorber.

2. e_{rp}: a loss fraction when the solar radiation at T_s is absorbed by the absorber at T_c. (The high quality energy is degraded by absorption at low temperature.)

3. e_{pa}: a fraction of the exergy leakage from the absorber to the surroundings.

4. e_{pf}: Heat-conduction loss fraction accompanied with the heat transfer from the absorber to the fluid.

Two of the above loss fractions, e_{opt} and e_{pa} correspond to the terms $(1 - \eta_o)$ and $U_l(T_c - T_a)/I_T$ in well-known expression of energetic efficiency; the other two fractions have no corresponding term in the energetic analysis because they are not considered as loss processes. It should be noted here that the term given for heat-conduction loss e_{pf} is closely related with the collector efficiency factor. Considering the correlations of temperature distribution in the collector, the following correlation can be obtained (Duffie and Beckman 2006):

$$\frac{T_{f,out} - T_a - S/U_1}{T_{f,in} - T_a - S/U_1} = \exp\left(-\frac{U_1 A_p F'}{\dot{m}C_p}\right)$$

(3.29)

Here also, using the above equation, the component of outlet fluid temperature is omitted from Eq. (3.27) and the correlation of collector exergy efficiency is rearranged into the following form (Jafarkazemi and Ahmadifard 2012):

$$\eta_{Ex} = \frac{\dot{m}C_p\left[\left(T_{f,in}-T_a-\dfrac{S}{U_1}\right)\left(\exp\left(-\dfrac{U_1 A_p F'}{\dot{m}C_p}\right)-1\right)\right]-\dot{m}C_p\left[T_a\left(\dfrac{\exp\left(-\dfrac{U_1 A_p F'}{\dot{m}C_p}\right)-1}{T_{f,in}}\left(T_{f,in}-T_a-\dfrac{S}{U_1}\right)+1\right)\right]}{A_p I_T\left[1-\left(\dfrac{T_a}{T_s}\right)\right]}$$

(3.30)

Various components of this correlation can be calculated based on the descriptions in the previous section.

3.1.2 Experimental Investigation of Nanofluids Flat-Plate Solar Collectors

This section explains the experimental procedure of testing SiO_2 nanofluid as working fluid in a flat-plate solar collector. After that, method of analyzing data obtained from the experiment is also included in this section.

3.1.2.1 Preparation and characterization of SiO_2 nanofluids

Stability of nanofluids for long term is the major issue for the engineering applications (Liu and Liao 2008). Nanoparticles in the base fluid naturally will aggregate and sediment. In theory, there are existence of both attractive and repulsive forces between particles (Ise and Sogami 2005). The attractive force is the van der Waals force and the repulsive force is the electrostatic repulsion when particles get too close together. If the repulsive force is stronger than the attractive force, nanoparticles in the base fluid can remain stable or otherwise it will aggregate and serious aggregation will lead to sedimentation. Adding surfactants to the nanofluid can enhance the electrostatic repulsion of nanoparticles. Surfactants such as sodium dodecyl benzene

sulfonate, sodium dodecyl sulfate or Triton X-100 had been tested and proven to stabilize nanofuid (Wang 2009). However, the effect might be weakened when the Brownian motion of nanoparticles is too strong or when the nanofluid is heated. Another way to stabilize nanofluid is by changing the pH value of the solution (Yousefi et al. 2012a). The pH of isoelectric point for nanoparticles carries no electrical charge and therefore causes no interparticle repulsion force which in turn causing more aggregated solution. The more differences between the pH of nanofluid and pH of isoelectric point may cause less aggregation and better dispersion. The pH of SiO_2 in this study had been measured to be 6.5 by using Hanna Instruments microprocessor pH meter while the pH of isoelectric point for SiO_2 is around 3 (Kosmulski 2001). A better way to stabilize nanofluid was proposed by Yang and Liu (2010) is to graft polymers on to the surface of nanoparticles and also known as surface functionalization. Silanes were grafted on silica nanoparticles making "Si-O-Si" covalent bonding and resulting in steric stabilization effect even when heated. Functionalized SiO_2 nanoparticles have been reported to keep dispersing well after 12 months and no sedimentation was observed (Chen et al. 2013).

The SiO_2 nanoparticles used in this experiments were obtained from US Research Nanomaterials, Inc with 15 nm in outer diameter, coated with 2wt% Silane, have a density of 2.4 g/cm^3 and a PH value of 6 - 6.5. For this study, 3L of 0.2% and 0.4% volume fraction of SiO_2 nanofluid were prepared. The amount of nanoparticles needed for the solution was calculated first by using Eq. (3.31).

$$\varphi_n = \frac{m_n / \rho_n}{m_n / \rho_n + m_w / \rho_w}$$

(3.31)

Where φ_n is the volume fraction of nanoparticles in nanofluid (%), m_n is the mass of nanoparticle (kg), m_w is the mass of water (kg), ρ_n is the density of nanoparticle (kg/m^3) and ρ_w is the density of water (kg/m^3).

The nanofluids were prepared by using two-step method. It was prepared by dispersing nanoparticles into distilled water by using ultrasonicator and high pressure homogenizer (up to 2000 bar capacity) to obtain a homogenously dispersed solution. The microstructure and composition of the nanoparticles are characterized using field emission scanning electron microscopy (FESEM) (Model AURIGA, Zeiss, Germany). Nanoparticles are characterized before and after experiment with FESEM at 1 kV accelerating voltage. 50,000 times magnification is used to capture the images at the 100 nm scale. Figure 3.1 shows the FESEM images of SiO$_2$ nanoparticles mixed in distilled water. The FESEM images in Figure 3.2 indicate the sizes of SiO$_2$ nanoparticles. The picture of the prepared nanofluid is shown in Figure 3.3. As it is shown, the prepared nanofluid can still keep dispersing well after 6 months and no sedimentation was observed.
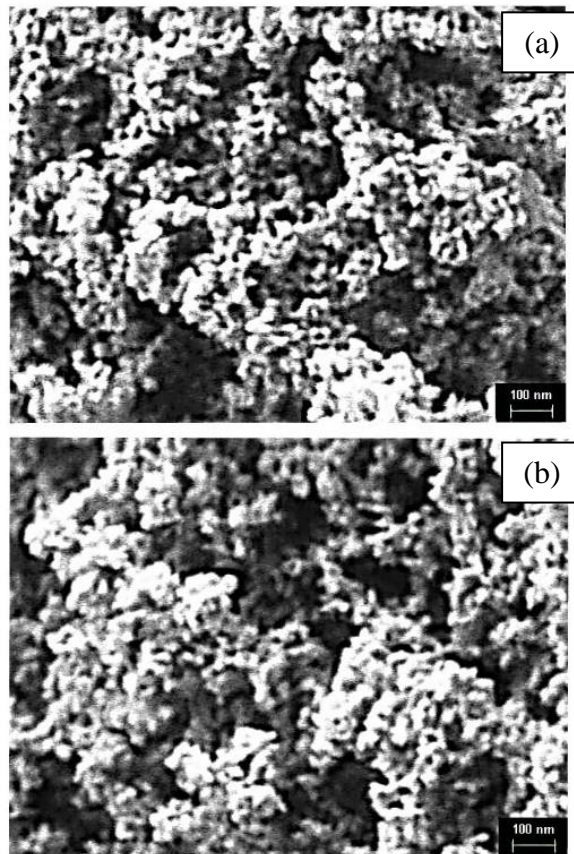
Figure 3.1: SEM images of SiO$_2$ nanoparticle (a) before and (b) after the

experiment
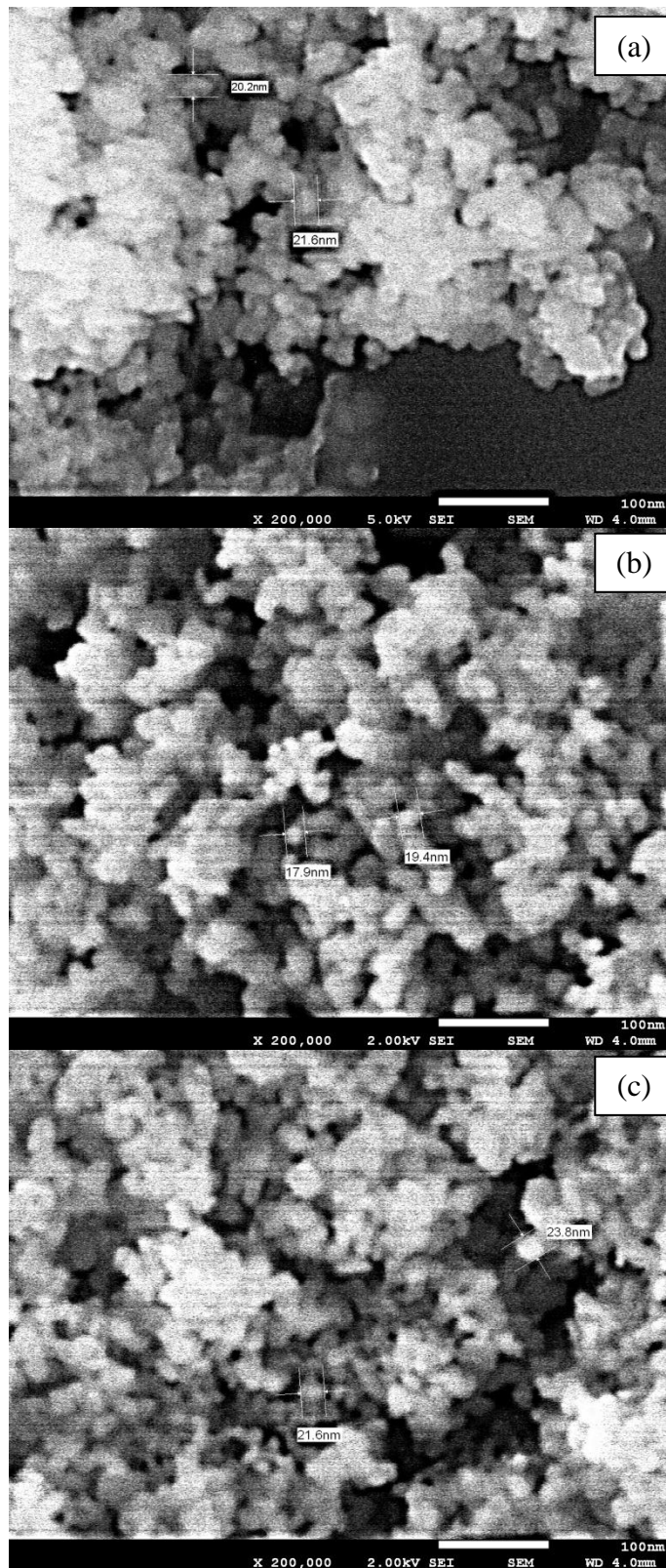
Figure 3.2: SEM images of (a) SiO$_2$ nanoparticles (b) 0.2% SiO$_2$ nanofluid and (c) 0.4% SiO$_2$ nanofluid
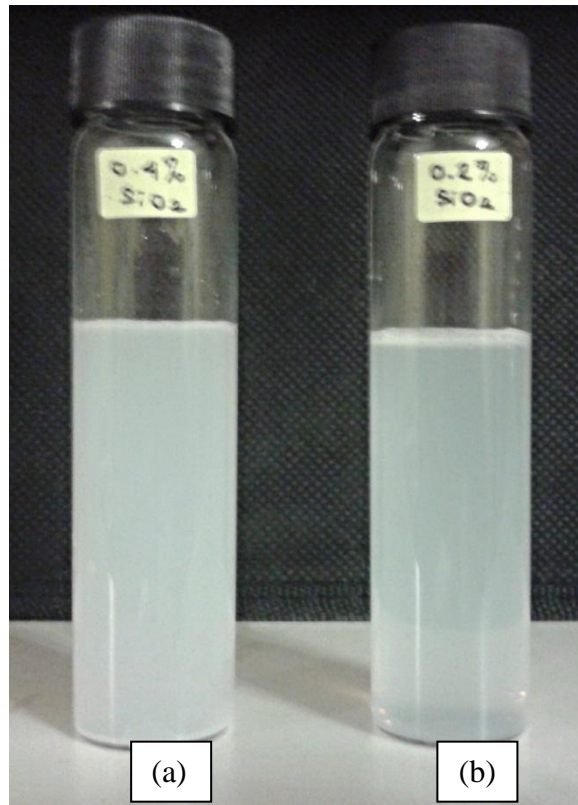
Figure 3.3: Pictures of (a) 0.4% and (b) 0.2% nanofluid after 6 months

The viscosity of prepared nanofluid was measured by using LVD-III ultra-programmable rheometer (Brookfield, USA) with ±0.5% uncertainty. The viscosity of all samples was measured at the constant shear rate of 73.38s^{-1}, while the ULA spindle rotating was 60 rpm. For the temperature variation, the refrigerated circulator bath (Model AD07R-40-12E, Polyscience, USA) with accuracy ±0.1°C was connected to the water jacket of ULA that was attached to the rheometer. The temperature of each sample was varied from 25 °C to 85 °C with 20 °C intervals to investigate the effect of temperature on the viscosity of nanofluid. Each experiment was repeated three times to get the more precise values. The mean value of the three data was considered for the analysis.

3.1.2.2 Experimental procedure

A schematic diagram of the experiment is shown in Figure 3.4. The solar collector experimental set up indicated in Figure 3.5 was constructed at the University of Malaya, Kuala Lumpur, Malaysia. The specifications of the flat-plate solar collector used in this study are given in Table 3.1. The tilt angle of this solar collector is 22°. Two electrical pumps were used in this system to pump the working fluid and water from the tank. The water from the tank is used to absorb the heat from the system cycle. A plate heat exchanger is used to transfer the heat from the working fluid of the solar thermal system cycle to the water inside the tank. The experiments were conducted by using different volume flow rates from 1 to 3 L/s for each type of the working fluids. A flow meter with a controlling valve was connected to control the mass flow rate of the working fluid. The tests have been carried out from 10 am to 3 pm. Following the requirement of the ASHRAE (2010) standard, each test was performed in several days and the best experimental data were chosen. For steady-state efficiency tests, the mass

flow rate must be held within ±1%, solar radiation must be steady within ±50 W/m^2, the variation of environment temperature must not more than ±1.5 K and the inlet temperature must be within ±0.1 K. Steady-state conditions must be maintained for data period length of 5 minutes and pre-data period of 15 minutes. Thermocouples were used in this experiment to measure the plate temperature, the fluid temperatures at the inlet and outlet of the solar collector and the environment temperature. A pressure transducer was used to measure the pressure difference from the inlet and outlet of the solar collector. All readings from the thermocouples and the pressure transducer were recorded in the data logger. Solar radiation was recorded by using a TES 1333R solar meter. The wind speed was measured by an anemometer. The entire measuring devices had been carefully calibrated before the experiment.

1–Flat plate solar collector,
2–Water tank,
3–Heat exchanger,
4–Flow meter,
5–Drain,
6–Pump,
7–Valve,
8–Thermocouple (plate temperature),
9–Thermocouple (working fluid out),
10–Thermocouple (working fluid in),
11–Thermocouple (ambient),
12–Thermometer,
13–TES 1333R solar meter,
14–PROVA (AV M–07) Anemometer,
15–Data logger,
16–Pressure transducer.
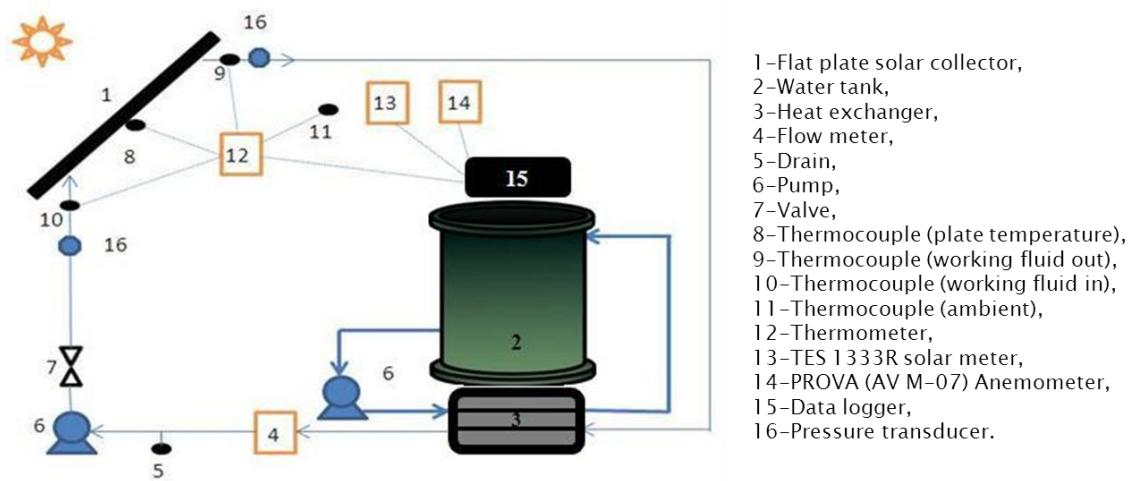
Figure 3.4. A schematic diagram of the experiment.

Table 3.1. Solar collector's specification.

Specification	Dimension
Dimension	2000 mm x 1000 mm x 80 mm (LxWxH)
Aperture area	1.84 m^2
Weight	36 kg
Cover material	4 mm tempered texture glass
Heat transfer coefficient	4.398 $W/(m^2 \cdot K)$
Absorber material	0.4 mm aluminum
Header material	Copper TP2
Header tube size	22 mm x 0.6 mm (Φxt), 2 pcs
Riser tube material	Copper TP2
Riser tube size	10 mm x 0.45 mm (Φxt), 8 pcs
Absorption rate	0.94
Emittance	0.12
Frame	Aluminum alloy, anodized

Figure 3.5: Experimental set up

3.1.3 Calculation from experimental data

3.1.3.1 Error analysis

In any experiment, the measured quantities subject to uncertainties or error. Errors can be caused by various factors. The errors can be classified as systematic and random error. Systematics errors are errors that shifted or displaced the measurement values systematically such as incorrect calibration of equipment or incorrect adjustment of that device. Usually, systematic errors can be avoided and eliminated. Random errors, on the other hand are errors which fluctuate from one measurement to the next.

Random errors are unavoidable and must be accounted to indicate the accuracy of the measured data (Kotulski and Szczepinski 2010).

For a collection of measured data, it is very important to calculate the average or mean value $\bar{x}$. The mean value can be calculated as follows:

$$\bar{x} = \frac{\sum x_i}{n}$$

(3.32)

Where n is the number of times and x_i is the measured quantity.

The measure of dispersion in the data collection relative to its average value is an important parameter in error analysis. The variance s^2 is the usual measure for estimating distribution dispersion. Variance is the arithmetical mean value of all squares of deviations of particular values x_i from $\bar{x}$ the average value of the entire samples and can be defined by the formula (Kotulski and Szczepinski 2010):

$$s^2 = \frac{\sum(x_i - \bar{x})^2}{n-1}$$

(3.33)

The quantity s is called the standard deviation which determines the width of the distribution and can be calculated by:

$$s = \sqrt{s^2}$$

(3.34)

The uncertainty given by the manufacturer for all the measuring devices is ±2% for PROVA (AV M-07) anemometer, ≤±0.06°C for thermocouples and ≤±2% for flow meter. After the uncertainty of measured data have been accounted, the uncertainty for calculated results will also be quantified by using (Kline and McClintock 1953) method.

3.1.3.2 Surface state of the heated surface

Nanoparticles had been reported to precipitate or fouled on the heated surface or on the flow conduit wall which will significantly change the surface characteristics that can potentially affect the thermal performance as well. Conventional SiO_2 nanofluid (without surface coating) formed a fouling layer of nanoparticles on the heated surface after the boiling experiment and the fouling layer cannot be flushed away by water. However, for SiO_2 nanoparticles coated with silane, no fouling layer exists after the boiling process. The SEM images of heated surface are shown in Figure 3.6 (Yang and Liu 2010). As seen in Fig. 3.6, only scattered functionalized nanoparticles are observed on the heated surface which can be easily flushed away by water. Similar result was also shown by Chen et al. (2013) indicating that no deposition layer exists for functionalized nanofluid., In this study, the test has been repeated by using distilled water again after nanofluid experiment to check if the nanoparticle precipitation on the flow conduits will significantly change the surface characteristics that can potentially affecting the thermal performance of the solar collector. From the test, the results showed that there is no significant impact of using functionalized nanofluid on surface characteristics of solar collector. The results obtained by using distilled water after nanofluid experiment was similar to the one before nanofluid had been applied in the solar collector.
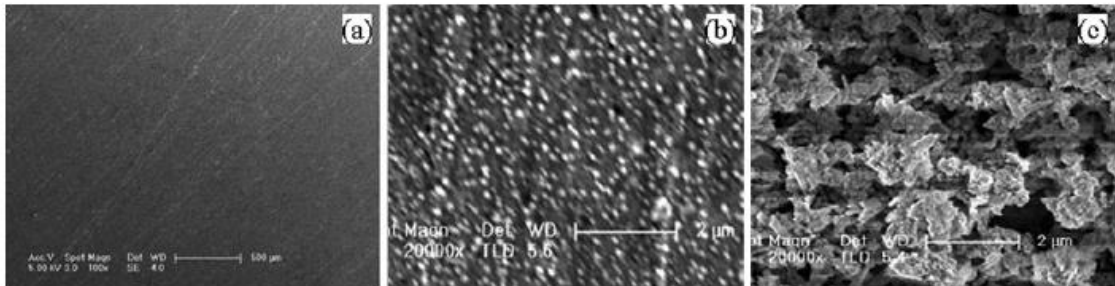
Figure 3.6: SEM images of the heated surface of (a) before the experiment, (b) using the functionalized nanofluid and (c) using the conventional nanofluid (Yang and Liu 2010).

3.1.3.3 Efficiency calculation from experimental data

The collector's thermal efficiency can be calculated from the ratio of useful energy to the energy incident on the collector. Flat-plate collectors can collect both direct and diffuse solar radiation. To predict and model the collector performance, information on the solar energy absorbed by the collector absorber plate is needed. The solar energy incident radiation on a tilted surface consists of beam, diffuse and ground-reflected radiation (Kalogirou 2009).

Beam and diffuse solar radiation will travels through the transparent cover. When the transmittance (τ) of the glazing increase, the absorber plate will have more radiation reached. The energy will be absorbed in a fraction equal to the absorbtivity (α) of the black absorber plate. Absorbtivity would be one for the perfect blackbody absorber. The instantaneous energy gained by the receiver can be determined by (Foster et al. 2009):

$$\dot{Q}_r = \dot{q}_r A_c = (\tau\alpha)_{eff} I_T A_c \tag{3.35}$$

The radiation will be absorbed and heat the absorber plate. Generally, solar collectors have great heat losses. The purpose of glazing is to prevent infrared-thermal energy to escape. However, the temperature difference between the absorber plate and the ambient causes heat losses by convection to the surroundings. This heat loss can be calculated by (Foster et al, 2010):

$$\dot{Q}_{conv} = \dot{q}_{conv} A_r = UA_r(T_r - T_a) \tag{3.36}$$

The heat lost by radiation can be calculated by (Foster et al, 2010):

$$\dot{Q}_{rad} = \dot{q}_{rad} A_r = \varepsilon_{eff}\sigma A_r(T_r{}^4 - T_a{}^4) \tag{3.37}$$

The heat losses from the bottom and from the edges of the collector are very small due to insulation and can be neglected. Combining the equations above, the useful energy collected can be represented as:

$$\dot{Q}_u = \dot{q}_u A_c = (\tau\alpha)_{eff} I_T A_c - UA_r\left(T_r - T_a\right) - \varepsilon_{eff}\sigma A_r(T_r{}^4 - T_a{}^4) \tag{3.38}$$

The important of all for this analysis is the heat-conducting fluid. The fluid will pass through pipes attached to the absorber plate. The fluid will absorb heat from the plate and as it flows through the pipes an increase in its temperature occur and will be carried for useful application. The thermal efficiency of a solar collector can be calculated as:

$$\eta = \frac{\dot{Q}_u}{I_T A_c} \tag{3.39}$$

To relate the collector's actual performance directly and in terms of the temperature of the useful heat energy from the circulating fluid, the efficiency and the useful heat gain can be calculated from:

$$\eta = F_R \left[(\tau\alpha)_{eff} - \frac{UA_r}{I_T A_c} (T_{in} - T_a) \right] \tag{3.40}$$

$$\dot{Q}_u = \eta I_T A_c = I_T A_c F_R \left[(\tau\alpha)_{eff} - \frac{UA_r}{I_T A_c} (T_{in} - T_a) \right] \tag{3.41}$$

The important useful heat gain by the working fluid can be expressed as:

$$\dot{Q}_u = \dot{m} C_p (T_{out} - T_{in}) \tag{3.42}$$

The heat capacity of water or nanofluid can be calculated by (Zhou and Ni 2008a):

$$C_{p,nf} = C_{p,np} (\varphi) + C_{p,bf} (1 - \varphi) \tag{3.43}$$

When there is no fluid flow, the temperature of the absorber can be defined as stagnation temperature (Singal, 2008):

$$T_{stag} = T_a + \frac{I_c F_R (\tau\alpha)_{eff}}{(F_R U_c) R} \tag{3.44}$$

From all these expressions, the useful heat gain and collectors efficiency can be calculated and compared between the conventional working fluid and proposed nanofluids.

3.1.3.4 Exergy calculation from experimental data

Exergy is the maximum output that can be achieved relative to the environment temperature. The general equation of the exergy balance is (Farahat et al. 2009; Suzuki 1988b):

$$\dot{E}_{in} + \dot{E}_{s} + \dot{E}_{out} + \dot{E}_{l} + \dot{E}_{d} = 0$$

(3.45)

Where $\dot{E}_{in}$ is the inlet exergy rate, $\dot{E}_{s}$ is the stored exergy rate, $\dot{E}_{out}$ is the outlet exergy rate, $\dot{E}_{l}$ is the leakage exergy rate and $\dot{E}_{d}$ is the destroyed exergy rate.

The inlet exergy rate measures the fluid flow and the absorbed solar radiation rate. The inlet exergy rate with fluid flow can be calculated by (Farahat et al. 2009)

$$\dot{E}_{in,f} = \dot{m}C_{p}\left(T_{in} - T_{a} - T_{a}\ln\left(\frac{T_{in}}{T_{a}}\right)\right) + \frac{\dot{m}\Delta P_{in}}{\rho}$$

(3.46)

Where ΔP_{in} is the pressure difference of the fluid with the surroundings at entrance and ρ is the fluid density.

The absorbed solar radiation exergy rate can be calculated as:

$$\dot{E}_{in,Q} = \eta I_{T} A_{P}\left(1 - \frac{T_{a}}{T_{s}}\right)$$

(3.47)

Where is apparent sun temperature and equals to 75% of blackbody temperature of the sun (Bejan et al. 1981).

Total inlet exergy rate of the solar collector can be calculated as:

$$\dot{E}_{in} = \dot{E}_{in,f} + \dot{E}_{in,Q}$$
(3.48)

At steady state conditions, where the fluid is flowing, the stored exergy rate is zero.

$$\dot{E}_s = 0$$
(3.49)

When only the exergy rate of outlet fluid flow is considered, the outlet exergy rate can be defined as (Kotas 1995):

$$\dot{E}_{out,f} = -\dot{m}C_p\left(T_{out} - T_a - T_a \ln\left(\frac{T_{out}}{T_a}\right)\right) + \frac{\dot{m}\Delta P_{out}}{\rho}$$
(3.50)

The heat leakage from the absorber plate to the environment can be defined as the leakage exergy rate and calculated as (Gupta and Saha 1990):

$$\dot{E}_l = -UA_P(T_P - T_a)\left(1 - \frac{T_a}{T_p}\right)$$
(3.51)

The destroyed exergy rate caused by the temperature difference between the absorber plate surface and the sun can be expressed as (Gupta and Saha 1990):

$$\dot{E}_{d,\Delta T_S} = -\eta I_T A_P T_a\left(\frac{1}{T_p} - \frac{1}{T_s}\right)$$
(3.52)

The destroyed exergy rate by pressure drop is expressed by (Suzuki 1988b):

$$\dot{E}_{d,\Delta P} = -\frac{\dot{m}\Delta P}{\rho} \frac{T_a \ln\left(\dfrac{T_{out}}{T_a}\right)}{\left(T_{out} - T_{in}\right)} \tag{3.53}$$

The destroyed exergy rate caused by the temperature difference between the absorber plate surface and the agent fluid can be calculated from (Suzuki 1988b):

$$\dot{E}_{d,\Delta T_f} = -\dot{m}C_p T_a \left(\ln\left(\frac{T_{out}}{T_{in}}\right) - \frac{\left(T_{out} - T_{in}\right)}{T_p} \right) \tag{3.54}$$

So, the total destroyed exergy rate can be calculated from:

$$\dot{E}_d = \dot{E}_{d,\Delta T_S} + \dot{E}_{d,\Delta P} + \dot{E}_{d,\Delta T_f} \tag{3.55}$$

The exergy destruction rate can also be expressed from:

$$\dot{E}_d = T_a \dot{S}_{gen} \tag{3.56}$$

where $\dot{S}_{gen}$ is the overall rate of entropy generation and can be calculated from (Bejan 1996):

$$\dot{S}_{gen} = \dot{m}C_p \ln\frac{T_{out}}{T_{in}} - \frac{\dot{Q}_S}{T_S} + \frac{\dot{Q}_O}{T_a} \tag{3.57}$$

where $\dot{Q}_S$ is the solar energy rate absorbed (W) by the collector surface as expressed by (Esen 2008)

$$\dot{Q}_S = I_T(\tau\alpha)A_P \tag{3.58}$$

And $\dot{Q}_O$ is the heat loss rate to the environment (W),

$$\dot{Q}_O = \dot{Q}_S - \dot{m}C_P(T_{out} - T_{in}) \tag{3.59}$$

Ultimately, combining all the expression above, the exergy efficiency equation of the solar collector can be analyzed (Farahat et al. 2009):

$$\eta_{ex} = \frac{\dot{m}\left[C_p\left(T_{out} - T_{in} - T_a \ln\left(\frac{T_{out}}{T_{in}}\right)\right) - \frac{\Delta P}{\rho}\right]}{I_T A_p \left(1 - \frac{T_a}{T_s}\right)}$$

(3.60)

3.2 The flow and heat transfer performance of flat-plate solar collectors with nanofluid

3.2.1 Pumping power

In this system, an electrical powered pump is required to pump the working fluid throughout the collector. To analyze the pumping energy needed by the system, expressions from (Garg and Agarwal 1995; White 2003) were used. It had been proven and well known for more than 100 years that thermal conductivity of a fluid can be enhanced by suspending millimeter or micrometer sized particles (Lee et al. 1999). However, it is not practical to use them because of problems such as sedimentation, erosion and increased pressure drop. The introduction of nanometer sized particles in the industry is believed to be able to overcome all these problems. The pressure drop in the system can be calculated from:

$$\Delta p = f \frac{\rho V^2}{2} \frac{\Delta L}{D} + K \frac{\rho V^2}{2}$$

(3.61)

Where f is the friction factor, K is the loss coefficient and D is the diameter of the pipe. V is the velocity (m/s) of the working fluid and can be calculated from:

$$V = \frac{\dot{m}}{\rho_{nf} \pi D^2 / 4}$$

(3.62)

Density of nanofluids is one of the most important thermo physical properties. Density of nanofluids will give direct impact on the pressure drop and pumping power of solar collector. Density of nanofluids will normally only be affected by the material of nanoparticle being used. Other factors such as shape, size, zeta potential and surfactants will not directly change the density of nanofluids (Timofeeva et al. 2011). The density of nanofluid can be calculated from:

$$\rho_{nf} = \rho_{np}(\varphi_n) + \rho_{bf}(1 - \varphi_n)$$

(3.63)

For the SiO_2 nanofluids used in this study, the density was measured by using a density meter KEM-DA 130N for both 0.2% and 0.4% concentration. This density meter can measure the density of fluid between 0 to 2000 kg/m^3 with uncertainty of ±0.001 kg/m3. The measured densities will then be compared with Equation (3.63) above.

The friction factors for laminar flow (Re $\leq$ 2 x 10^5) and turbulent flow (Re $\leq$ 2 x 10^5) can be calculated from (3.64) and (3.65) respectively (Bergman et al. 2011; Kahani et al. 2013):

$$f = \frac{64}{Re}$$
for laminar

(3.64)

$$f = \frac{0.079}{(Re)^{1/4}}$$
for turbulent

(3.65)

Another good parameter for fluid flow is the Reynolds number that was popularized by Reynolds Osborne (1842-1912) who was an English engineer that investigated flow in pipes (Cengel and Cimbala 2006). Based on mean velocities, Reynolds developed viscous flow equation. The Reynolds number can be expressed as:

$$\text{Re} = \frac{\rho V D}{\mu} \tag{3.66}$$

where μ is the viscosity of the working fluid (0.0008 kg/m s for water) and the viscosity of nanofluid can be calculated as (Einstein 1956):

$$\mu_{nf} = (1 + 2.5\varphi_n) \times \mu_{bf} \tag{3.67}$$

However, Einstein's theoretical equations to calculate density of fluid are only applicable to Newtonian fluids while nanofluids often displayed non-Newtonian rheological behavior. Therefore, viscosity of nanofluids in this study for different concentration and temperatures was measured by using LVD-III ultra-programmable rheometer (Brookfield, USA). The rheometer's calibrated spring can measure viscosity ranging from 1 to 6 x 10^6 MPa.s. The Brookfield ultra-low adapter (ULA) with spindle model ULA-49EAY code 01 has been used in this experiment. Viscosity of the fluid is directly related to pressure drop which in turn related to pumping power.

Finally, the pumping power can be calculated from:

$$\dot{W}_{pumping} = \left(\frac{\dot{m}}{\rho_{nf}} \right) \times \Delta p \tag{3.68}$$

Where $\dot{m}$ is mass flow rate, ρ_{nf} is density of nanofluid and Δp is the pressure difference.

3.2.2 Heat transfer

The major drawback of the flat-plate solar collectors is high heat losses from the absorber plate to surroundings and reducing the useful energy gain of the system. The enhancement of heat transfer rate in solar collectors could improve the overall performance of the heating system. Enhancement of heat transfer rate can be achieved by increasing the heat transfer coefficient by disrupting boundary layer, increasing the Reynolds number or increasing the temperature gradient.

Heat transfer will occur whenever there is temperature difference. In a solar collector system, water is normally used as heat transfer fluid. To improve the heat transfer characteristics of working fluids in the system, the key to it is to improve the thermal conductivity of the fluid. Solid particle has a larger thermal conductivity than water. So, by dispersing nano size particles into the fluid, it is expected to increase the thermal conductivity of that fluid. Heat transfer that occurs between the pipes surfaces and a flowing fluid refers to heat transfer by convection. The convective heat transfer coefficient in this study can be calculated from:

$$h = \frac{Q_u}{A_p(T_p - T_b)}$$

(3.69)

Where T_b is the bulk temperature and can be calculated from:

$$T_b = \frac{T_{in} + T_{out}}{2}$$

(3.70)

The heat transfer coefficient can also be calculated from (Li et al. 2003)

$$h = \frac{q}{T_p - T_{nf}}$$

(3.71)

Where q is the heat flux (W/m^2).

From there, the Nusselt number can be calculated:

$$Nu_{nf} = \frac{h_{nf}D}{k_{nf}}$$

(3.72)

In the area of heat transfer analysis, Nusselt number is one of the important dimensionless quantities to quantify. It was developed by Nusselt Wilhem (1882-1957) who was a German engineer that applied similarity theory to heat transfer. Nusselt number can be defined as the ratio of convection to conduction heat transfer at a surface of a fluid. For the laminar flow of circular pipe, the Nusselt number can be calculated from Reynolds and Prandtl number expressed by (Owhaib and Palm 2004):

$$Nu = 0.000972\mathrm{Re}^{1.17}\,\mathrm{Pr}^{1/3} \quad \text{for Re} < 2000$$

(3.73)

The Prandtl number is a dimensionless quantity that is often found in property tables alongside other properties such as viscosity and thermal conductivity. It was named after Prandtl Prandtl Ludwig (1875-1953) who was a German engineer that developed the boundary layer theory. Prandtl is considered the founder of modern fluid mechanics. Prandtl developed the relationship between viscous diffusion and thermal diffusion. Prandtl number can be calculated from:

$$Pr = \frac{C_{p,nf}\,\mu_{nf}}{k_{nf}}$$

(3.74)

Thermal conductivity can be expressed by:

$$\frac{k_{nf}}{k_f} = \frac{k_p + (SH-1)k_f - (SH-1)\varphi(k_f - k_p)}{k_p + (SH-1)k_f + \varphi(k_f - k_p)}$$

(3.75)

Where SH is the shape factor and assuming the spherical shape of nanoparticle, the factor can be taken as 3 (Li et al. 2013).

3.3 The economic and environmental impact of solar collector utilizing nanofluid

In household energy usage, a large portion of energy consumption is used to heat water for shower, cooking or washing. In Malaysia, the average energy demand for water heating is around 11.03% (Lalchand 2012). Most of this heat energy demand is supplied by electrical energy or burning of petroleum gas that will contribute to environmental problems. Solar thermal energy is an unlimited and free source of energy that can meet the world's future energy needs without harming the earth. Switching to solar water heating system will reduce the greenhouse gas and smog forming emissions from the combustion of fossil fuels in addition to economic advantage of the system.

Economic and environmental impact of solar collectors can be assessed by using life cycle assessment (LCA) method. Tsillingiridis et al. (2004), Ardante et al. (2005) and Kalogirou (2008) are some example of many researchers that have used life cycle assessment methods on solar hot water heating systems to evaluate the economic and environmental impact of it. However, all these studies were focusing on solar water heating system in European countries with more emphasize were put on the environmental impact. The life cycle assessment method can effectively be used to evaluate the impact of manufacturing solar collectors on environment from initial resources to its disposal after being used by consumer. The life cycle assessment in this study focuses on the embodied energy of manufacturing and the operation of the solar

collector. Only energy used to manufacture the solar collector is considered where else the distribution, maintenance and disposal phase of the collectors are neglected. According to Ardante et al. (2005), more than 70% of the embodied energy of the system comes from the manufacturing of the collector. The analysis was done with the reduction of collector area as the functional unit that influences the overall weight and embodied energy of the collector. By using the thermal efficiency data of solar collector, the potential of reduction of the size of collector's area can be estimated by:

$$A_p = \frac{\dot{m}C_p(T_{out} - T_{in})}{I_T\eta}$$

(3.76)

Two major materials that are being used in solar collector are glass and copper with the weight ratio of 27 kg glass and 9 kg copper for a 36 kg collector. The embodied energy index is 15.9 MJ/kg and 70.6 MJ/kg for glass and copper respectively (Otanicar et al. 2010). By using the result of size reduction, the weight and the embodied energy for solar collector can be calculated accordingly.

The results of the thermal performance of nanofluid solar collector and size reduction can also be used to estimate the cost saving. By using nanofluid as working fluid in solar collector, large portion of copper and glass used in the system can be eliminated based on the scaling of the overall percentage weight of the collector. The capital cost of the collector will then be offset by the cost of the nanoparticles. The energy usage per day in conjunction with the local electricity rates based from RM 0.218 per kWh for the first 200 kWh and RM 0.334 for subsequent hour is used to determine the amount saved by using solar thermal system. The electricity rates used throughout this study were based on the TNB tariff in the year 2013.

Burning of fossil fuels to generate the energy to heat water will result in harmful gas emissions. Switching to solar hot water system can reduce that problem. The distribution of electricity from various fuel types and the key pollutants generated in Malaysia is shown in Table 3.2.

Table 3.2: Electricity generation by fuel type and primary emissions mix for Malaysia (Sustainable Energy Development 2010)

Fuel	% of Electricity generated	Carbon dioxide, CO_2 (kg/MJ)	Sulfur oxides, SO_x (kg/MJ)	Nitrogen oxides, NO_x (kg/MJ)
Coal	36.5	0.274	0.00031	0.0005
Oil	0.2	0.220	0	0
Natural gas	55.9	0.113	0	0.00003
Hydro	5.6	0	0	0
Others	1.8	0	0	0

With the data of embodied energy index of solar collector achieved, the emissions from the manufacturing of the collectors can be determined. The offset damage costs can be calculated for the three main pollutants of CO_2, NO_x and SO_x based on the damage cost factors (Spardo and Rabl 1999). These offset damage cost are not costs directly applicable to the collector owner. The results will be shown in Chapter 4 section next.

CHAPTER 4: RESULTS & DISCUSSION

4.1 The thermodynamics performance of flat-plate solar thermal collector utilizing SiO$_2$ nanofluid

4.1.1 Density of nanofluids

Density of the working fluid in solar collector is a very important thermo physical property and must be accounted. Before experimental investigation was carried out, analytical analyses had been made on 4 types of metal oxides nanofluids including SiO$_2$, CuO, TiO$_2$ and Al$_2$O$_3$ to form a basis in theoretical comparison. Figure 4.1 shows the calculated theoretical density from Eq. (3.4) of various types of metal oxides nanofluids. As portrayed, density of nanofluids is proportional to volume fraction of nanoparticles. In all cases, nanofluid gave higher density than water. It can be explained by Eq. (3.4) and data from Table 2.3 where density of nanofluids will increase by increasing the volume fraction of nanoparticles. Nanoparticles have higher density than water and dispersing it in base fluid gave higher density than the base fluid. Figure 4.1 also shows that CuO nanofluids have the highest possible density compared to other fluids based on the higher density of CuO nanoparticles. The trend in these results are also similar to studies by Pandey and Nema (2012).
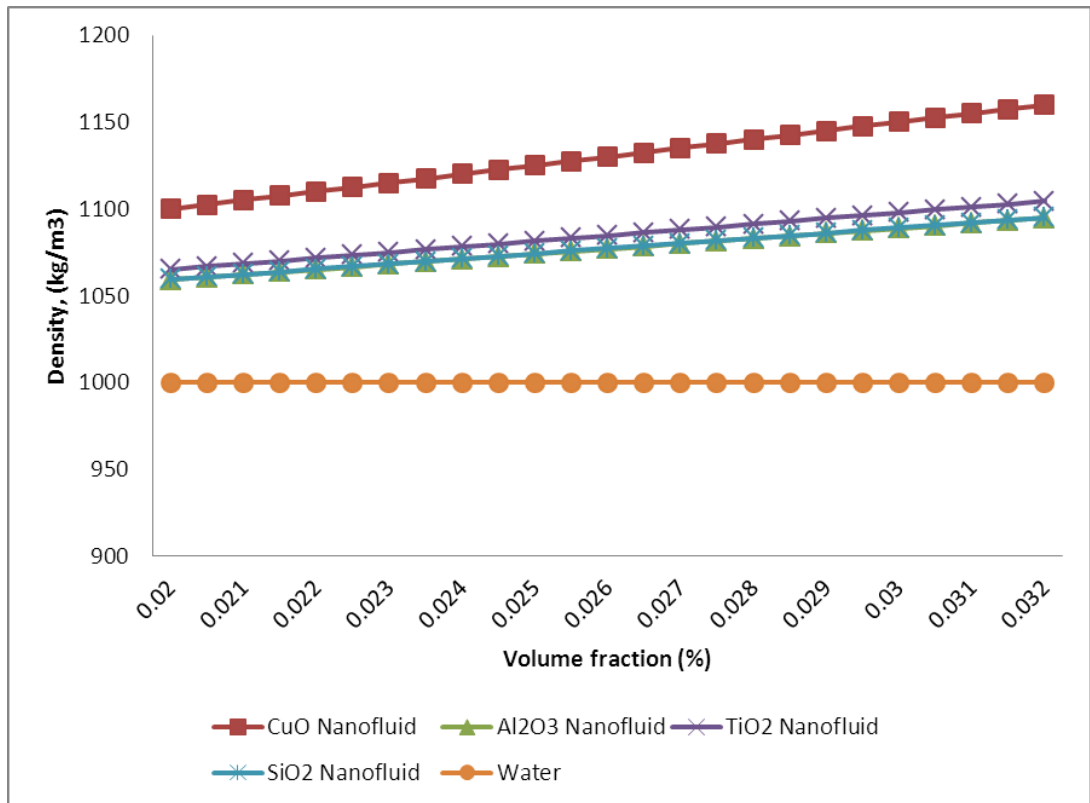
Figure 4.1: Effect of varying volume fraction to the density of working fluids

For SiO$_2$ nanofluids that were used specifically in this study, the densities for 0.2% to 1.0% volume fraction SiO$_2$ nanofluids were measured by using KEM-DA 130N density meter. The measured densities are then compared with the theoretical model from Eq. (3.4). The values of the densities of SiO$_2$ nanofluids were measured at temperature 30°C. The measured density and the theoretical density are displayed in Figure 4.2. It can be seen that the measured nanofluid densities present almost similar values and only small average deviation of 4.5% can be detected from the theoretical model.
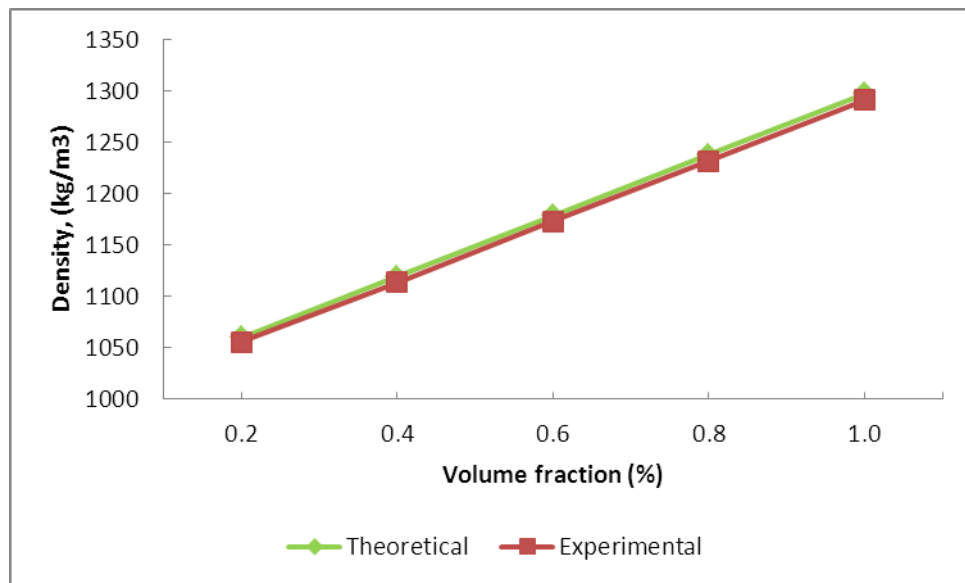
Figure 4.2: Comparison of measured density of SiO$_2$ nanofluids used in this study with theoretical calculation

4.1.2 Specific heat

Specific heat of nanofluid must be determined to study the performance of solar collectors. Figure 4.3 shows that the theoretical values of specific heats of various nanofluids are inversely proportional to volume fraction of nanoparticles as calculated from Eq. (3.3). Similar results had also been shown by other researchers like Pandey and Nema (2012), Kamyar et al. (2012b) and Sohel et al. (2013). Substitution of lower value of specific heats of nanoparticles from Table 2.3 will decrease the overall specific heats of nanofluids as stated in Eq. (3.3). Specific heat can be explained as the energy required raising the temperature of a unit mass of a substance by one degree. It means that a different amount of heat energy is needed to raise the temperature of similar

masses of different substances by one degree. Smaller number of specific heats for nanofluids will leads to smaller amount of energy needed to raise the temperature of it. Hence, output temperature for solar collectors using nanofluids will rise and lead to higher efficiency of the system.
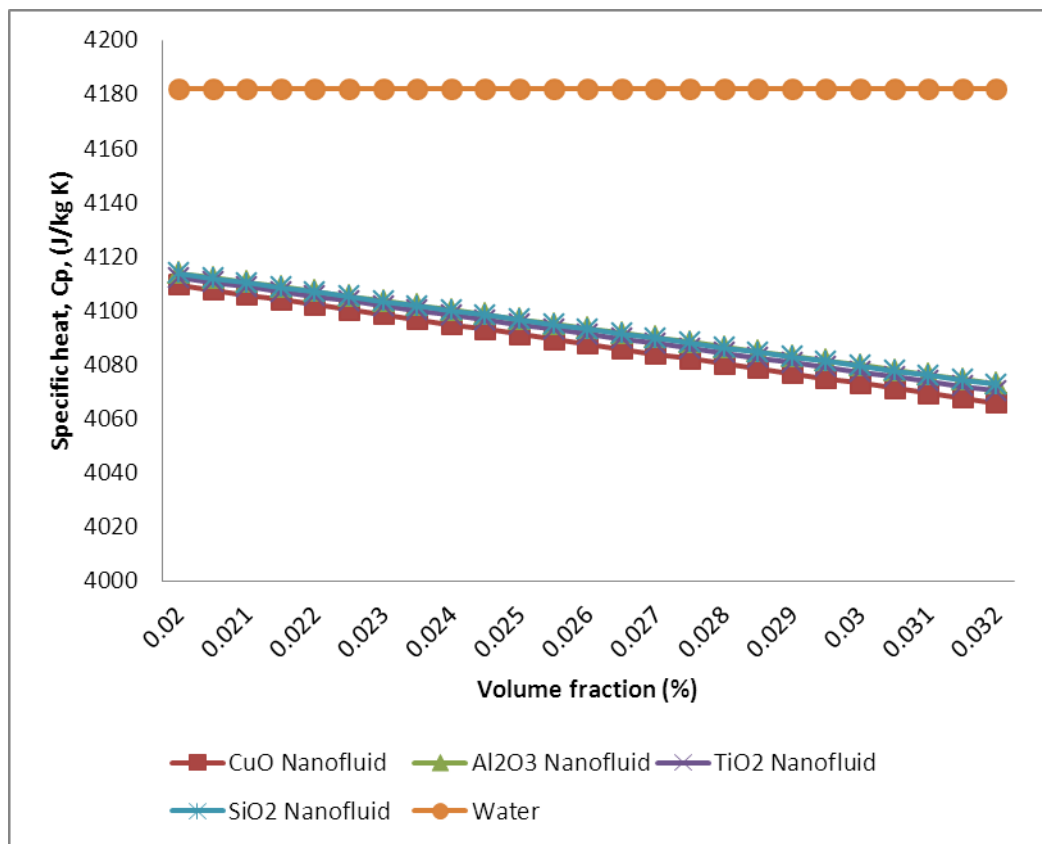
Figure 4.3: Effect of varying volume fraction to the specific heat of working fluids

The specific heat for SiO_2 nanofluids used in this study was measured by using DSC 4000, Perkin Elmer differential Scanning Calorimeter. The measured specific heats are then compared with the theoretical model from Eq. (3.3). Measured values of the heat capacity of nanofluids at temperature 30°C and the theoretical heat capacity are

displayed in Figure 4.4. It can be seen that the measured nanofluid capacities present almost similar values and only small deviation of 2.4% can be detected from the theoretical model.
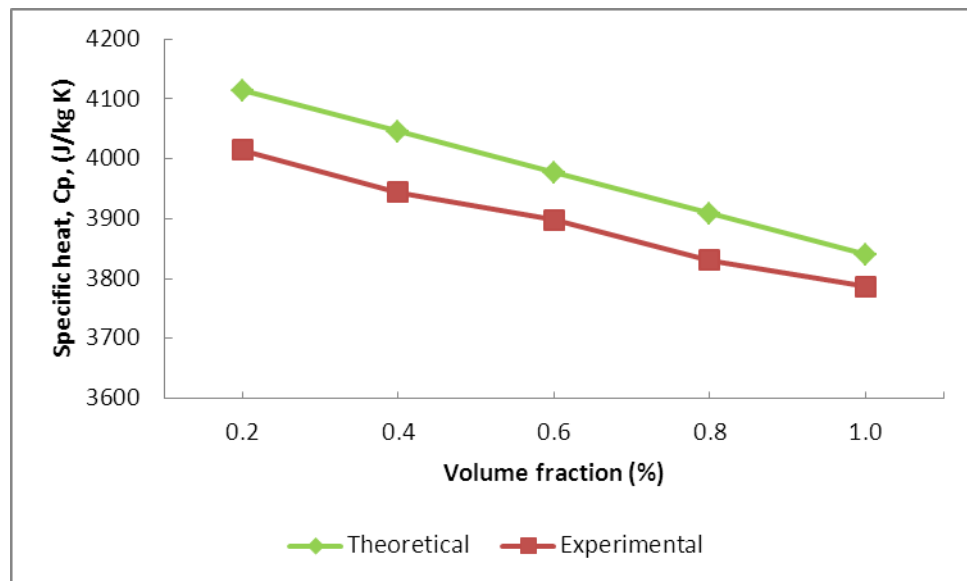
Figure 4.4: Comparison of measured specific heat of SiO$_2$ nanofluids used in this study with theoretical calculation

4.1.3 Efficiency analysis

The thermal efficiency of solar collectors was calculated from the ratio of useful energy to the energy incident on the collector. Figure 4.5 presented the theoretical values of efficiency for various types of nanofluids including CuO, Al$_2$O$_3$, SiO$_2$ and TiO$_2$ based nanofluids. Figure 4.5 shows that efficiency of nanofluids is proportional to

the volume fraction of nanoparticles. In Eq. (3.2), the important useful heat gain by the working fluid is calculated and the value is then substituted in Eq. (3.8) to determine its efficiency. As shown in Figure 4.5, the efficiency of solar collector increased by 38.5% by using CuO nanofluid and 28.8% for Al_2O_3, SiO_2 and TiO_2 nanofluids compared to water as working fluid. These results are in good agreement with experimental results by other researchers like Yousefi et al. (2012c) and Tyagi et al. (2009).

There are reasons for the higher efficiency of nanofluids solar collector compared to water. One of it is the higher output temperature associated with nanofluids solar collector (Yousefi et al. 2012a; Yousefi et al. 2012b; Yousefi et al. 2012c). Output temperature of solar collector can be influenced by the specific heat of working fluids. As seen in Table 2.3, nanoparticles and nanofluids have lower specific heat than water and Copper have the lowest value of all others. Because of that, less heat is required to raise the temperature of nanofluids and thus making the output temperature and efficiency becomes higher (Kamyar et al. 2012b; Sohel et al. 2013).
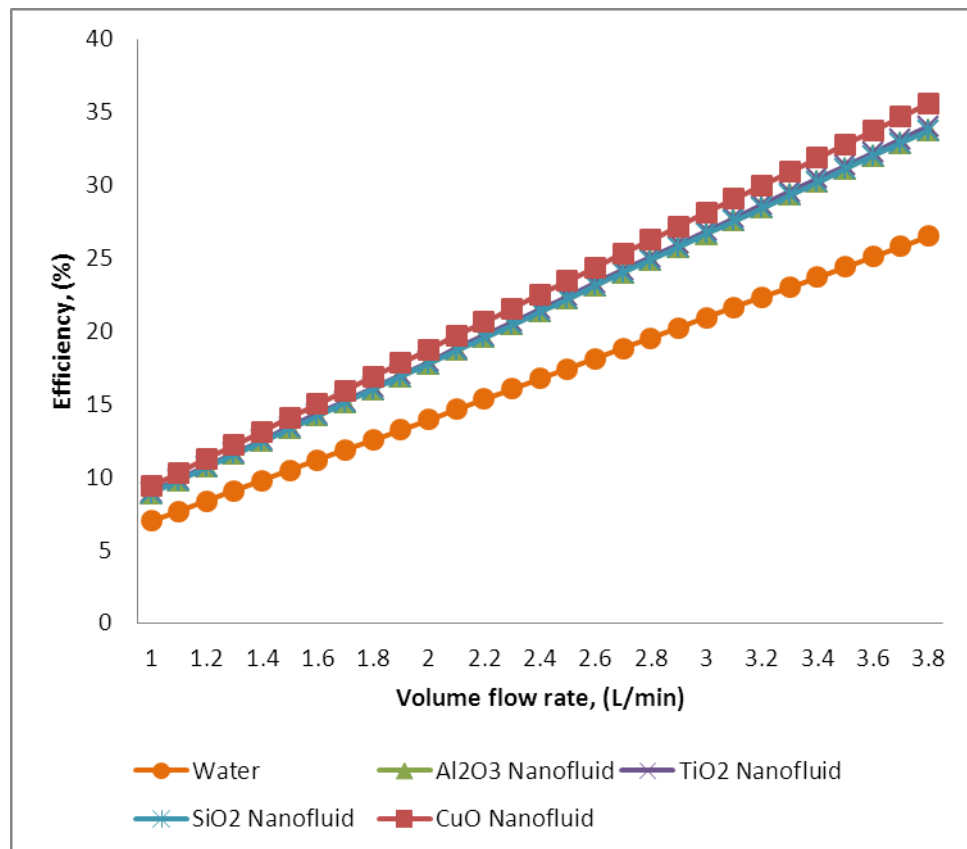
Figure 4.5: Effect of varying volume fraction to the efficiency of working fluids

The experimental results include the performance of solar collector using water and SiO_2 nanofluids at various concentrations and volume flow rates. The tests were performed around solar noon at 10 am to 3 pm. Figure 4.6 shows the effect of the volume flow rate of the working fluid on the efficiency of the solar collector. The volume flow rates of the working fluid were regulated to keep in between 1 - 3 L/min. For a steady state condition in compliance with ASHRAE Standard, the maximum variation in mass flow rate was kept at (<1%). The uncertainty for collector efficiency calculation at various tests was around 4.1% including both measurement and scatter uncertainties and was quantified by using Kline and McClintock method (Kline and McClintock 1953).
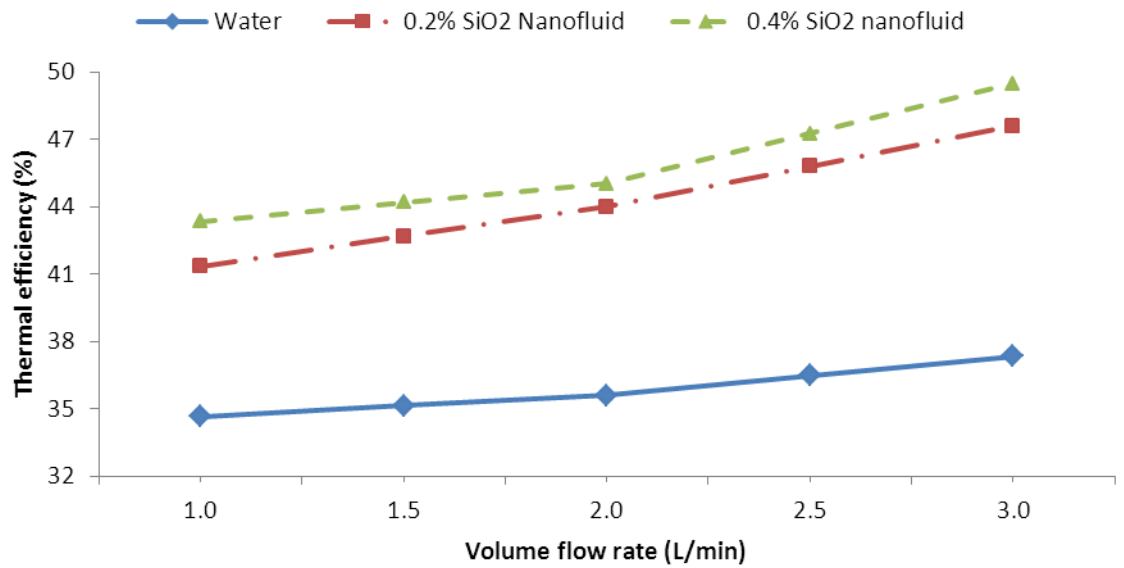
Figure 4.6: Effect of volume flow rates of working fluids on the efficiency of the solar collector.

As shown in Figure 4.6, the efficiency of the solar collector with SiO_2 nanofluids is higher than that of the water while the efficiency is increased by increasing the volume flow rates. There are some reasons for the higher efficiency of nanofluids solar collector compared to water. One of it is the higher output temperature associated with nanofluids solar collector (Yousefi et al. 2012a; Yousefi et al. 2012b; Yousefi et al. 2012c). The efficiency of solar collector increased by 23.5% by using 0.2% SiO_2 nanofluid. However, only an increase of around 3.7% was achieved by adding the concentration to 0.4% compared to 0.2% concentration nanofluid. The similar findings were reported from an experimental investigation on Al_2O_3 nanofluid by (Yousefi et al. 2012c) where the absorptance of 0.2 wt% nanofluid is higher than 0.4 wt% in lower temperature difference, but lower in higher temperature differences. This phenomenon

had been explained by some investigators (i.e., Rojas et al., 2008; (Zhou and Ni 2008a);(Vatanpour et al. 2011). However, higher temperature increased the speed of molecules and collisions between the nanoparticles that increased the thermal conductivity for higher concentration nanofluid (Das and Choi 2009). Comparison of results obtained for thermal efficiency from this study with other researches is shown in Table 4.1.

Table 4.1: Comparison of results obtained for thermal efficiency from this study with other researches.

Researcher	Solar thermal system	Nano particle	Efficiency improvement
(Otanicar 2009)	micro-solar-collector	Diversity of nanoparticles	5%
(Taylor et al. 2011)	high flux solar collectors	Graphite	10%
(Yousefi et al. 2012c)	flat-plate solar collector	Aluminium (III) Oxide (Al2O3)	28.30%
(Lenert and Wang 2012)	concentrated solar power	Carbon coated cobalt (C-Co)	35%
(Zamzamian et al. 2014)	flat-plate solar collector	Copper (Cu)	28.60%
This study	flat-plate solar collector	SiO2	23.50%

4.1.4 Exergy analysis

The exergy analysis of a flat plat solar collector using different nanofluid was carried out in the present study to evaluate the enhancement of exegetic efficiency with comparison to a conventional collector. Figure 4.7 shows the behaviour of the exergy efficiency as a function of the volume fraction of nanofluid as calculated from Eq. (3.60). The analysis represents that the lowest efficiencies belong with the collector, operated by water; therefore, a large amount of irreversibility belonged with the

traditional solar collector. By using nanofluid in solar collector, exergy efficiency can be increased. CuO nanofluid may be a good choice as an absorbing medium because of their exergy efficiency is higher than the other considering nanofluid and water. From Hamilton and Crosser model (Hamilton and Crosser 1962), it is stated that the thermal conductivity of nanofluid is directly related to the volume fraction and the shape of the nanoparticle. It can be explained that addition of more particles leads to increased effective surface area for heat transfer. Additionally, the inherently higher thermal conductivity of nanoparticles will improve the thermal conductivity of the nanofluid. This may cause an improvement in exergy efficiency. For a fixed volume flow rate, solar collector with CuO nanofluid had implied highest exergy efficiency. Its maximum value is higher than the conventional solar collector by 15.52%. Al_2O_3 and SiO_2 showed approximately same exergy but higher than water, besides TiO_2 may provide a good exergy with comparison to water, Al_2O_3 and SiO_2 nanofluids, although it carry more cost than water. Thus, the analytical results indicated that in flat plate solar collector, there is a definite probability to get maximum exergy by using nanofluid as agent medium. The possible reason for this enhancement may be associated with the following: (I) the nanofluid with suspended nanoparticles increases the thermal conductivity of the mixture and (II) it is also known that the convective heat transfer coefficient of the nanofluid is higher than that of the base fluid (water) at a given Reynolds number. The results complied with those obtained from Duangthongsuk and Wongwises (2009), Xuan and Li (2003a) and He et al. (2007). Exergy efficiency is calculated from Eq. (3.60). According to this equation, mass flow rate and specific heat might have great impact on exergy efficiency of solar collector with considering collector absorber area as constant.
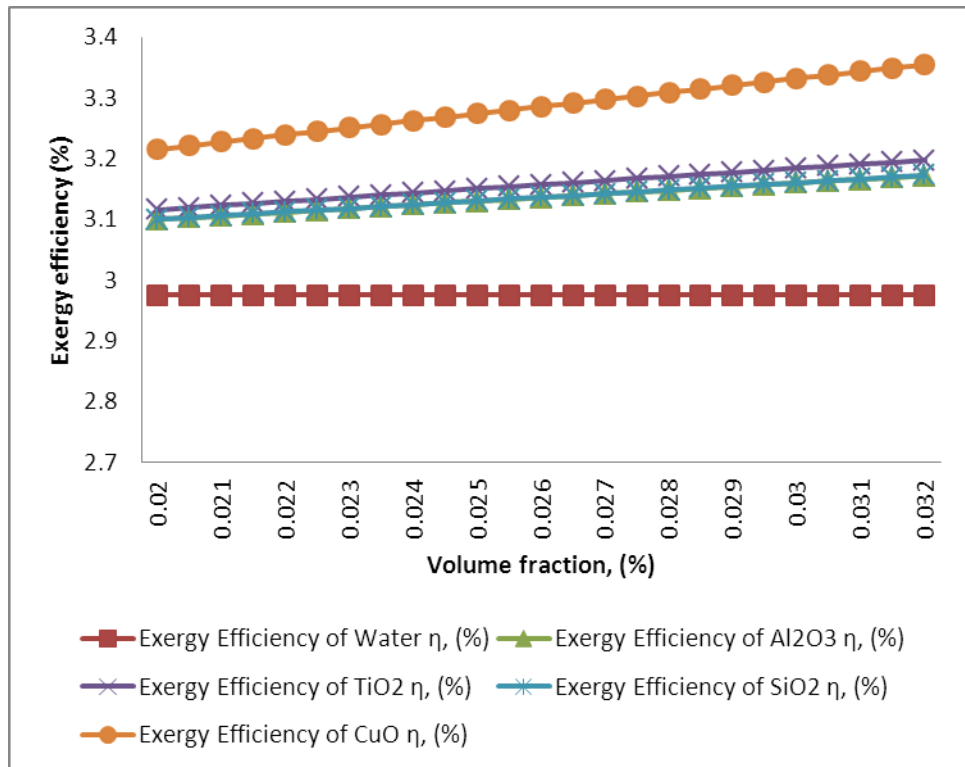
Figure 4.7: Effect of varying volume fraction to the exergy efficiency of working fluids

Figure 4.8 shows the exergy efficiency of various flow rates with different working fluid types for the flat-plate solar collector experiment. Based on the efficiency equations (3.39) and (3.42) as well as efficiency data shown in Figure 4.6, increasing mass flow rate will increase the exergy efficiency of the system. Adding more SiO_2 nanoparticles to the system, from 0.2% to 0.4% can produce higher exergy efficiency than the water. The uncertainty for collector exergy efficiency calculation at various tests was around 8.5%. The results indicate that in solar collector, there is a definite probability to get maximum exergy by using SiO_2 nanofluid as medium. The possible reason for this enhancement may be associated with the increase in thermal conductivity of the mixture and higher convective heat transfer coefficient of nanofluid. The results

complied with those obtained from Duangthongsuk and Wongwises (2009), Xuan and

Li (2003b) and He et al. (2007).
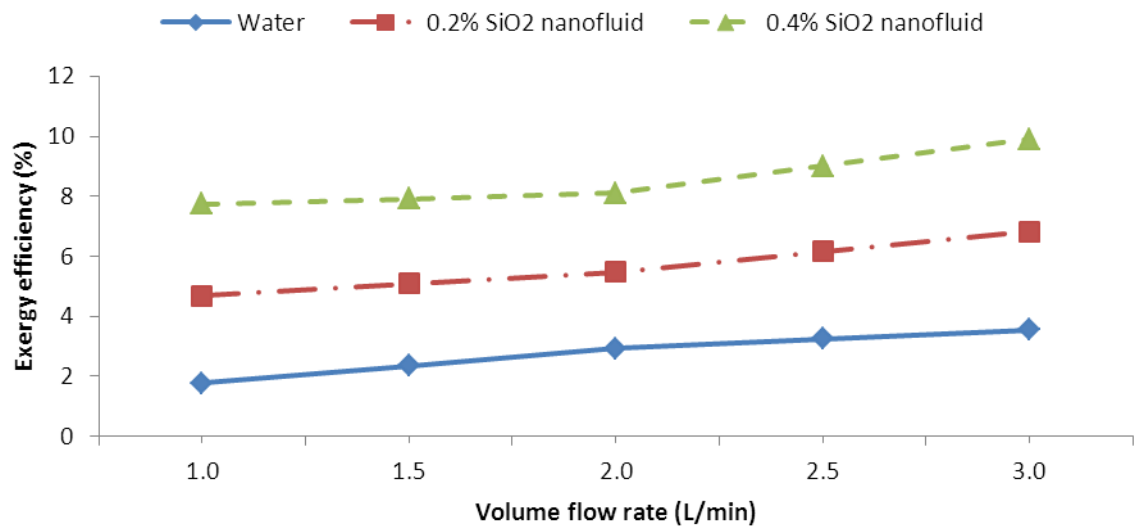
Figure 4.8: Effect of volume flow rate of working fluid on the exergy efficiency of the solar collector.

4.1.5 Exergy destruction and entropy generation

The exergy destruction and entropy generation rates are presented in Figure 4.9. As shown in the figure, the rates decreased by increasing the volume flow rates for all types of the working fluids. Exergy is the maximum output potential that can be achieved by a system relative to the dead state or environment temperature. Exergy efficiency implied how close the performance of the system had achieved relative to its theoretical limit. Exergy destruction however, is the cause of a system not achieving its maximum capabilities and it can be avoided. This exergy destruction, if minimized and managed further, can increase the energy and exergy efficiency of the system even more. Adding nanoparticles in the base fluid can be seen to lower down the entropy

generation and exergy destruction. Thermal conductivity and heat absorption rate increases with the increment of nanoparticles volume fraction and thus result in reduction of entropy generation and exergy destruction. Although adding nanoparticles in the fluid will increase the viscosity and fluid friction that will lead to increase of the entropy generation in the system, but, entropy generation will decrease far greater than fluid friction due to the gap of contribution of heat transfer. Similar result was reported by Mahian et al. (2012).
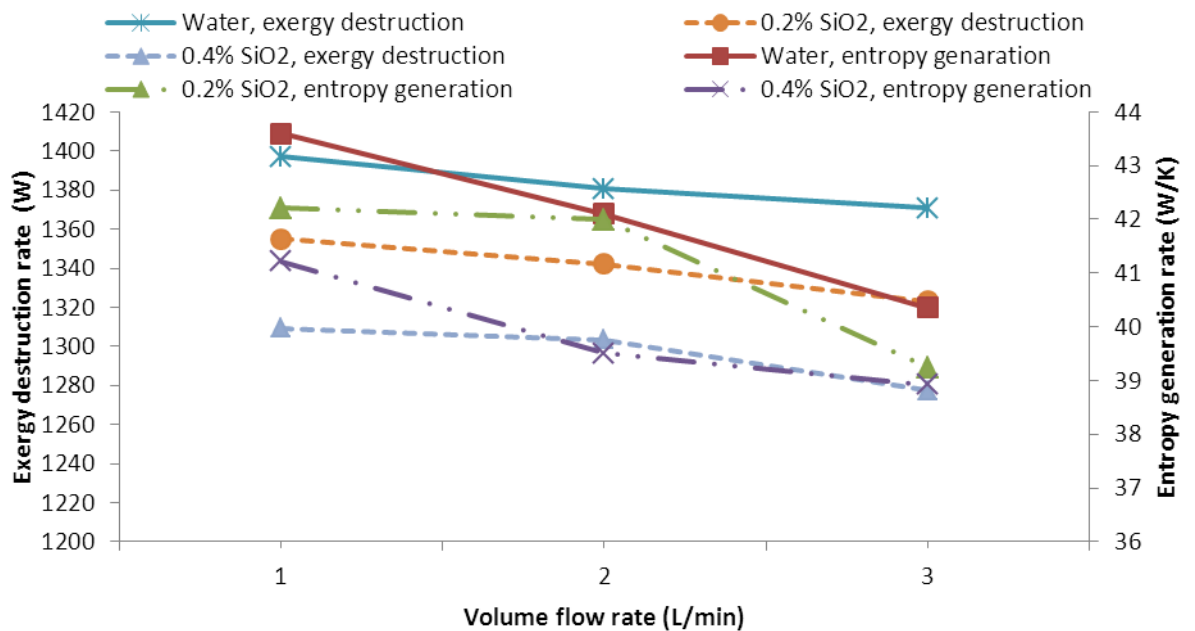
Figure 4.9: Effect of volume flow rate of working fluid on the exergy destruction and entropy generation of the solar collector.

4.2 The flow and heat transfer performance of flat-plate solar collectors with nanofluid

4.2.1 Heat transfer and fluid flow

Figure 4.10 illustrates the effect of SiO_2 nanoparticles concentration and volume flow rate on the heat transfer coefficient. The uncertainty for collector heat transfer coefficient calculation at various tests was around 4.9%. Enhanced heat transfer coefficient is observed in the results by increasing the volume flow rate after adding SiO_2 nanoparticles in the base fluid due to the improvement of thermal conductivity of nanofluids as shown in (Table 2.3). Liquids have relatively low heat transfer properties and adding small amount of solid nanoparticles with higher heat transfer properties will enhance the thermal conductivity of the fluid.
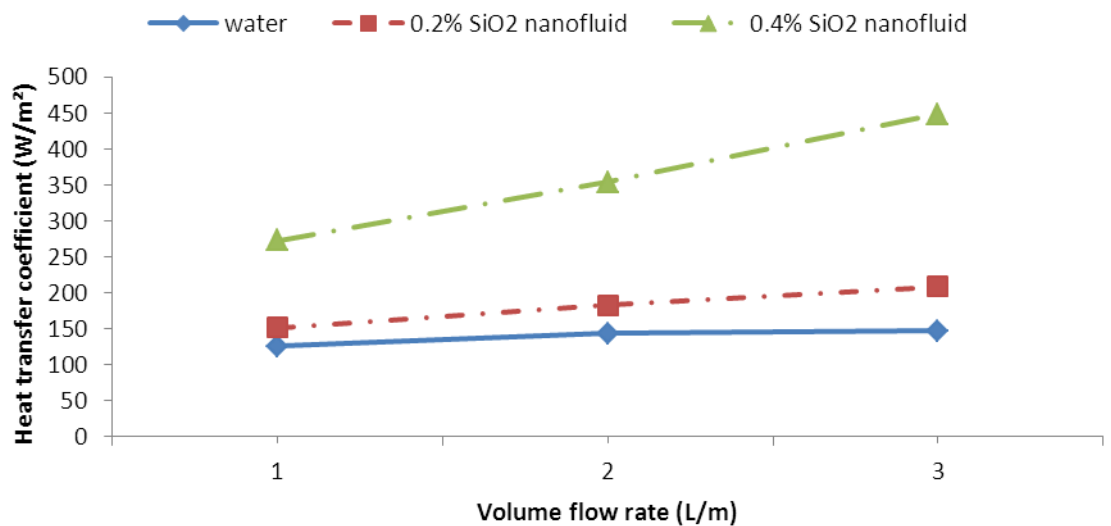
Figure 4.10: Effect of volume flow rates of working fluids on the heat transfer coefficient of the solar collector.

Thermal conductivity is normally proportional to the heat transfer coefficient. Jiang et al. (2014) indicated that for an identical nusselt number condition, heat transfer coefficient of a fluid is higher when the thermal conductivity of the fluid becomes higher. At higher particle volume fraction, higher convective heat transfer coefficient was observed. Suspension of thermal boundary layer formation and disturbance of the SiO_2 nanoparticles in the mixture could also rise at higher concentration of nanofluid and therefore resulting in higher heat transfer coefficient. Comparison of results obtained for heat transfer coefficient from this study with other researches is shown in Table 4.2.

Table 4.2: Comparison of results obtained for heat transfer coefficient with other researches.

Researcher	Nanoparticles	Heat transfer coefficient increase by
Kim et al. (2009)	amorphous carbonic	8%
Hwang et al. (2009)	Al_2O_3	8%
Duangthongsuk and Wongwises (2010)	TiO_2	26%
Fotukian and Nasr (2010)	CuO	25%
Haghighi et al. (2014)	Al_2O_3	15%
This study	SiO_2	17%

Table 4.3: Specific heat, density and Prandtl number of the working fluids.

	Specific heat, C_p, (J/kg K)	Density, ρ, (kg/m^3)	Prandtl number, Pr
Water	4182.00	1000.0	5.58
0.2% SiO$_2$ nanofluid	4113.66	1059.4	4.83
0.4% SiO$_2$ nanofluid	4045.32	1118.8	3.79

Table 4.3 shows the value of the specific heat, the density and the Prandtl number of the working fluid calculated from Eq. (3.14), Eq. (3.34) and Eq. (3.44) respectively. Adding SiO$_2$ nanoparticles to the water has increased the density of the fluid while decreasing the specific heat and the Prandtl number. A decrease in the specific heat has led to smaller amount of the heat energy needed to raise the temperature that will lead to higher output temperature when applied in the solar collector. Decreasing the Prandtl number has resulted in bigger thickness of the thermal boundary layer than the velocity boundary layer.

The theoretical viscosities as calculated from Eq. (3.67) are 0.8, 1.2 and 1.6 mPas respectively for water, 0.2% SiO$_2$ nanofluid and 0.4% SiO$_2$ nanofluid. The measured viscosity of nanofluids in this study is shown in Figure 4.11. It is shown in Figure 4.11 that, the viscosity of nanofluid exponentially decreases with the increase of temperature and the viscosity value of the nanofluid is higher than the base fluid for every addition of volume concentration.
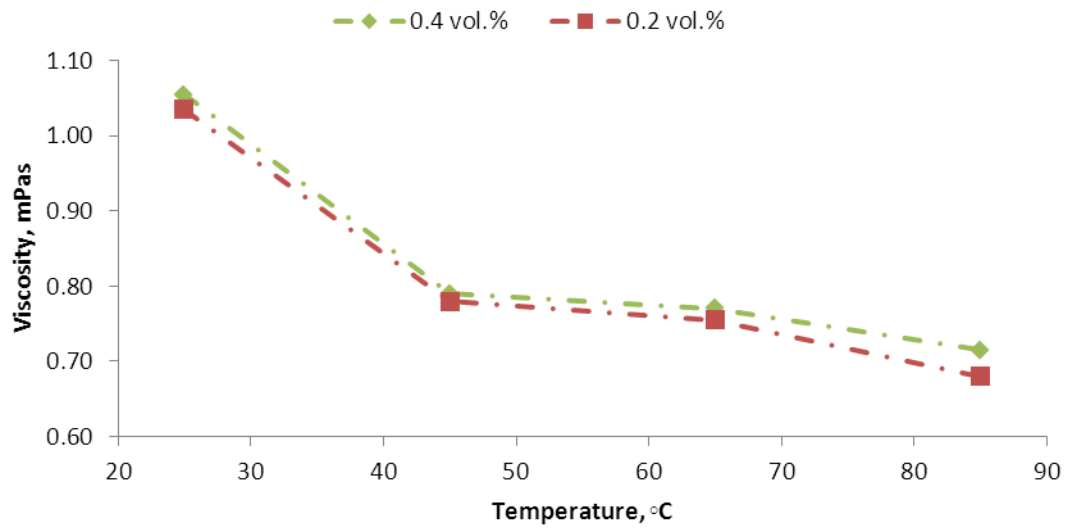
Figure 4.11: Measured value of viscosity for nanofluids in this study.

The Reynolds number is a dimensionless value of the ratio of inertial force to viscous force in fluid flow. Figure 4.12 indicates that the Reynolds number increased by increasing the volume flow rate of the working fluid and by adding SiO_2 nanoparticles, the value of the Reynolds number can be enhanced further. The maximum uncertainty calculated for Reynolds number was around 1.1%.
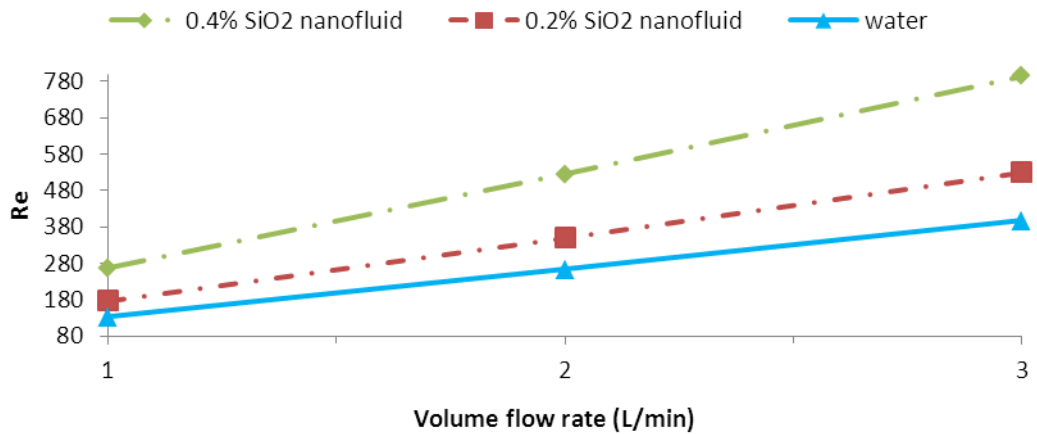
Figure 4.12: Effect of volume flow rate on Reynolds numbers.

For a forced convection flow, the Nusselt number is a very important parameter because it deals with the heat transfer at the boundary layer of fluid. The Nusselt number is a dimensionless ratio of convective to the conductive heat transfer normal to the boundary while it is a function of the Reynolds and Prandtl numbers. As seen in Figure 4.13, the Nusselt number increased by adding nanoparticles inside the working fluid and thus managed to improve the heat transfer characteristic in the system for the corresponding Reynolds number, as reported by other researchers (Alim et al. 2013; Azmi et al. 2013).
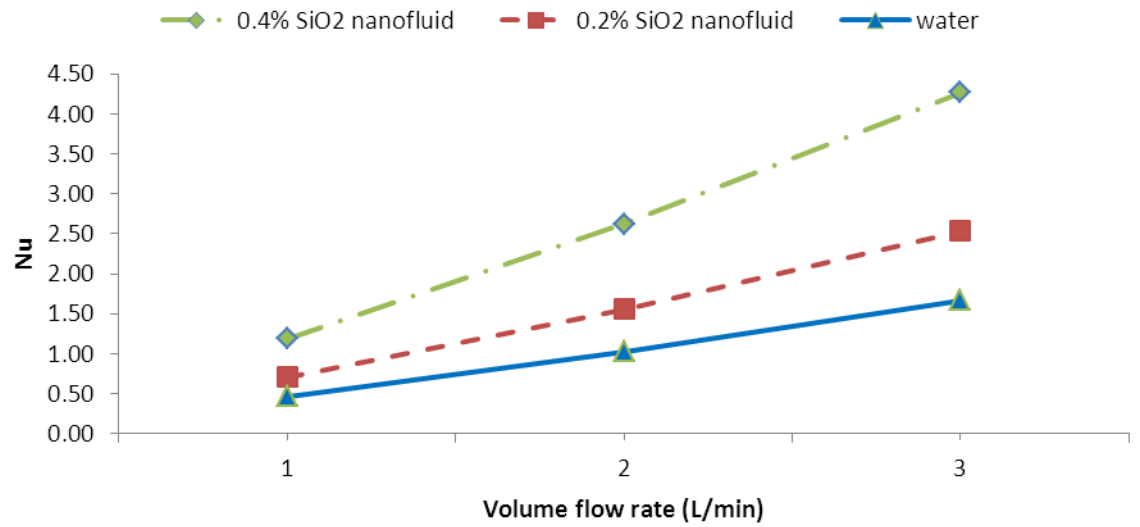
Figure 4.13: Effect of volume flow rate on Nusselt numbers.

4.2.2 Pumping power

Suspending solid particles to enhance the heat transfer and efficiency in fluids had been tested many times before by using millimeter or micrometer-sized particles. However, the effort was not very practical due to problems such as increased pressure drop of the flow channel and thus increasing the pumping power needed by the system. The production of nanometer-sized particles brings little or no penalty in pressure drop and pumping power because the nanoparticles are ultrafine. In this section, the results in pressure drop and pumping power of using nanofluids in solar collectors are shown and discussed.
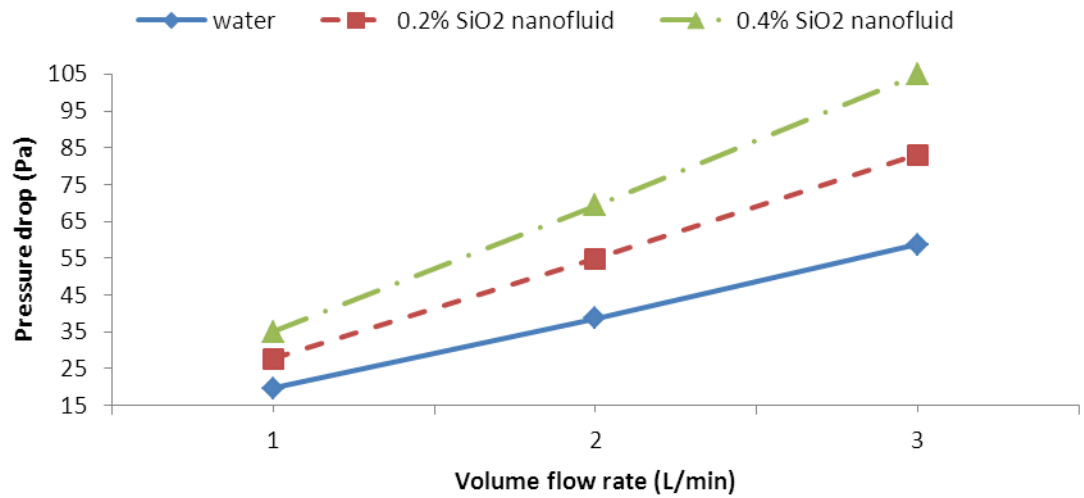
Figure 4.14: Effect of volume flow rate of working fluid on the pressure drop.

Figure 4.14 shows the pressure drop in the system as a function of volume flow rate for different type of working fluids. The pressure drop increased by increasing the working fluid flow rate and by adding nanoparticles concentration. The higher pressure drop experience by using nanofluid is because of its higher density as explained by (Tiwari et al. 2013). When using nanofluid, the pressure drop also occurred because of frictional effect between particles and flow conduit walls or pipes.
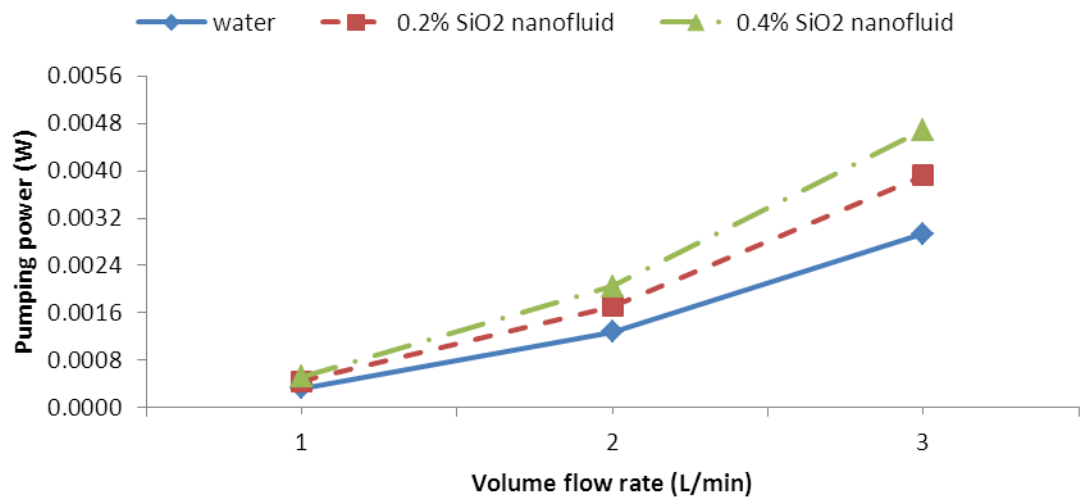
Figure 4.15: Effect of volume flow rate of working fluid on the pumping power.

Figure 4.15 demonstrates the effect on pumping power for variation of nanoparticles concentration in different volume flow rates. As shown in the figure 4.15, pumping power needed for SiO_2 nanofluid is higher compared to water and it increases by increasing nanoparticles volume fraction. Pumping power is associated with the mass flow rates, density and pressure drop of working fluids as expressed in Eq. (3.68). Adding more nanoparticles in the working fluid will result to increase in density and pressure drop and thus increasing the pumping power for the system. Similar results had also been reported by (Kabeel et al. 2013) and (Khairul et al. 2014). However, the increase in pumping power needed when nanofluid is being utilized is too small and will not significantly affect the overall efficiency of the system.

4.3 The economic and environmental impact of solar collector utilizing nanofluid

Economic and environmental impact of solar collectors can be assessed by using life cycle assessment (LCA) method. Tsillingiridis et al. (2004), Ardante et al. (2005) and Kalogirou (2008) are some example of many researchers that have used life cycle assessment methods on solar hot water heating systems to evaluate the economic and environmental impact of it. The life cycle assessment method can effectively be used to evaluate the impact of manufacturing solar collectors on environment from initial resources to its disposal after being used by consumer. The life cycle assessment in this study focuses on the embodied energy of manufacturing and the operation of the solar collector. Only energy used to manufacture the solar collector is considered where else the distribution, maintenance and disposal phase of the collectors are neglected. According to Ardante et al. (2005), more than 70% of the embodied energy of the system comes from the manufacturing of the collector. The analysis was done with the

reduction of collector area as the functional unit that influences the overall weight and embodied energy of the collector. The results will be shown in the next section.

4.3.1 Energy savings

The potential of size reduction of solar collector by using various nanofluids is shown in Figure 4.16. Compared to water, solar collector's area can be reduced up to 25.6%, 21.6%, 22.1% and 21.5% for CuO, SiO_2, TiO_2 and Al_2O_3 respectively as calculated from Eq. (3.76). Potential of collector's area reduction is calculated by substituting efficiency data in Figure 4.5 into Eq. (3.76). Because of higher efficiency of nanofluids solar collector, the surface area of the solar collector that acts as the input energy of the system can be reduced to give the same amount of output temperature with water as conventional working fluid for solar thermal collector.

The weight reduction of solar collector can be estimated by using the area reduction data in Figure 4.16. As shown in Figure 4.17, the total weight for 1000 units of solar collectors can be reduced up to 10 239 kg for CuO nanofluid solar collector and around 8 624.6 kg, 8 856.5 kg and 8 617.8 kg for SiO_2, TiO_2 and Al_2O_3 respectively.
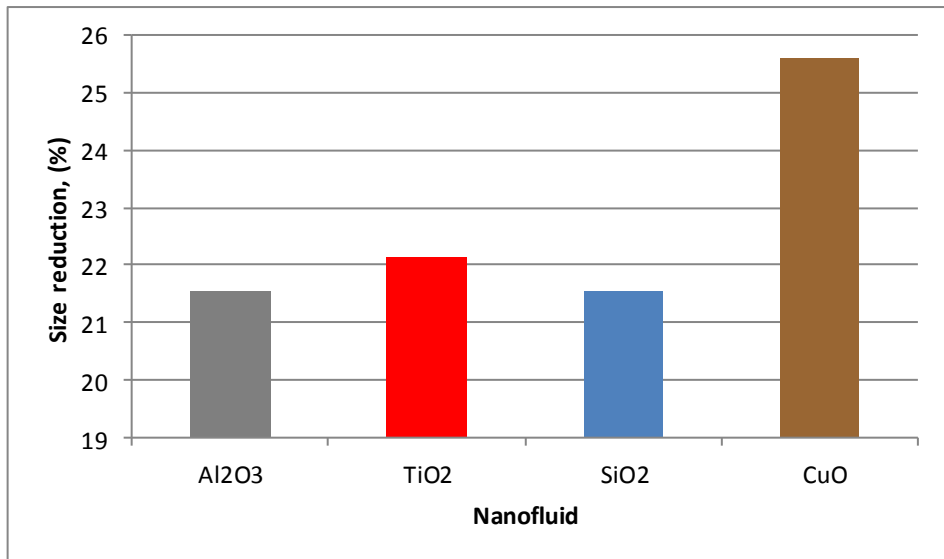
Figure 4.16: Percentage of size reduction for solar collector by applying different nanofluids
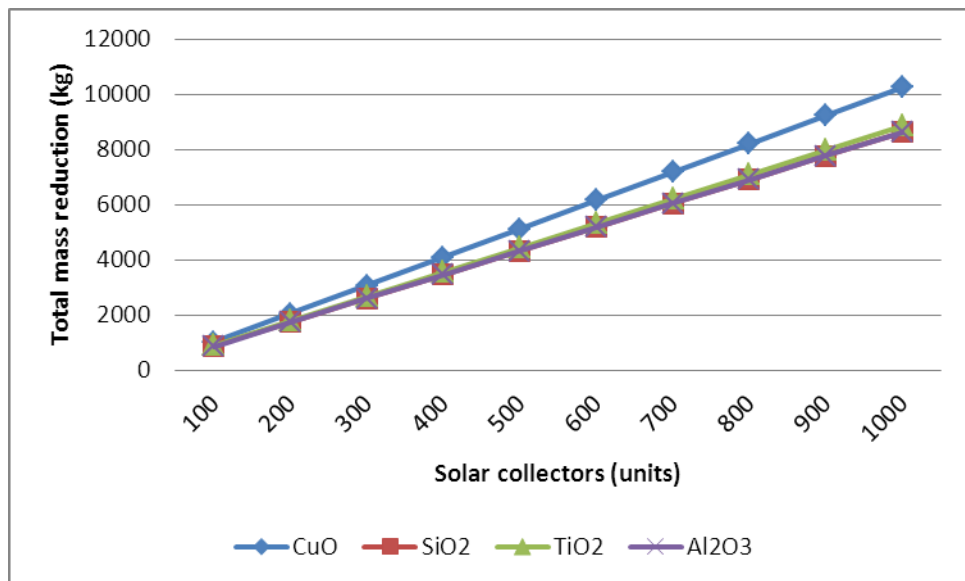
Figure 4.17: Weight reduction of solar collector when applying different nanofluids

Table 4.4 presents the embodied energy for each collectors as well as the percentage of energy savings when applying nanofluids solar collectors compared to water as working fluid. As seen in Table 4.4, the reduction in copper and glass material in the nanofluid based solar collector results in a reduction of around 220 MJ average when compared to the water based collector. Similar results had also been shown by Otanicar (2009) for graphite nanofluids direct absorption solar collector.

Table 4.4: Embodied energy and percentage of energy savings to manufacture solar thermal collector when using different nanofluids

	water	CuO nanofluid	SiO$_2$ nanofluid	TiO$_2$ nanofluid	Al$_2$O$_3$ nanofluid
Embodied Energy (MJ)	1183	880	928	921	928
Energy saving (%)		25.60	21.56	22.14	21.54

4.3.2 Cost savings

The size reduction of nanofluid based solar collector can lead to electricity cost savings calculated based on the current prices for electricity in Malaysia as shown in Table 4.5. Energy load for electric heater is estimated to be around 11 kWh/day for a typical household with 4 family members. (Otanicar, 2009). This electrical energy load was used to calculate the electricity cost per year by using electric heater based on the electricity tariff by TNB in year 2013. The current market cost of the nanoparticles in the year 2013 is RM7.33/g, RM6.87/g, RM5.88/g and RM4.63/g respectively for CuO,

Al$_2$O$_3$, TiO$_2$ and SiO$_2$. In the experiment, 3L of water have been used and 16 gram of nanoparticles has been mixed to make 0.2% concentration for each nanofluid. Because of the higher efficiency of the nanofluid based solar collector, the cost savings per year for all nanofluids is greater than the water based solar collector.

Table 4.5: Economic comparison for solar collectors with different based fluids

	Electric heater	Solar heater (water)	Solar heater (Al$_2$O$_3$)	Solar heater (TiO$_2$)	Solar heater (SiO$_2$)	Solar heater (CuO)
Capital costs (RM)	400.00					
Independent costs (RM)		3000.00	3000.00	3000.00	3000.00	3000.00
Area based costs (RM)		1000.00	784.55	778.59	784.38	744.02
Nanoparticles (RM)			109.96	94.13	74.10	117.30
Total cost (RM)	400.00	4000.00	3894.51	3872.71	3858.48	3861.32
Electricity cost saving per year (RM)		1606.00	1606.00	1606.00	1606.00	1606.00
Years until electricity savings = Costs		2.49	2.42	2.41	2.40	2.40

The payback period for the nanofluid collector is less than the conventional collector primarily due to the reduced capital cost needed for the nanofluid collector. The payback period is shortest for SiO$_2$ and CuO nanofluid solar collector. The higher efficiency and higher area reduction of CuO based nanofluid solar collector can compensate the higher cost of CuO nanoparticles and thus making it almost equal to

SiO_2 nanofluid solar collector. Further savings with nanofluid based solar collector can be achieved if the price of nanoparticles is expected to drop as they become more widely used and produced.

4.3.3 Emissions and damage cost reduction

Table 4.6: Embodied energy emissions from various working fluid solar collector

	Solar heater (water)	Solar heater (CuO)	Solar heater (SiO_2)	Solar heater (TiO_2)	Solar heater (Al_2O_3)
Embodied Energy (MJ)	1183	880	928	921	928
Emission (kg)					
Carbon Dioxide, CO2	718.08	534.16	563.30	559.05	563.30
Sulfur Oxides, SOx	0.37	0.27	0.29	0.29	0.29
Nitrogen Oxides, NOx	0.63	0.47	0.49	0.49	0.49

As seen in Table 4.6 the manufacturing of the nanofluid based solar collector results in around 170 kg less CO_2 emissions in average compared to a conventional solar collector. The differences between the other emissions, Sulfur Oxides, SO_x and Nitrogen Oxides, NO_x, are of a much smaller scale. CuO nanofluid based collector can offset more than 180 kg of CO_2 followed by TiO_2 with 159 kg of CO_2 and the lowest will be SiO_2 and Al_2O_3 with the same amount of 155 kg of CO_2 compared to the traditional solar heaters. Finally the offset damage costs from the pollution savings of the collectors can be established.

Table 4.7: Yearly damage costs for various working fluid solar collectors

			Damage Costs (RM)			
	Cost (RM/kg)	Solar heater (water)	Solar heater (CuO)	Solar heater (SiO$_2$)	Solar heater (TiO$_2$)	Solar heater (Al$_2$O$_3$)
Carbon Dioxide, CO$_2$	0.09	64.63	48.07	50.70	50.31	50.70
Sulfur Oxides, SO$_x$	36.81	13.50	10.04	10.59	10.51	10.59
Nitrogen Oxides, NO$_x$	55.84	35.01	26.04	27.46	27.26	27.46
Total (RM)		113.14	84.16	88.75	88.08	88.75

Table 4.7 shows that the damage cost is lower with the nanofluid based solar collector. This costs savings are not directly applicable to the collector owner but distributed throughout the installer of the collector, the utility or the state and federal government. This damage costs showed the impact of the pollutants from the manufacturing of the collector but the economic or environmental impacts of nanoparticles is not included. Some work have been done on the impact of nanoparticles on the environment, especially human health and ecological systems (Chen et al. 2008) but these studies focus on nanoparticles which are not suspended in liquid. Nanoparticles used in solar collector are suspended in liquid and flowing in a closed loop system which can eliminate the risk for inhalation.

From all the findings in the analytical analysis above, it can be summed up that although output temperature has a greater effect on energy efficiency; it also enhances absorber plate temperature, which may cause exergy loss. As it is mentioned in many articles, the main reason of exergy loss in collector is the difference between absorber plate temperature and the sun temperature *(Ts)*. Since the increase in the absorber plate temperature leads to an increase in this difference and consequently a decrease in collector exergy loss. Jafarkazemi and Ahmadifard (2012) stated in their investigation, increasing the flow rate to approximately 0.01 kg/s leads to a considerable decrease in the absorber plate's temperature. The decrease in temperature gradient between the absorber plate and the environment leads to a decrease in overall heat loss coefficient and consequently to an increase in the thermal efficiency of the collector. Figure 4.3 directly supports that statement. By increasing nanoparticles volume concentration, mass flow rate is increased significantly. Table 4.6 lists the parameters or a bird's eye views of this present study and represents the possible good outcome comparing between conventional and nanofluid based flat plate solar collector.

Table 4.8: Analytical findings of a flat plate solar collector for different nanofluids and base fluid (equal nanoparticles volume fraction and volume flow rate).

Base fluid	C_p, (J/kg.K)	A_p, (m^2)	Mass flow Rate, enhancement, (%)	Efficiency enhancement, (%)	Exergy enhancement, (%)
Water	4182.00	1.61	-	-	-
Al_2O_3	4113.82	1.51	9.47	28.84	4.25
TiO_2	4112.20	1.52	10.38	28.84	4.25
CuO	4109.38	2.24	15.95	38.46	15.52
SiO_2	4113.66	1.50	9.47	28.84	4.25

The above table makes it clear that the CuO nanofluid provides maximum efficiency for both energy and exergy. However, the price of CuO nanoparticles is also higher than other nanoparticles. This leads to higher cost. But other nanofluids have similar behaviour in terms of energy and exergy efficiency which makes SiO_2 the better choice because it has the cheapest price compared to other nanoparticles and the abundance of the source of SiO_2 can make it the best option in terms of sustainability.

4.4 Error analysis

The distribution of the measured values of solar radiation and temperatures are specified in Table 4.9.

Table 4.9: Mean value, variance and standard deviation of the measurements.

	Solar radiation, I_T (W/m2)	Plate temperature, Tp (°C)	Inlet temperature, Tin (°C)	Outlet temperature, Tout (°C)	Ambient temperature, Ta(°C)
Mean, $\bar{x}$	756.76	54.69	35.26	46.53	33.46
Variance, s^2	749.94	32.13	0.11	47.08	1.46
Standard deviation, s	27.39	5.67	0.34	6.86	1.21

Standard deviation determines the width of the distribution. Errors are quoted in terms of the standard deviation. For measured solar radiation, the standard deviation was around 27.39 W/m^2 for the average value of 756.76 W/m^2. The standard deviation for measured plate temperature, inlet temperature, outlet temperature and ambient temperature are 5.67°C, 0.34°C, 6.86°C and 1.21°C respectively. The maximum uncertainty obtained by combining both measurement and random uncertainties at various tests was around 3.77% in which the random uncertainty due to random fluctuation of the process contributes greater.

CHAPTER 5: CONCLUSION

Present study focuses on the benefits of using different nanofluids in a flat plate solar collector. The effects of volume flow rate, nanoparticles volume fraction, mass flow rate, density and specific heat on energy and exergy efficiency of the solar collector are studied. Analytical outcomes reveal that using CuO nanofluid increases energy and exergy efficiency of a flat plate solar collector in analogy with water as absorbing fluid by 38.46% and 15.52%, respectively. Analytical study also remarks that the increment of volume fraction, mass flow rate and density can enhance both energy and exergy efficiency. For equal volume flow rate, mass flow rate could be increased by injecting nanoparticles in base fluid only and represents higher efficiency.

In terms of economic and environmental perspective, SiO_2 nanofluids are more advantageous compared to other metal oxides nanoparticles. Therefore, the study continues further by focusing on SiO_2 nanofluid. The analysis and performance assessment of a flat-plate solar thermal collector using SiO_2 nanofluid as absorbing medium had been dealt with energetic, exergetic, heat transfer, economic and environmental aspects in this study. An experimental investigation had also been taken and the relevant relations used in the analyses had been presented. Nanofluids containing small amount of nanoparticles have higher energy and exergy efficiency than base fluids. The efficiency of solar collector increased by 23.5% by using 0.2% SiO2 nanofluid. In term of heat transfer, addition of a small amount of SiO2 nanoparticles has resulted in the increased Nusselt and Reynolds number. As a result, the heat transfer characteristic in the system has enhanced. The negative impact of adding nanoparticles in the base fluids is the increase in viscosity of the working fluid that has led to increase in pumping power and pressure drop. However, for low concentration nanofluids, only

negligible effect in the pumping power and pressure drop is noticed. Due to higher efficiency of the solar collector operated by nanofluid, smaller and compact solar collector could be manufactured that would reduce the energy and cost to manufacture it and therefore would result in lower emission and lower impact on the environment compared to a conventional collector.

From this study, the work shown in the previous sections has added to the scientific community in the following ways:

1. In term of thermodynamic performance of flat-plate solar collector by using nanofluid:

   a) Higher density and lower specific heat of nanoparticles leads to a higher thermal efficiency and CuO nanofluid have the highest value compared to other 3 nanofluids.

   b) SiO2 nanoparticles coated with silanes are very stable as additives and will not precipitate or fouling the conduits walls of solar collectors.

   c) Using 0.2% SiO_2 nanofluid increases the efficiency of solar collector by 23.5% and increasing volume concentration will increase the efficiency.

   d) Increasing volume fraction and volume flow rate of nanofluid will also increase the exergy efficiency of the system.

   e) Thermal conductivity and heat absorption rate increases with the increment of nanoparticles volume fraction and thus result in reduction of entropy generation and exergy destruction.

2. In term of heat transfer and fluid flow of nanofluid in solar collector:

a) At higher particle volume fraction, higher convective heat transfer coefficient was observed.

b) Adding small amount of SiO2 nanoparticles can increase the Nusselt and Reynolds number and therefore enhance the heat transfer characteristic in the system.

c) The viscosity of nanofluid exponentially decreases with the increase of temperature and the viscosity value of the nanofluid is higher than the base fluid for every addition of volume concentration.

d) Because of that, the pressure drop and pumping power in solar collector increased by increasing the nanofluid flow rate and by increasing the concentration.

e) However, for low concentration nanofluids, only negligible effect in the pumping power and pressure drop is noticed.

3. In term of economic and environmental impact of applying nanofluid in solar collector:

a) Due to higher efficiency of solar collector operated by nanofluid, smaller and compact solar collector can be manufactured that will reduce the energy and cost of manufacturing processes and materials.

b) 25.6%, 21.6%, 22.1% and 21.5% solar collector area reduction are achieved for CuO, SiO_2, TiO_2 and Al_2O_3 respectively.

c) It was estimated that 10 239 kg, 8 625 kg, 8 857 kg and 8 618 kg total weight for 1000 units of solar collectors can be saved for CuO, SiO_2, TiO_2 and Al_2O_3 nanofluid respectively.

d) The average value of 220 MJ embodied energy can be saved for each collector by using various types of metal oxides nanofluids.

e) 280 MJ embodied energy can be saved when manufacturing each solar collector operated by SiO_2 nanofluid.

f) The payback period of using nanofluid solar collector is around 2.4 years compared to conventional one with 2.49 years

g) The manufacturing of nanofluid based solar collector will results in lower emission and lower impact on environment compared to a conventional collector.

h) The manufacturing of the nanofluid based solar collector results in around 170 kg less CO_2 emissions in average compared to a conventional solar collector

i) Environmental damage cost is lower with the nanofluid based solar collector

The analytical and experimental work presented in this study has shown some of the potential improvements created by using nanofluids in solar thermal collectors. However, a variety of questions still remains unanswered and need researching. Further studies should be addressed in future work on solar system that utilizes nanofluids:

1. Can different combinations of nanoparticles mixtures lead to enhanced efficiencies? There is a possibility that making right combinations of different nanoparticles can lead to enhanced efficiencies in terms of both performance and economic advantages.

2. Can the reduced sized collector perform as good as the theoretical results? In this study, only theoretical results have been obtained for the reduced size collector. The actual reduced sized collector must be tested in the future to validate the claim.

3. How will the nanofluids perform in flat-plate solar thermal collectors over a long time periods? The experiment conducted in this study and all other studies are laboratory experiments for only a short time periods since the application of nanofluids is still relatively new in heat transfer device. Effect of nanofluids on the device for the long time periods is still unknown and must be quantified.

REFERENCES

Abbasian Arani AA, Amani J (2012) Experimental study on the effect of TiO2–water nanofluid on heat transfer and pressure drop. Experimental Thermal and Fluid Science 42:107-115

Abbasian Arani AA, Amani J (2013) Experimental investigation of diameter effect on heat transfer performance and pressure drop of TiO_2–water nanofluid. Experimental Thermal and Fluid Science 44:520-533

Akhtar N, Mullick SC (2007) Computation of glass-cover temperatures and top heat loss coefficient of flat-plate solar collectors with double glazing. Energy 32:1067-1074

Aladag B, Halelfadl S, Doner N, Maré T, Duret S, Estellé P (2012) Experimental investigations of the viscosity of nanofluids at low temperatures. Applied Energy 97:876-880

Albadr J, Tayal S, Alasadi M (2013) Heat transfer through heat exchanger using Al_2O_3 nanofluid at different concentrations. Case Studies in Thermal Engineering 1:38-44

Alim MA, Abdin Z, Saidur R, Hepbasli A, Khairul MA, Rahim NA (2013) Analyses of entropy generation and pressure drop for a conventional flat plate solar collector using different types of metal oxide nanofluids. Energy and Buildings 66:289-296

Anderson TN, Duke M, Carson JK (2010) The effect of colour on the thermal performance of building integrated solar collectors. Solar Energy Materials and Solar Cells 94:350-354

Ardante F, Beccali G, Cellura M, Brano VL (2005) Life cycle assessment of a solar thermal collector. renewable Energy 30:1031-1054

Ardente F, Beccali G, Cellura M, Brano LV (2005) Life cycle assessment of a solar thermal collector. Renewable Energy 30:1031-1054

ASHRAE (2007) Handbook of HVAC Applications. ASHRAE, Atlanta, USA.

ASHRAE (2010) Methods of Testing to Determine the Thermal Performance of Solar Collectors (ANSI approved). Atlanta, USA.

Azmi WH, Sharma KV, Sarma PK, Mamat R, Anuar S, Dharma Rao V (2013) Experimental determination of turbulent forced convection heat transfer and friction factor with SiO2 nanofluid. Experimental Thermal and Fluid Science 51:103-111

Bejan A (1996) Entropy Generation Minimization: The method of Thermodynamic Optimization of Finite-size Systems and Finite-time Processes vol 2. CRC Press. USA.

Bejan A, Keary DW, Kreith F (1981) Second law analysis and synthesis of solar collector systems. Journal of Solar Energy Engineering 103:23-28

Bejan A, Kestin J (1983) Entropy generation through heat and fluid flow. Journal of Applied Mechanics 50:475

Bergman TL, Lavine AS, Incropera FP, DeWitt DP (2011) Fundamentals of Heat and Mass Transfer. 7th edn. Wiley. USA.

Bliss Jr RW (1959) The derivations of several "Plate-efficiency factors" useful in the design of flat-plate solar heat collectors. Solar Energy 3:55-64

Cengel YA, Boles MA (2010) Thermodynamics: An Engineering Approach. 7th edn. McGrawHill. USA.

Cengel YA, Cimbala JM (2006) Fluid Mechanics Fundamentals and Applications. McGraw Hill. USA.

Chen Y-j, Wang P-y, Liu Z-h (2013) Application of water-based SiO_2 functionalized nanofluid in a loop thermosyphon. International Journal of Heat and Mass Transfer 56:59-68

Chen Z, Furbo S, Perers B, Fan J, Andersen E (2012) Efficiencies of Flat Plate Solar Collectors at Different Flow Rates. Energy Procedia 30:65-72

Chen Z et al. (2008) Age-Related Differences in Pumonary and Cardiovascular Response to SiO2 Nanoparticles Inhalation: Nanotoxicity Has Susceptible Population. Environmental Science and Technology 42:8985-8992

Chiou JP (1982) The effect of nonuniform fluid flow distribution on the thermal performance of solar collector. Solar Energy 29:487-502

Cooper PI (1981) The effect of inclination on the heat loss from flat-plate solar collectors. Solar Energy 27:413-420

Das SK, Choi SUS (2009) A Review of Heat Transfer in Nanofluids. In: Thomas FI, James PH (eds) Advances in Heat Transfer, vol Volume 41. Elsevier, pp 81-197.

Das SK, PutraThiesen PN, Roetzel W (2003) Temperature dependance of thermal conductivity enhancement for nanofluids. J Heat Transfer 125:567-574

Ding Y, Chen H, He Y, Lapkin A, Yeganeh M, Šiller L, Butenko YV (2007) Forced convective heat transfer of nanofluids. Advanced Powder Technology 18:813-824

Duangthongsuk W, Wongwises S (2009) Heat transfer enhancement and pressure drop characteristics of TiO$_2$–water nanofluid in a double-tube counter flow heat exchanger. International Journal of Heat and Mass Transfer 52:2059-2067

Duangthongsuk W, Wongwises S (2010) An experimental study on the heat transfer performance and pressure drop of TiO$_2$-water nanofluids flowing under a turbulent flow regime. International Journal of Heat and Mass Transfer 53:334-344

Duffie JA, Beckman WA (2006) Solar engineering of thermal processes. vol 13. Wiley New York.

Eastman JA, Choi SUS, Li S, Yu W, Thompson LJ (2001) Anomalously increased effective thermal conductivities of ethylene glycol-based nanofluids containing copper nanoparticles Applied Physics Letters 78:718

Einstein A (1956) Investigation on the Theory of the Brownian Movement. Courier Dover Publications. USA.

Elias MM, Shahrul IM, Mahbubul IM, Saidur R, Rahim NA (2014) Effect of different nanoparticle shapes on shell and tube heat exchanger using different baffle angles and operated with nanofluid. International Journal of Heat and Mass Transfer 70:289-297

Esen H (2008) Experimental energy and exergy analysis of double-flow solar air heater having different obstacles on absorber plates. . Building and Environment 43:1046-1054

Farahat S, Sarhaddi F, Ajam H (2009) Exergetic optimization of flat plate solar collectors. Renewable Energy 34:1169-1174

Fazeli SA, Hosseini Hashemi SM, Zirakzadeh H, Ashjaee M (2012) Experimental and numerical investigation of heat transfer in a miniature heat sink utilizing silica nanofluid. Superlattices and Microstructures 51:247-264

Fedele L, Colla L, Bobbo S (2012) Viscosity and thermal conductivity measurements of water-based nanofluids containing titanium oxide nanoparticles. International Journal of Refrigeration 35:1359-1366

Foster R, Witcher J, Nelson V, Ghassemi M, Mimbela LE, Ghassemi A (2009) Solar Energy: Renewable Energy and the Environment. Taylor & Francis. New Mexico. USA.

Fotukian SM, Nasr Esfahany M (2010) Experimental study of turbulent convective heat transfer and pressure drop of dilute CuO/water nanofluid inside a circular tube. International Communications in Heat and Mass Transfer 37:214-219

Francey JLA, Paraioannou J (1985) Wind-related heat losses of a flat-plate collector. Solar Energy 35:15-19

Garg HP, Agarwal RK (1995) Some aspects of a PV/T collector/forced circulation flat plate solar water heater with solar cells. Energy Conversion and Management 36:87-99

Ghadimi A, Saidur R, Metselaar HSC (2011) A review of nanofluid stability properties and characterization in stationary conditions. International Journal of Heat and Mass Transfer 54:4051-4068

Ghanbarpour M, Bitaraf Haghigi E, Khodabandeh R (2014) Thermal properties and rheological behavior of water based Al_2O_3 nanofluid as a heat transfer fluid. Experimental Thermal and Fluid Science 53:227-235

Goswami DY, Kreith F, Kreider JF (2000) Principles of Solar Engineering CRC. Florida. USA.

Goswami YD (2007) Energy: the burning issue: There are no easy answers to the energy conundrum, but a fundamental agreement on the questions is essential. Refocus 8:22-25. USA.

Groenhout NK, Behnia M, Morrison GL (2002) Experimental measurement of heat loss in an advanced solar collector. Experimental Thermal and Fluid Science 26:131-137

Gupta KKD, Saha SK (1990) Energy analysis of solar thermal collectors. Renewable Energy and Environment:283-287

Haddon RC (2002) Carbon nanotubes. Acc Chem Res 35:977-1113

Haghighi EB et al. (2014) Experimental Study on Convective Heat Transfer of Nanofluids in Turbulent Flow: Methods of Comparison of Their Performance. Experimental Thermal and Fluid Science 57:378-387

Hahne E (1985) Parameter effects on design and performance of flat plate solar collectors. Solar Energy 34:497-504

Hamilton R, Crosser O (1962) Thermal conductivity of heterogeneous two-component systems. Industrial & Engineering chemistry fundamentals 1:187-191

Han D, Meng Z, Wu D, Zhang C, Zhu H (2011) Thermal properties of carbon black aqueous nanofluids for solar absorption. Nanoscale Research Letters 6:1-7

He Y, Jin Y, Chen H, Ding Y, Cang D, Lu H (2007) Heat transfer and flow behaviour of aqueous suspensions of TiO_2 nanoparticles (nanofluids) flowing upward through a vertical pipe. International Journal of Heat and Mass Transfer 50:2272-2281

Hollands KGT, Lightstone MF (1989) A review of low-flow, stratified-tank solar water heating systems. Solar Energy 43:97-105

Hottel HC, Woertz BB (1942) Performance of Flat Plate Solar Heat Collectors. Transactions ASME 64:91-104

Hwang KS, Jang SP, Choi SUS (2009) Flow and convective heat transfer characteristics of water-based Al2O3 nanofluids in fully developed laminar flow regime. International Journal of Heat and Mass Transfer 52:193-199

Indhuja A, Suganthi K, Manikandan S, Rajan KS (2013) Viscosity and thermal conductivity of dispersions of gum arabic capped MWCNT in water: Influence of MWCNT concentration and temperature. Journal of the Taiwan Institute of Chemical Engineers 44:474-479

IPCC (2014) Climate Change 2014, Fifth Assessment Report. United Nations, New York.

Ise N, Sogami I (2005) Structure Formation in Solution: Ionic Polymers and Colloidal Particles. Springer. USA.

Jafarkazemi F, Ahmadifard E (2012) Energetic and exergetic evaluation of flat plate solar collectors. Renewable Energy 56:55-63

Jeter SM, Stephens JH (2012) SYSTEMS AND METHODS OF THERMAL ENERGY STORAGE AND RELEASE. EP Patent 2,475,885,

Jiang H, Li H, Zan C, Wang F, Yang Q, Shi L (2014) Temperature dependence of the stability and thermal conductivity of an oil-based nanofluid. Thermochimica Acta 579:27-30

Kabeel AE, Abou El Maaty T, El Samadony Y (2013) The effect of using nano-particles on corrugated plate heat exchanger performance. Applied Thermal Engineering 52:221-229

Kahani M, Heris SZ, Mousavi SM (2013) Effects of Curvature Ratio and Coil Pitch Spacing on Heat Transfer Performance of Al2O3/Water Nanofluid Laminar Flow through Helical Coils. Journal of Dispersion Science and Technology 34:1704-1712

Kalogirou S (2004a) Environmental benefits of domestic solar energy systems. energy Conversion and Management 45:3075-3092

Kalogirou S (2008) Thermal performance, economic and environmental life cycle analysis of thermosyphon solar water heaters. Journal of Solar Energy

Kalogirou S (2009) Solar Energy Engineering: Processes and Systems Academic Press. California. USA.

Kalogirou SA (2004b) Solar thermal collectors and applications. Progress in Energy and Combustion Science 30:231-295

Kamyar A, Saidur R, Hasanuzzaman M (2012) Application of Computational Fluid Dynamics (CFD) for nanofluids. International Journal of Heat and Mass Transfer 55:4104-4115

Keblinski P, Phillpot SR, Choi SUS, Eastman JA (2002) Mechanism of heat flow in suspensions of nanosized particles (nanofluids). International Journal of Heat and Mass Transfer 45:855-863

Kenna JP (1983) The thermal trap solar collector. Solar Energy 31:335-338

Khairul MA, Alim MA, Mahbubul IM, Saidur R, Hepbasli A, Hossain A (2014) Heat transfer performance and exergy analyses of a corrugated plate heat exchanger using metal oxide nanofluids. International Communications in Heat and Mass Transfer 50:8-14

Kikas NP (1995) Laminar flow distribution in solar systems. Solar Energy 54:209-217

Kim D et al. (2009) Convective heat transfer characteristics of nanofluids under laminar and turbulent flow conditions. Current Applied Physics 9:e119-e123

Kline SJ, McClintock FA (1953) Describing Uncertainties in Single-Sample Experiments. Mechanical Engineering 75:3-8

Kosmulski M (2001) Chemical Properties of Material Surfaces. Marcel Dekker, New York.

Kotas TJ (1995) The exergy method of thermal plant analysis. Krieger Publish Company, Malabar, FL.

Kotulski ZA, Szczepinski W (2010) Error Analysis with Applications in Engineering. Springer. Netherland.

Kulkarni DP, Das DK, Vajjha RS (2009) Application of nanofluids in heating buildings and reducing pollution. Applied Energy 86:2566-2573

Lalchand G (2012) Electricity demand and supply in Peninsular Malaysia: Energy efficiency, renewable energy, or nuclear? http://www.christopherteh.com/. Accessed 21 December 2012

Langston LS (2009) Efficiency by the Numbers. Mechanical Engineering Magazine (ASME).

Laquil PD, Kearney D, Geyer M, Diver R (1993) Solar-Thermal Electric Technology. In: Renewable Energy: Sources for Fuels and Electricity. Earthscan, Island Press, Washington DC, pp 213-296.

Larsen SF, Altamirano M, Hernández A (2012) Heat loss of a trapezoidal cavity absorber for a linear Fresnel reflecting solar concentrator. Renewable Energy 39:198–206

Lee S, Choi SU-S, Li S, Eastman JA (1999) Measuring Thermal Conductivity of Fluids Containing Oxide Nanoparticles. J Heat Transfer 121:280-289

Lee SW, Park SD, Kang S, Bang IC, Kim JH (2011) Investigation of viscosity and thermal conductivity of SiC nanofluids for heat transfer applications. International Journal of Heat and Mass Transfer 54:433-438

Lenert A, Wang EN (2012) Optimization of nanofluid volumetric receivers for solar thermal energy conversion. Solar Energy 86:253-265

Leong KY, Saidur R, Kazi SN, Mamun AH (2010) Performance investigation of an automotive car radiator operated with nanofluid-based coolants. Applied Thermal Engineering 30:2685-2692

Leong KY, Saidur R, Mahlia TMI, Yau YH (2012) Predicting size reduction of shell and tube heat recovery exchanger operated with nanofluids based coolants and its associated energy saving. Energy Education Science and Technology Part A 30:1-14

Li FC, Yang JC, Zhou WW, He YR, Huang YM, Jiang BC (2013) Equation experimental study on the characteristics of thermal conductivity and shear viscosity of viscoelastic-fluid-based nanofluids containing multiwalled carbon nanotubes. Thermochimica Acta 556:47-53

Li Q, Xuan Y, Wang J (2003) Investigation on convective heat transfer and flow features of nanofluids. Journal of Heat Transfer 125:151-155

Liu BYH, Jordan RC (1963) The long-term average performance of flat-plate solar-energy collectors: With design data for the U.S., its outlying possessions and Canada. Solar Energy 7:53-74

Liu Z-h, Liao L (2008) Sorption and agglutination phenomenon of nanofluids on a plain heating surface during pool boiling. International Journal of Heat and Mass Transfer 51:2593-2602

Lu L, Liu Z-H, Xiao H-S (2011) Thermal performance of an open thermosyphon using nanofluids for high-temperature evacuated tubular solar collectors: Part 1: Indoor experiment. Solar Energy 85:379-387

Ma L, Lu Z, Zhang J, Liang R (2010) Thermal performance analysis of the glass evacuated tube solar collector with U-tube. Building and Environment 45:1959-1967

Mahbubul IM, Saidur R, Amalina MA (2012) Latest developments on the viscosity of nanofluids. International Journal of Heat and Mass Transfer 55:874-885

Mahian O, Kianifar A, Kleinstreuer C, Al-Nimr MA, Pop I, Sahin AZ, Wongwises S (2013) A review of entropy generation in nanofluid flow. International Journal of Heat and Mass Transfer 65:514-532

Mahian O, Mahmud S, Heris SZ (2012) Analysis of entropy generation between co-rotating cylinders using nanofluids. Energy 44:438-446

Mekhilef S, Safari A, Mustaffa WES, Saidur R, Omar R, Younis MAA (2012) Solar energy in Malaysia: Current state and prospects. Renewable and Sustainable Energy Reviews 16:386-396

Mintsa HA, Roy G, Nguyen CT, Doucet D (2009) New temperature dependent thermal conductivity data for water-based nanofluids. International Journal of Thermal Sciences 48:363-371

Mullick SC, Samdarshi SK (1988) Improved technique for computing the top heat loss factor of a flat-plate collector with a single glazing. Journal of Solar Energy Engineering, Transactions of the ASME 110:262-267

Murshed SMS, Leong KC, Yang C (2005) Enhanced thermal conductivity of TiO$_2$ - water based Nanofluids. International Journal of Thermal Sciences 44:367-373

Murshed SMS, Nieto de Castro CA, Lourenço MJV, Lopes MLM, Santos FJV (2011) A review of boiling and convective heat transfer with nanofluids. Renewable and Sustainable Energy Reviews 15:2342-2354

Nagar VK, Vaishya JS, Bhide VG (1984) Emittance from stagnation temperature study. Solar Energy 32:633-636

Namburu P, Kulkarni D, Dandekar A, Das D (2007a) Experimental investigation of viscosity and specific heat of silicon dioxide nanofluids. Micro & Nano Letters, IET 2:67-71

Namburu PK, Kulkarni DP, Misra D, Das DK (2007b) Viscosity of copper oxide nanoparticles dispersed in ethylene glycol and water mixture. Experimental Thermal and Fluid Science 32:397-402

Naraki M, Peyghambarzadeh SM, Hashemabadi SH, Vermahmoudi Y (2013) Parametric study of overall heat transfer coefficient of CuO/water nanofluids in a car radiator. International Journal of Thermal Sciences 66:82-90

Natarajan E, Sathish R (2009) Role of nanofluids in solar water heater. The International Journal of Advanced Manufacturing Technology. DOI 10.1007/s00170-008-1876-8.

Nemet A, Kravanja Z, Klemeš JJ (2012) Integration of solar thermal energy into processes with heat demand. Clean Technologies and Environmental Policy 14:453-463

Nguyen CT, Desgranges F, Roy G, Galanis N, Maré T, Boucher S, Angue Mintsa H (2007) Temperature and particle-size dependent viscosity data for water-based nanofluids – Hysteresis phenomenon. International Journal of Heat and Fluid Flow 28:1492-1506

Nugroho AM (2010) The impact of solar chimney geometry for stack ventilation in Malaysia's single storey terraced house. . Malaysia's Geography 2010:163–177.

Otanicar T, Phelan PE, Prasher RS, Rosengarten G, Taylor RA (2010) Nanofluid-based direct absorption solar collector. J Renewable Sustainable Energy 2

Otanicar TP (2009) Direct absorption solar thermal collectors utilizing liquid-nanoparticle suspensions. Arizona State University. USA.

Owhaib W, Palm B (2004) Experimental investigation of single-phase convective heat transfer in circular microchannels. Experimental Thermal and Fluid Science 2:105-110

Pacheco JE (2001) Demonstration of solar-generated electricity on demand: the solar two project. J Sol Energy:123-125

Pandey SD, Nema VK (2012) Experimental analysis of heat transfer and friction factor of nanofluid as a coolant in a corrugated plate heat exchanger. Experimental Thermal and Fluid Science 38:248-256

Pastoriza-Gallego MJ, Casanova C, Legido JL, Piñeiro MM (2011) CuO in water nanofluid: Influence of particle size and polydispersity on volumetric behaviour and viscosity. Fluid Phase Equilibria 300:188-196

Phuoc TX, Massoudi M (2009) Experimental observations of the effects of shear rates and particle concentration on the viscosity of Fe_2O_3–deionized water nanofluids. International Journal of Thermal Sciences 48:1294-1301

Ranjan KR, Kaushik SC (2013) Exergy analysis of the active solar distillation systems integrated with solar ponds. Clean Technologies and Environmental Policy 16:791-805

Reddy VS, Kaushik SC, Tyagi SK (2012) Exergetic analysis and performance evaluation of parabolic trough concentrating solar thermal power plant (PTCSTPP). Energy 39:258–273

Roberts DE, Forbes A (2012) An analytical expression for the instantaneous efficiency of a flat plate solar water heater and the influence of absorber plate absorptance and emittance. Solar Energy 86:1416-1427

Romero M, Buck R, Pacheco JE (2002) An update on solar central receiver systems, projects, and technologies. J Sol Energy:98-108

Said Z, Sajid MH, Alim MA, Saidur R, Rahim NA (2013) Experimental investigation of the thermophysical properties of Al_2O_3-nanofluid and its effect on a flat plate solar collector. International Communications in Heat and Mass Transfer 48:99-107

Saidur R, BoroumandJazi G, Mekhlif S, Jameel M (2012) Exergy analysis of solar energy applications. Renewable and Sustainable Energy Reviews 16:350-356

Saidur R, Lai YK (2011) Nanotechnology in vehicle's weight reduction and associated energy savings. Energy Education Science and Technology Part A 26:87-101

Saidur R, Leong KY, Mohammad HA (2011) A review on applications and challenges of nanofluids. Renewable and Sustainable Energy Reviews 15:1646-1668

Sajadi AR, Kazemi MH (2011) Investigation of turbulent convective heat transfer and pressure drop of TiO_2/water nanofluid in circular tube. International Communications in Heat and Mass Transfer 38:1474-1478

Samdarshi SK, Mullick SC (1991) Analytical equation for the top heat loss factor of a flat-plate collector with double glazing. Journal of Solar Energy Engineering, Transactions of the ASME 113:117-122

San Martin RL, Fjeld GJ (1975) Experimental performance of three solar collectors. Solar Energy 17:345-349

Sanchez-Bautista AdF, Santibanez-Aguilar JE, Ponce-Ortega JM, Napoles-Rivera F, Serna-Gonzalez M, El-Halwagi MM (2015) Optimal design of domestic water-heating solar systems. Clean Technol Environ Policy 17:637-656

Sani E, Mercatelli L, Barison S, Pagura C, Agresti F, Colla L, Sansoni P (2011) Potential of carbon nanohorn-based suspensions for solar thermal collectors. Solar Energy Materials and Solar Cells 95:2994-3000

Sarhaddi F, Farahat S, Ajam H, Behzadmehr A (2010) Exergetic performance assessment of a solar photovoltaic thermal (PV/T) air collector. Energy and Buildings 42:2184-2199

Shin D, Banerjee D (2011) Enhancement of specific heat capacity of high-temperature silica-nanofluids synthesized in alkali chloride salt eutectics for solar thermal-energy storage applications. International Journal of Heat and Mass Transfer 54:1064-1070

Siebers DL, Viskanta R (1977) Comparison of predicted performance of constant outlet temperature and constant mass flow rate collectors. Solar Energy 19:411-413

Singal RK (2008) Non-Conventional Energy Resources (Alternative Energy Sources and Systems). S.K. KATARIA & SONS, Delhi.

Sohel MR, Saidur R, Sabri MFM, Kamalisarvestani M, Elias MM, Ijam A (2013) Investigating the heat transfer performance and thermophysical properties of nanofluids in a circular micro-channel. International Communications in Heat and Mass Transfer 42:75-81

Sokhansefat T, Kasaeian AB, Kowsary F (2014) Heat transfer enhancement in parabolic trough collector tube using Al_2O_3/synthetic oil nanofluid. Renewable and Sustainable Energy Reviews 33:636-644

Spardo JV, Rabl A (1999) Estimates of Real Damage from Air Pollution: Site Dependence and Simple Impact Indices for LCA. International Journal of LCA 4:229-243

Struckmann F (2008) Analysis of a flat-plate solar collector. Project Report, MVK160 Heat and Mass Transport, Lund, Sweden

Sukhatme K, Sukhatme S (1996) Solar Energy 2E. Tata McGraw-Hill Education.

Sustainable Energy Development (2006). Ninth Malaysia Plan 2006-2010. Dewan Rakyat. Malaysia.

Suzuki A (1988a) A fundamental equation for exergy balance on solar collectors. Journal of solar energy engineering 110:102-106

Suzuki A (1988b) General theory of exergy balance analysis and application to solar collectors. Energy 13:153-160

Taylor RA, Phelan PE, Otanicar TP, Adrian R, Prasher R (2011) Nanofluid optical property characterization: towards efficient direct absorption solar collectors. Nanoscale Research Letters 6

Timofeeva lV, Yu W, France DM, Singh D, Routbort JL (2011) Nanofluids for heat transfer: an engineering approach. Nanoscale Research Letters 6:182

Tiwari AK, Ghosh P, Sarkar J (2013) Heat transfer and pressure drop characteristics of CeO2/water nanofluid in plate heat exchanger. Applied Thermal Engineering 57:24-32

Tora EA, El-Halwagi MM (2009) Optimal design and integration of solar systems and fossil fuels for sustainable and stable power outlet. Clean Technologies and Environmental Policy 11:401-407

Trisaksri V, Wongwises S (2007) Critical review of heat transfer characteristics of nanofluids. Renewable and Sustainable Energy Reviews 11:512-523

Tsillingiridis G, Martinopoulos G, Kyriakis N (2004) Life cycle environmental impact of a thermosyphon domestic solar hot water system in comparison with electrical and gas water heating. renewable Energy 29:1277-1288

Tyagi H, Phelen P, R.Prasher (2009) Predicted efficiency of a low-temperature nanofluid based direct absorption solar collector. Journal of Solar Energy Engineering 131:41004-41010

UNPF (2014) Population Dynamics in the Post-2015 Development Agenda.

Valero A, Valero A, Martínez A (2010) Inventory of the exergy resources on earth including its mineral capital Energy 35:989-995

Vatanpour V, Madaeni SS, Moradian R, Zinadini S, Astinchap B (2011) Fabrication and characterization of novel antifouling nanofiltration mambrane prepared from oxidized multiwalled carbon nanotube/polyethersulfone nanocomposite. J Membr Sci 375:284-294

Wang H (2009) Dispersing carbon nanotubes using surfactants. Current Opinion in Colloid & Interface Science 14:364-371

Wang L, Fang X, Zhang Z (2010) Design methods for large scale dye-sensitized solar modules and the progress of stability research. Renewable and Sustainable Energy Reviews 14:3178-3184

Weitbrecht V, Lehmann D, Richter A (2002) Flow distribution in solar collectors with laminar flow conditions. Solar Energy 73:433-441

Wen D, Ding Y (2004) Experimental investigation into convective heat transfer of nanofluids at the entrance region under laminar flow conditions. International Journal of Heat and Mass Transfer 47:5181-5188

White FM (2003) Fluid Mechanics. 5th edn. McGraw-Hill, Boston. USA.

Xie HQ, Wang JC, Xi TG, Liu Y, Ai F, Wu QR (2002) Thermal conductivity enhancement of suspensions containing nanosized alumina particles. Journal Applied Physics 91:4568-4572

Xuan Y, Li Q (2003) Investigation on convective heat transfer and flow features of nanofluids. Journal of Heat Transfer 125:151

Xuan Y, Roetzel W (2000) Conceptions for heat transfer correlation of nanofluids. International Journal of Heat and Mass Transfer 43:3701-3707

Yang X, Liu Z-h (2010) A Kind of Nanofluid Consisting of Surface-Functionalized Nanoparticles. Nanoscale Research Letters 5:1324-1328

Yousefi T, Shojaeizadeh E, Veysi F, Zinadini S (2012a) An experimental investigation on the effect of pH variation of MWCNT–H_2O nanofluid on the efficiency of a flat-plate solar collector. Solar Energy 86:771-779

Yousefi T, Veisy F, Shojaeizadeh E, Zinadini S (2012b) An experimental investigation on the effect of MWCNT-H_2O nanofluid on the efficiency of flat-plate solar collectors. Experimental Thermal and Fluid Science 39:207-212

Yousefi T, Veysi F, Shojaeizadeh E, Zinadini S (2012c) An experimental investigation on the effect of Al_2O_3–H_2O nanofluid on the efficiency of flat-plate solar collectors. Renewable Energy 39:293-298

Zamzamian A, KeyanpourRad M, KianiNeyestani M, Jamal-Abad MT (2014) An experimental study on the effect of Cu-synthesized/EG nanofluid on the efficiency of flat-plate solar collectors. Renewable Energy 71:658-664

Zhou SQ, Ni R (2008a) Measurement of the specific heat capacity of water-based Al_2O_3 nanofluid. Appl Phys Lett 92:1-3

LIST OF PUBLICATIONS AND PAPERS PRESENTED

LIST OF PUBLICATIONS

1. M. Faizal, R. Saidur, S.Mekhilef, Potential of Size Reduction of Flat-plate Solar Collectors When Applying Al2O3 Nanofluid. Advanced Material Research, 832 (2014) 149-153 (accepted; published)

2. M. Faizal, R. Saidur, S.Mekhilef, Potential of size reduction of flat-plate solar collectors when applying MWCNT nanofluid. Earth Environ. Sci. 16 (2013), (accepted; published)

3. M. Faizal, R. Saidur, S.Mekhilef, M. A. Alim, Energy, Economic and Environmental Analysis of Metal Oxides Nanofluid for Flat-Plate Solar Collector, Energy Conversion and Management 76 (2013) 162-168 (accepted; published)

4. M.A. Alim, R. Saidur, N.A. Rahim, M.A. Khairul, M. Faizal, M.R. Islam, Z. Abdin, Energy and Exergy Analysis of a Flat Plate Solar Collector Using Different Nanofluids, Numerical Heat Transfer A (submitted; under review)

5. M. Faizal, R. Saidur, S.Mekhilef, A. Hepbasli. Energy, economic and environmental analysis of a flat plate solar collector operated with SiO_2 nanofluid, Clean Technologies and Environmental Policy (accepted; published)

CONFERENCE PRESENTED

1. International Conference on Nanoscience and Nanotechnology 2013 (NANO-SciTech 2013), 1st - 4th March 2013, Grand Bluewave Hotel, Shah Alam, Malaysia

2. International Conference on Energy and Environment 2013 (ICEE2013), 5th - 6th March 2013, Universiti Tenaga Nasional, Putrajaya Campus, 43000 Kajang, Selangor, Malaysia

Potential of size reduction of flat-plate solar collectors when applying MWCNT nanofluid

M Faizal[1, 2]*, R Saidur[2, 3] and S Mekhilef[4]
[1]Engineering Division, ADP, Taylor's University Lakeside Campus, 47500 Selangor, Malaysia
[2]Department of Mechanical Engineering, University of Malaya, 50603 Kuala Lumpur, Malaysia
[3]UM Power Energy Dedicated Advanced Centre (UMPEDAC), Level 4, Wisma R&D, University of Malaya, 59990 Kuala Lumpur, Malaysia
[4]Department of Electrical Engineering, University of Malaya, 50603 Kuala Lumpur, Malaysia

E-mail: mohdfaizalfauzan@yahoo.com

Abstract. Flat-plate solar collector is the most popular type of collector for hot water system to replace gas or electric heater. Solar thermal energy source is clean and infinite to replace fossil fuel source that is declining and harmful to the environment. However, current solar technology is still expensive, low in efficiency and takes up a lot of space. One effective way to increase the efficiency is by applying high conductivity fluid as nanofluid. This paper analyzes the potential of size reduction of solar collector when MWCNT nanofluid is used as absorbing medium. The analysis is based on different mass flow rate, nanoparticles mass fraction, and presence of surfactant in the fluid. For the same output temperature, it can be observed that the collector's size can be reduced up to 37% of its original size when applying MWCNT nanofluid as the working fluid and thus can reduce the overall cost of the system..

1. Introduction

In Malaysia, most houses are using Electric Water Heater for shower due to the cheap price and easy installation of it. However, Malaysia has a good potential for solar hot water system. Located on the equatorial, Malaysia's climate is hot and humid throughout the year with monthly solar radiation is approximately around 400-600 MJ/m^2 [1]. Solar energy source is sustainable, free, clean and infinite. However, currently solar heater is still expensive, low in efficiency and bulky. One of the effective methods to increase the efficiency is to replace the working fluid with nanofluids. Researches on thermal efficiency by applying nanofluids on flat-plate solar collector have been made in the past few years [2-11]. Experimental investigation conducted by Yousefi, et al. [4] on the effect of Al_2O_3 based nanofluid shown the increase of 28.3% efficiency of flat-plate solar collectors. Lenert and Wang [12] presented a model and experimental study of concentrated solar power application using carbon-coated cobalt (C-Co) nanoparticles and Therminol VP-1 base fluid and concluded that the efficiency is more than 35% with nanofluid and the efficiency will increase with increasing nanofluid height. Lu, et al. [13] shown that the application of Copper Oxide (CuO) nanoparticles in evacuated tubular solar collector will significantly enhance the thermal performance of evaporator and evaporating heat transfer coefficient increased by 30% compared to water as working fluid. 5% improvement in

Energy, economic and environmental analysis of metal oxides nanofluid for flat-plate solar collector

M. Faizal [a,b,*], R. Saidur [b], S. Mekhilef [c], M.A. Alim [b]

[a]Engineering Division, ADP, Taylor's University Lakeside Campus, 47500 Selangor, Malaysia
[b]Department of Mechanical Engineering, University of Malaya, 50603 Kuala Lumpur, Malaysia
[c]Department of Electrical Engineering, University of Malaya, 50603 Kuala Lumpur, Malaysia

ARTICLE INFO

ABSTRACT

For a solar thermal system, increasing the heat transfer area can increase the output temperature of the system. However, this approach leads to a bigger and bulkier collector. It will then increase the cost and energy needed to manufacture the solar collector. This study is carried out to estimate the potential to design a smaller solar collector that can produce the same desired output temperature. This is possible by using nanofluid as working fluid. By using numerical methods and data from literatures, efficiency, size reduction, cost and embodied energy savings are calculated for various nanofluids. From the study, it was estimated that 10,239 kg, 8625 kg, 8857 kg and 8618 kg total weight for 1000 units of solar collectors can be saved for CuO, SiO_2, TiO_2 and Al_2O_3 nanofluid respectively. The average value of 220 MJ embodied energy can be saved for each collector, 2.4 years payback period can be achieved and around 170 kg less CO_2 emissions in average can be offset for the nanofluid based solar collector compared to a conventional solar collector. Finally, the environmental damage cost can also be reduced with the nanofluid based solar collector.

1. Introduction

The population and world energy demand is increasing and accelerating while fossil fuel sources are declining fast. The environment is polluted by fuel burning and climate change has becoming huge global problem. Therefore, a lot of studies related to energy efficiency and renewable energy have been conducted to address this issue [1–42]. Commonly, most houses in Malaysia are using Electric Water Heater for shower. This is mainly because the price of Electric Heater is cheap and relatively easy to install. However, the world is facing a huge problem now because of declining source of energy and using the precious electrical energy for heating does not really a good idea since heat can be harnessed directly from the sun. Potentially, Malaysia is located on the equatorial, with hot and humid climate throughout the year and monthly solar radiation approximately around 400–600 MJ/m^2 [26]. Solar energy source is sustainable, free, clean and infinite. However, current solar heater is still expensive, low in efficiency and big in size. One of the effective methods to increase the efficiency is to replace the working fluid with nanofluids. Researches on thermal efficiency by applying nanofluids on flat-plate solar collector have been made in the past few years by numerous researchers [43–52]. Experimental investigation conducted by Yousefi et al. [45] on the effect of Al_2O_3 based nanofluid shown the increase of 28.3% efficiency of flat-plate solar collectors. Lenert and Wang [53] presented a model and experimental study of concentrated solar power application using carbon-coated cobalt (C–Co) nanoparticles and Therminol VP-1 base fluid and concluded that the efficiency is more than 35% with nanofluid and the efficiency will increase with increasing nanofluid height. Lu et al. [54] shown that the application of Copper Oxide (CuO) nanoparticles in evacuated tubular solar collector will significantly enhance the thermal performance of evaporator and evaporating heat transfer coefficient increased by 30% compared to water as working fluid. Five percentage improvement in efficiency was found out by Otanicar et al. [55] by using diversity of nanoparticles with water as base fluid for micro-solar-thermal collector. Shin and Banerjee [56] applied novel nanomaterials in molten salts base fluid for concentrated solar power coupled with thermal storage and experienced an enhancement in operational efficiencies. They also concluded that the cost of electricity will be reduced. Taylor et al. [51] used graphite based nanofluid in high flux solar collectors that resulting in 10% increase in efficiency.

Because of higher thermal conductivity and efficiency of nanofluids, smaller and compact design of solar thermal collector has become possible without affecting the output desired. Smaller size collector can reduced the material usage, cost and energy required

* Corresponding author at: Engineering Division, ADP, Taylor's University Lakeside Campus, 47500 Selangor, Malaysia.
E-mail addresses: mohdfaizal.fauzan@taylors.edu.my, mohdfaizalfauzan@yahoo.com (M. Faizal).

Potential of Size Reduction of Flat-plate Solar Collectors When Applying Al2O3 Nanofluid

M. Faizal[1, 2, a], R. Saidur[2, b], S.Mekhilef[3, c]

[1]Engineering Division, ADP, Taylor's University Lakeside Campus, 47500 Selangor, Malaysia

[2]Department of Mechanical Engineering, University of Malaya, 50603 Kuala Lumpur, Malaysia

[3]Department of Electrical Engineering, University of Malaya, 50603 Kuala Lumpur, Malaysia

[a]mohdfaizal.fauzan@taylors.edu.my, [b]saidur@um.edu.my, [c]saad@um.edu.my

Abstract. The source of fossil fuel is decreasing. The price increased rapidly. Population and demand of energy increased significantly over the years. Carbon pollution and global warming are becoming major issues. The best way to overcome this problem is by changing to renewable source of energy. One of it is solar thermal energy. However, a solar technology is currently still expensive, low in efficiency and takes up a lot of space. Nanofluid is recognized as a solution to overcome this problem. Due to the high thermal conductivity of nanofluids, the thermal efficiency of a solar collector can be increased and thus decreasing the size of the system. This paper analyzes the efficiency of using the Al_2O_3 nanofluid as absorbing medium in flat-plate solar collector and estimated the potential of size reduction. When applying the same output temperature of Al_2O_3 nanofluid as with water, it can be observed that the collector's size can be reduced up to 24% of its original size.

Introduction

Commonly, most houses in Malaysia are using Electric Water Heater for shower mainly because the price is cheap and installation is easy. However, the world is facing a huge problem now because of declining source of energy and using the precious electrical energy for heating does not really a good idea since heat can be harnessed directly from the sun. Potentially, Malaysia is located on the equatorial, with hot and humid climate throughout the year and with monthly solar radiation is approximately around 400-600 MJ/m^2 [1]. Solar energy source is sustainable, free, clean and infinite. However, current solar heater is still expensive, low in efficiency and big in size. One of the effective methods to increase the efficiency is to replace the working fluid with nanofluids. Researches on thermal efficiency by applying nanofluids on flat-plate solar collector have been made in the past few years by numerous researchers [2-11]. Experimental investigation conducted by Yousefi, Veysi, Shojaeizadeh and Zinadini [4] on the effect of Al_2O_3 based nanofluid shown the increase of 28.3% efficiency of flat-plate solar collectors. Lenert and Wang [12] presented a model and experimental study of concentrated solar power application using carbon-coated cobalt (C-Co) nanoparticles and Therminol VP-1 base fluid and concluded that the efficiency is more than 35% with nanofluid and the efficiency will increase with increasing nanofluid height. Lu, Liu and Xiao [13] shown that the application of Copper Oxide (CuO) nanoparticles in evacuated tubular solar collector will significantly enhance the thermal performance of evaporator and evaporating heat transfer coefficient increased by 30% compared to water as working fluid. 5% improvement in efficiency was found out by Otanicar, Phelan, Prasher, Rosengarten and Taylor [14] by using diversity of nanoparticles with water as base fluid for micro-solar-thermal collector. Shin and Banerjee [15] applied novel nanomaterials in molten salts base fluid for concentrated solar power coupled with thermal storage and experienced an enhancement in operational efficiencies. They also concluded that the cost of electricity will be reduced. Taylor, Phelan, Otanicar, Adrian and Prasher [10] used graphite based nanofluid in high flux solar collectors that resulting in 10% increase in efficiency.

ORIGINAL PAPER

Energy, economic, and environmental analysis of a flat-plate solar collector operated with SiO$_2$ nanofluid

M. Faizal · R. Saidur · S. Mekhilef ·
A. Hepbasli · I. M. Mahbubul

Abstract To overcome the environmental impact and declining source of fossil fuels, renewable energy sources need to meet the increasing demand of energy. Solar thermal energy is clean and infinite, suitable to be a good replacement for fossil fuel. However, the current solar technology is still expensive and low in efficiency. One of the effective ways of increasing the efficiency of solar collector is to utilize high thermal conductivity fluid known as nanofluid. This research analyzes the impact on the performance, fluid flow, heat transfer, economic, and environment of a flat-plate solar thermal collector by using silicon dioxide nanofluid as absorbing medium. The analysis is based on different volume flow rates and varying nanoparticles volume fractions. The study has indicated that nanofluids containing small amount of nanoparticles have higher heat transfer coefficient and also higher energy and exergy efficiency than base fluids. The measured viscosity of nanofluids is higher than water but it gives negligible effect on pressure drop and pumping power. Using SiO$_2$ nanofluid in solar collector could also save 280 MJ more embodied energy, offsetting 170 kg less CO$_2$ emissions and having a faster payback period of 0.12 years compared to conventional water-based solar collectors.

Keywords SiO$_2$ nanofluid · Flat-plate solar collector · Heat transfer · Economic · Exergy

Introduction

Renewable energies are very important in the world economy today because they are sustainable, safe, and clean. World energy demand is increasing and expected to accelerate more in the future, while the fossil oil sources and production are declining. Climate change and environmental pollution are becoming huge global problems. Solar energy is an unlimited and free source of energy that can meet the world's future energy needs without harming the earth. Therefore, many studies have been conducted to address this issue. Tora and El-Halwagi (2009) had developed an optimal design of energy system to integrate solar systems and fossil fuel for sustainable and stable power outlet. Nemet et al. (2012) continued the work further by developing captured solar energy curve and minimal capture temperature curve to maximize the solar thermal energy delivered to the process. Ranjan and Kaushik (2013) performed an energy and exergy analysis of active solar distillation system integrated with solar pond that can contribute to water security and sustainability. Sanchez-Bautista et al. (2014) presented an optimization model for the optimal design of water-heating system for homes in Mexico. In that model, location, solar radiation, inhabitants, and time-based consumption pattern

M. Faizal
Department of Engineering, School of Liberal Arts and Sciences, Taylor's University Lakeside Campus, 47500 Selangor, Malaysia

M. Faizal · R. Saidur (✉) · I. M. Mahbubul
Department of Mechanical Engineering, Faculty of Engineering, University of Malaya, 50603 Kuala Lumpur, Malaysia
e-mail: saidur@um.edu.my; saidur912@yahoo.com

S. Mekhilef
Power Electronics and Renewable Energy Research Laboratory (PEARL), Department of Electrical Engineering, Faculty of Engineering, University of Malaya, 50603 Kuala Lumpur, Malaysia

A. Hepbasli
Department of Energy Systems Engineering, Faculty of Engineering, Yasar University, 35100 Izmir, Turkey

Ⓢ Springer

INTERNATIONAL CONFERENCE ON NANOSCIENCE & NANOTECHNOLOGY 2013
(NANO-SciTech 2013)
MARCH 1ST – 4TH, 2013
SHAH ALAM, SELANGOR, MALAYSIA

INVITATION LETTER

Date   : **30 January 2013**
Our Reference : **NANO-SciTech2013/P28**

Paper ID : **P28**
Paper Title : **Potential of Size Reduction of Flat-plate Solar Collectors When Applying Al2O3 Nanofluid**
Authors : **M. Faizal, R. Saidur, S.Mekhilef**
Address : **Engineering Division, ADP, Taylor's University Lakeside Campus, 47500 Selangor, Malaysia**
Registration fee : **RM1,000**

Dear **Mohd Faizal Fauzan**,

On behalf of the Organizing Committee of the International Conference on Nanoscience and Nanotechnology 2013 (NANO-SciTech 2013), we are delighted to inform you that your abstract has been accepted for **Oral Presentation** and that you are kindly requested to attend the conference for your presentation.

Please do browse the conference website from time to time for updates on the conference matters.

Please pay the registration fee as described in the website, **http://www.ios.uitm.edu.my/nano-scitech2013/**.

We look forward to seeing you in Shah Alam, Selangor, Malaysia in coming March. If you have any question, please do not hesitate to contact us at **nanoscitech13@gmail.com**.

Yours sincerely,

PROF. ENGR. DR. MOHAMAD RUSOP MAHMOOD
Chairman
NANO-SciTech 2013

The Secretariat
NANO-SciTech 2013
Institute of Science
Level 3, Block C
(Old Engineering Building)
Universiti Teknologi MARA (UiTM)
40450 Shah Alam, Selangor
MALAYSIA

Tel: +603 5544 4415
Fax: +603 5544 3870
Email: nanoscitech13@gmail.com

Organised by
NANO-SciTech Centre
Institute of Science,
Universiti Teknologi MARA (UiTM)
40450 Shah Alam,
Selangor,
MALAYSIA

Co-organised by
Department of Environmental
Technology & Urban Planning
Nagoya Institute of Technology
Nagoya,
JAPAN

140

Mohd Faizal Fauzan

Dear Faizal,

Thank you for submitting the manuscript/revised manuscript, "Energy, Economic and Environmental Analysis of Metal Oxides Nanofluid for Flat-Plate Solar Collector" to Energy Conversion and Management for publication. I apologize for the lengthy review period. I am pleased to inform you that the reviews are complete and that the paper is accepted for publication in Energy Conversion and Management.

The Production Unit of Elsevier Science will send you proofs of the paper, which should be corrected and returned promptly. A copyright agreement form for you to complete will be enclosed with the proofs.

I would like to inform you that, if your institution is a subscriber to Energy Conversion and Management, you may have full text access to the journal online at no additional cost to the print subscription through ScienceDirect Web Editions (http://www.sciencedirect.com/web-editions). Such access is limited to the last twelve months. For information on the status of accepted papers, after Elsevier has sent you proofs of the paper, please consult our Online Article Status Information System (OASIS) on the Internet at http://www.elsevier.com/locate/authors/.

Thank you for this contribution to Energy Conversion and Management. I hope your present research is progressing well, and I look forward to reading future contributions to Energy Conversion and Management from you and your colleagues. I would appreciate your recommendation to your other colleagues that they consider submitting their manuscripts to Energy Conversion and Management for review and publication.

When your paper is published on ScienceDirect, you want to make sure it gets the attention it deserves. To help you get your message across, Elsevier has developed a new, free service called AudioSlides: brief, webcast-style presentations that are shown (publicly available) next to your published article. This format gives you the opportunity to explain your research in your own words and attract interest. You will receive an invitation email to create an AudioSlides presentation shortly. For more information and examples, please visit http://www.elsevier.com/audioslides.

Sincerely yours,

Professor Moh'd A. Al-Nimr
Editor-in-Chief
Energy Conversion and Management

From:	confdeliver <confdeliver@163.com>
Sent:	Tuesday, September 24, 2013 10:17 AM
To:	Mohd Faizal Fauzan; mohdfaizalfauzan@yahoo.com
Subject:	Dear M. Faizal, invitation for presentation of your paper in Elsevier Journal.

Dear M. Faizal,

From the Elsevier Journal, we know your impressive paper ***Energy, economic and environmental analysis of metal oxides nanofluid for flat-plate solar collector***. We would like to invite you to make an oral presentation and introduce your research results in The 3rd Conference on Nanomaterials (CN 2014).

This year, The 3rd Conference on Nanomaterials (CN 2014), will be held from January 14 to 16, 2014 in Shenzhen, China.
We would extend our highest appreciation and warmest welcome to your attention and attendance

Invited Speaker
Prof. Manuel Vazquez, Institute of Materials Science of Madrid, Spain
Prof. V.K. Jindal, Panjab University, India
Prof. Jyh-Ping Chen, Chang Guang University, Chinese Taipei
Dr. SHIV KUMAR CHAKARVARTI, Manav Rachna International University, India
Dr. Michael Holzinger, Université Joseph Fourier，France
Dr. Qiao Chen, University of Sussex, UK
Dr. Igor A. Levitsky, University of RI, USA
More information, please refer:
http://www.engii.org/workshop/CN2014January/Home.aspx?utm_campaign=CN-hand

Publication
All the accepted papers will be published by "Journal of Materials Science and Chemical Engineering" (ISSN: 2327-6045), a peer-reviewed open access journal that can ensure the widest dissemination of your published work. For more information, please visit:
http: //www.scirp.org/journal/msce/

Venue
Shenzhen, one of five municipal cities, locates in the southeast coast of china neighboring Hong Kong. It ranks the fourth in terms of economic capacity in china mainland. It is an ideal city to settle down because of its pleasant oceanic climate and its open cultural environment caused by its geographical advantage. It is also a favorable place for hosting a conference, with sea view and beach, world-class hotels, resort and spa centers, golf courses, and some nationally renowned scenic spots.
Besides, more conferences information, please visit: www.engii.org

Secretary, Tony Zhang
CN 2014 Organizing Committee
E-mail: workshop_January@engii.org
Tel: +86- 132 6470 2250

Your article *Energy, Economic and Environmental Analysis of Metal Oxides Nanofluid for Flat-Plate Solar Collector*
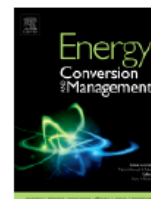
Dear Mr. Faizal,

We are pleased to present to you as a corresponding author, an overview of the performance of your article in *Energy Conversion and Management*. With Article Usage Alerts, a free service, you are able to measure the impact of your article via its usage on ScienceDirect.

Your article has been downloaded or viewed 744 times since publication (measured through 31 January).

For more details, please check here for your Article Usage Dashboard. For best results use Google Chrome or Firefox.

View Dashboard

This information is generated especially for you, however if you would like to share your results and/or article with peers, feel free to send it through via email or the social media buttons in the Dashboard. If you have any questions about this service, please consult our Support site. You receive this email as a service, however if you would like to stop receiving alerts, please use the unsubscribe option below.

You will receive quarterly Article Usage Alerts in the first year after publication of your article. If you would like to check your article more often, please bookmark your article's Dashboard page as the information on the Dashboard will be updated monthly.

Thank you for your interest.

Best wishes,

Elsevier

Article Usage Dashboard

Energy, economic and environmental analysis of metal oxides nanofluid for flat-plate solar collector

Faizal, M.; Saidur, R.; Mekhilef, S.; Alim, M.A.

Energy Conversion and Management, Volume(s) 76, 15-Aug-2013, Pages 162-168

Share your article   Tips and Tricks to let the world   Download this
                      know about your research   dashboard

                                                     View Article

Views by geography
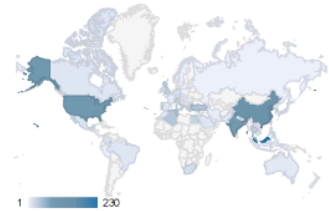
1   230

Top countries	Rank	Views	Pct
Malaysia	1	230	23%
China	2	125	12%
United States	3	97	10%
India	4	89	9%
Turkey	5	38	4%

Corporate versus Public Sector

Trend and cumulative views

1,200

1,000

800

600

1,020
total views

Article Usage Dashboard
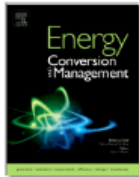
Energy, economic and environmental analysis of metal oxides nanofluid for flat-plate solar collector

Faizal, M.; Saidur, R.; Mekhilef, S.; Alim, M.A.

Energy Conversion and Management, Volume(s) 76, 15-Aug-2013, Pages 162-168

View Article

Views by geography

Top countries	Rank	Views	Pct
Malaysia	1	265	22%
China	2	151	12%
United States	3	119	10%
India	4	109	9%
Algeria	5	55	5%

Corporate versus Public Sector
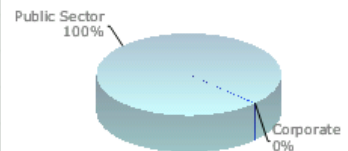
Public Sector
100%

Corporate
0%

Trend and cumulative views

1,400

1,200

1,000

800

600

400

200

1,210
total views

| 91 | 142 | 97 | 170 | 127 | 117 | 98 | 103 | 75 | 67 | 36 | 87 |
| Aug-13 | Sep-13 | Oct-13 | Nov-13 | Dec-13 | Jan-14 | Feb-14 | Mar-14 | Apr-14 | May-14 | Jun-14 | Jul-14 |

Scopus

Search   Alerts   My list   My Scopus

Energy, economic and environmental analysis of metal oxides nanofluid for flat-plate solar collector
Faizal M., Saidur R., Mekhilef S., Alim M.A.
(2013) Energy Conversion and Management, 76 , pp. 162–168.

Is cited by: Set feed

14 documents   Analyze search results   Sort on: Date Cited by | Relevance [...]

Energy, economic, and en	Export | Download | View citation overview | View Cited by | More...	Show all abstracts

Refine

Limit to   Exclude

1	Performance of copper oxide/water nanofluid in a flat plate solar water heater under natural and forced circulations View at Publisher	Michael, J.J., Iniyan, S. 2015 Energy Conversion and Management 0

Year
- 2015 (1)
- 2014 (13)

2	Numerical study on turbulent heat transfer and pressure drop of nanofluid in coiled tube-in-tube heat exchangers View at Publisher	Aly, W.I.A. 2014 Energy Conversion and Management 6

Author Name
- Aly, W.I.A. (1)
- Chabi, A.R. (1)
- Chen, C. (1)
- Chen, L. (1)
- De Rosa, M. (1)

3	Experimental investigation of the effects of silica/water nanofluid on PV/T (photovoltaic thermal units) View at Publisher	Sardarabadi, M., Passandideh-Fard, M., Zeinali Heris, S. 2014 Energy 5
4	Heat transfer enhancement in a PV cell using Boehmite nanofluid View at Publisher	Karami, N., Rahimi, M. 2014 Energy Conversion and Management 3

Subject Area
- Energy (13)
- Chemical Engineering (1)
- Environmental Science (1)
- Physics and Astronomy (1)

5	Effect of solid volume fraction and tilt angle in a quarter circular solar thermal collectors filled with CNT-water nanofluid View at Publisher	Rahman, M.M., Mojumder, S., Saha, S., Mekhilef, S., Saidur, R. 2014 International Communications in Heat and Mass Transfer 2

Document Type
- Article (13)
- Review (1)

6	Concentration photovoltaic-thermal energy co-generation system using nanofluids for cooling and heating View at Publisher	Xu, Z., Kleinstreuer, C. 2014 Energy Conversion and Management 1

Source Title
Keyword
Affiliation
Country/Territory
Source Type
Language

7	Experimental analysis on a novel solar collector system achieved by supercritical CO2 natural convection View at Publisher	Chen, L., Zhang, X.-R. 2014 Energy Conversion and Management 5

Limit to   Exclude

Export refine

8	Performance analysis of a minichannel-based solar collector using different nanofluids View at Publisher	Mahian, O., Kianifar, A., Sahin, A.Z., Wongwises, S. 2014 Energy Conversion and Management 1
9	Experimental study and performance analysis of a thermoelectric cooling and heating system driven by a photovoltaic/thermal system in summer and winter operation modes View at Publisher	He, W., Zhou, J., Chen, C., Ji, J. 2014 Energy Conversion and Management 5
10	Performance of water based CuO and Al2O3 nanofluids in a Cu-Be alloy heat sink with rectangular microchannels View at Publisher	Peyghambarzadeh, S.M., Hashemabadi, S.H., Chabi, A.R., Salimi, M. 2014 Energy Conversion and Management 1
11	Improving the performance of solar still by using nanofluids and providing vacuum View at Publisher	Kabeel, A.E., Omara, Z.M., Essa, F.A. 2014 Energy Conversion and Management 2
12	An experimental study on the effect of Cu-synthesized/EG nanofluid on the efficiency of flat-plate solar collectors View at Publisher	Zamzamian, A., KeyanpourRad, M., KianiNeyestani, M., Jamal-Abad, M.T. 2014 Renewable Energy 3
13	Energetic performances of an optimized passive Solar Heating Prototype used for Tunisian buildings air-heating application	Mehdaoui, F., Hazami, M., Naili, N., Farhat, A. 2014 Energy Conversion and Management 1

APPENDIX A: IMAGES OF OTHER TYPES OF SOLAR COLLECTORS
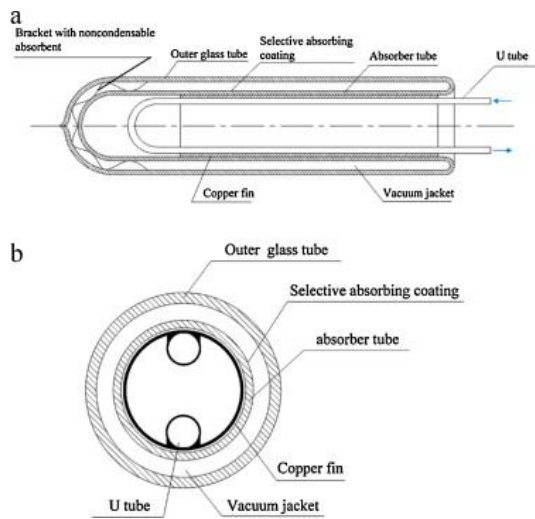
Glass evacuated tube solar collector with U-tube. (a) Illustration of the glass evacuated tube and (b) cross section (Ma et al. 2010)
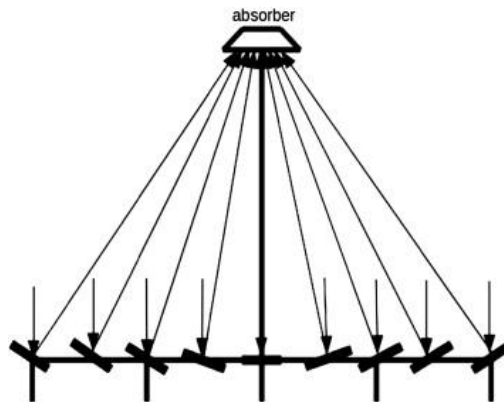
Linear Fresnel reflectors (Larsen et al. 2012)
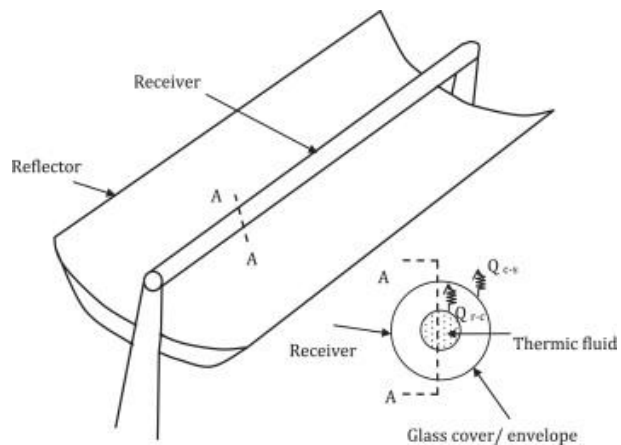
Parabolic trough collectors (Reddy et al. 2012)
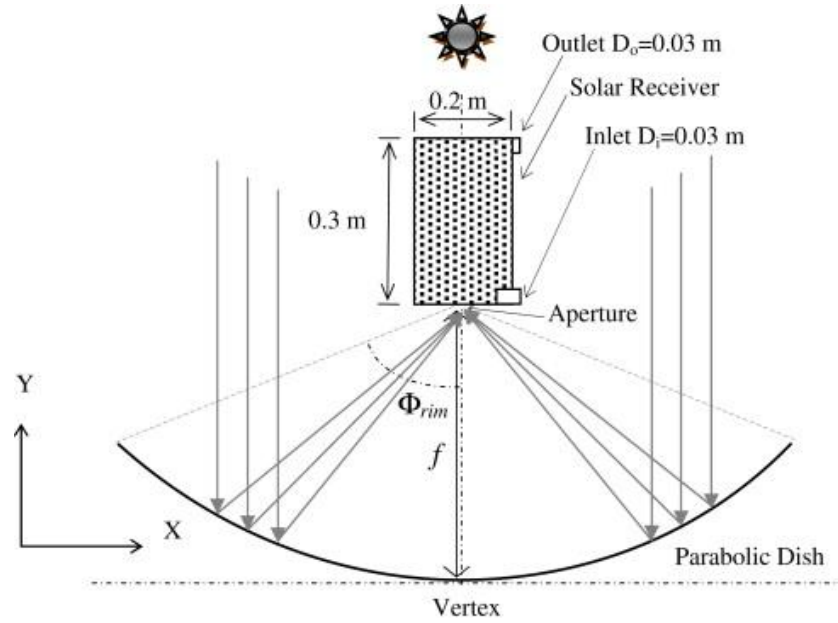
Parabolic dish reflectors (Wang et al. 2010)
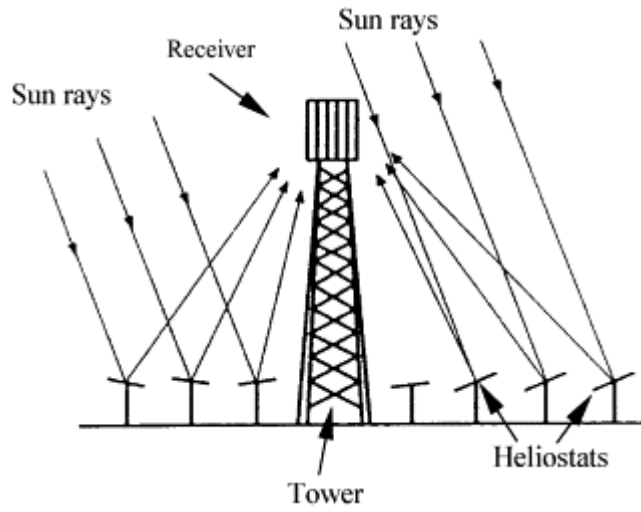
Heliostat field collectors (Kalogirou 2004b)

APPENDIX B: IMAGES OF EXPERIMENTAL APPARATUS
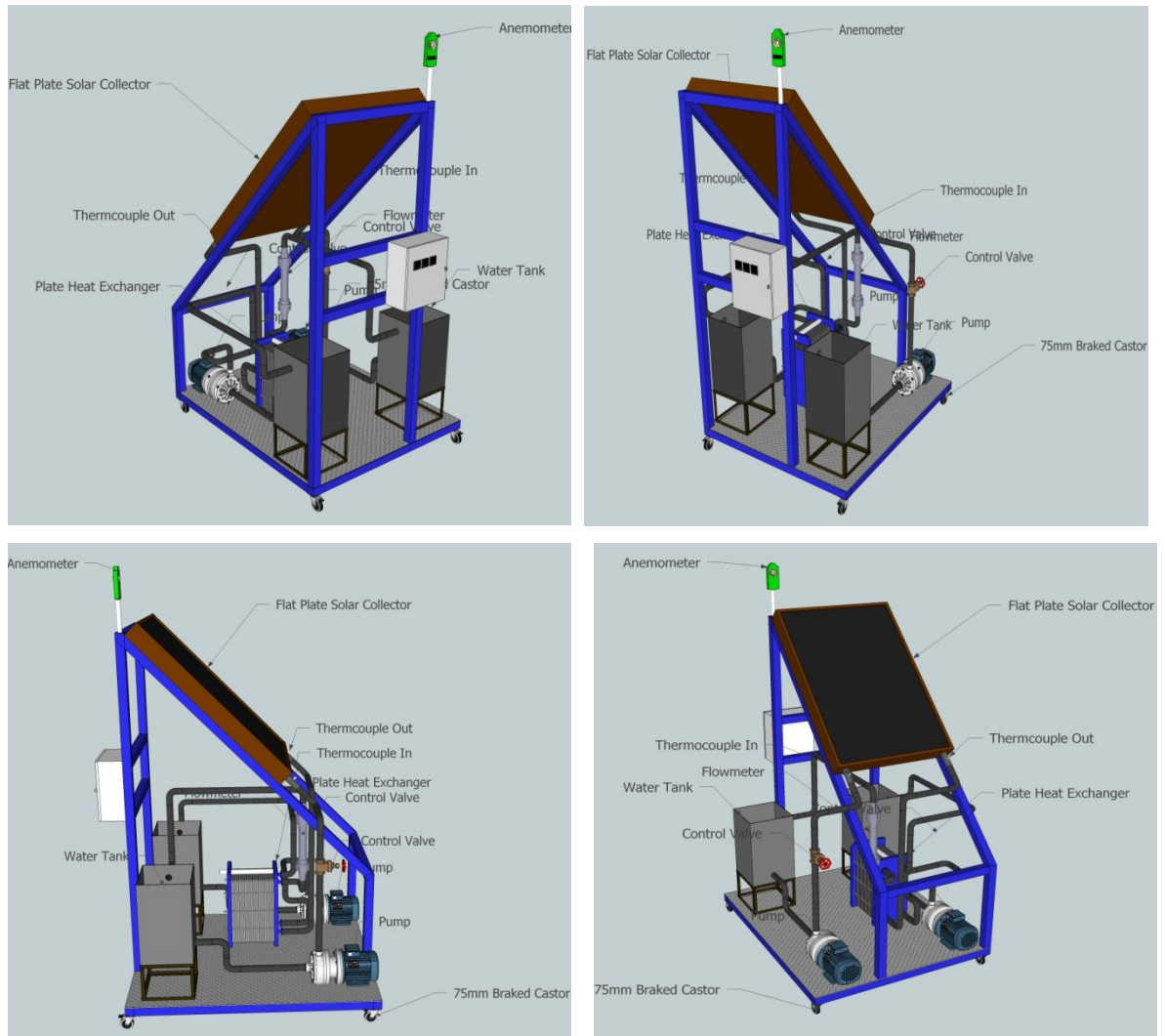
CAD images of experimental set up

The construction of experimental set up

Differential Scanning Calorimeter (DSC 4000 Perkin Elmer)

Programmable viscometer (Brookfield LVDV-III ultra)

Portable density meter (KEM-DA 130N)

Water distiller

Ultrasonic homogenizer.

Digital weighing machine.

Shaking incubator.

Water pump.

Heat exchanger.
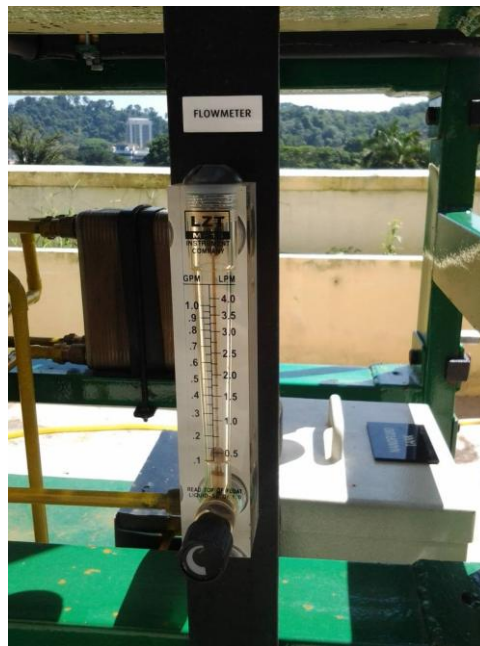
Flow meter.

Differential pressure transducer.

Data logger.

TES 1333R solar meter.

PROVA (AV M-07) anemometer.

PH meter

Field Emission Scanning Electron Microscope (FESEM) Physics Department
University of Malaya
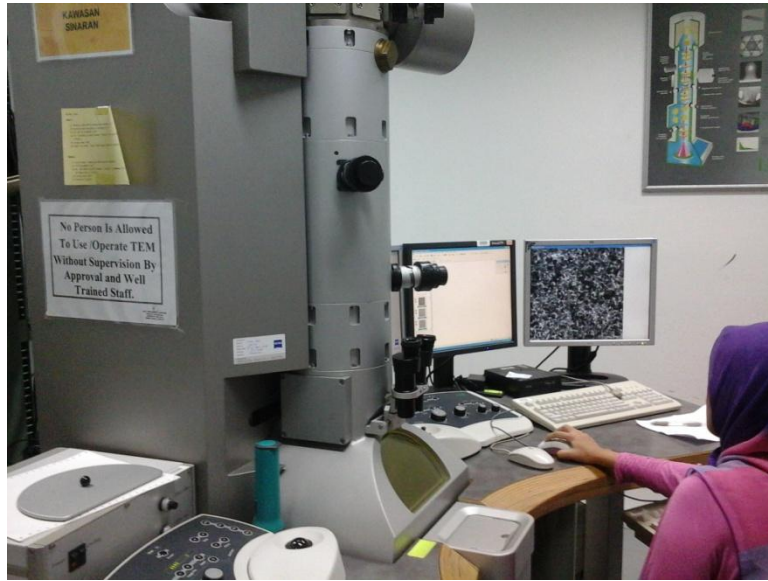
Transmission Electron Microscope (TEM) Medical Department University of Malaya

APPENDIX C: ADDITIONAL TABULATED DATA

3% volume fraction Al_2O_3 nanofluid

Volume flow Rate	Mass flow rate	Specific heat of nanofluid	Solar radiation	Inlet Temperature	Energy Efficiency
1	0.0181	4079.73	500	300	8.8840
1.1	0.0200	4079.73	500	300	9.7724
1.2	0.0218	4079.73	500	300	10.6608
1.3	0.0236	4079.73	500	300	11.5492
1.4	0.0254	4079.73	500	300	12.4376
1.5	0.0272	4079.73	500	300	13.3260
1.6	0.0290	4079.73	500	300	14.2144
1.7	0.0308	4079.73	500	300	15.1028
1.8	0.0327	4079.73	500	300	15.9912
1.9	0.0345	4079.73	500	300	16.8796
2	0.0363	4079.73	500	300	17.7680
2.1	0.0381	4079.73	500	300	18.6564
2.2	0.0399	4079.73	500	300	19.5448
2.3	0.0417	4079.73	500	300	20.4332
2.4	0.0436	4079.73	500	300	21.3216
2.5	0.0454	4079.73	500	300	22.2101
2.6	0.0472	4079.73	500	300	23.0985
2.7	0.0490	4079.73	500	300	23.9869
2.8	0.0508	4079.73	500	300	24.8753
2.9	0.0526	4079.73	500	300	25.7637
3	0.0544	4079.73	500	300	26.6521
3.1	0.0563	4079.73	500	300	27.5405
3.2	0.0581	4079.73	500	300	28.4289
3.3	0.0599	4079.73	500	300	29.3173
3.4	0.0617	4079.73	500	300	30.2057
3.5	0.0635	4079.73	500	300	31.0941
3.6	0.0653	4079.73	500	300	31.9825
3.7	0.0671	4079.73	500	300	32.8709
3.8	0.0690	4079.73	500	300	33.7593

3% volume fraction Al_2O_3 nanofluid

Qu	A	%	mass glass	mass copper	MJ/kg glass	MJ/kg copper	MJ total	mass total
3485	0.78	21.54	23.54	7.85	15.9	70.6	928.13	31.38
3834	0.78	21.54	23.54	7.85	15.9	70.6	928.13	31.38
4182	0.78	21.54	23.54	7.85	15.9	70.6	928.13	31.38
4531	0.78	21.54	23.54	7.85	15.9	70.6	928.13	31.38
4879	0.78	21.54	23.54	7.85	15.9	70.6	928.13	31.38
5228	0.78	21.54	23.54	7.85	15.9	70.6	928.13	31.38
5576	0.78	21.54	23.54	7.85	15.9	70.6	928.13	31.38
5925	0.78	21.54	23.54	7.85	15.9	70.6	928.13	31.38
6273	0.78	21.54	23.54	7.85	15.9	70.6	928.13	31.38
6622	0.78	21.54	23.54	7.85	15.9	70.6	928.13	31.38
6970	0.78	21.54	23.54	7.85	15.9	70.6	928.13	31.38
7319	0.78	21.54	23.54	7.85	15.9	70.6	928.13	31.38
7667	0.78	21.54	23.54	7.85	15.9	70.6	928.13	31.38
8016	0.78	21.54	23.54	7.85	15.9	70.6	928.13	31.38
8364	0.78	21.54	23.54	7.85	15.9	70.6	928.13	31.38
8713	0.78	21.54	23.54	7.85	15.9	70.6	928.13	31.38
9061	0.78	21.54	23.54	7.85	15.9	70.6	928.13	31.38
9410	0.78	21.54	23.54	7.85	15.9	70.6	928.13	31.38
9758	0.78	21.54	23.54	7.85	15.9	70.6	928.13	31.38
10107	0.78	21.54	23.54	7.85	15.9	70.6	928.13	31.38
10455	0.78	21.54	23.54	7.85	15.9	70.6	928.13	31.38
10804	0.78	21.54	23.54	7.85	15.9	70.6	928.13	31.38
11152	0.78	21.54	23.54	7.85	15.9	70.6	928.13	31.38
11501	0.78	21.54	23.54	7.85	15.9	70.6	928.13	31.38
11849	0.78	21.54	23.54	7.85	15.9	70.6	928.13	31.38
12198	0.78	21.54	23.54	7.85	15.9	70.6	928.13	31.38
12546	0.78	21.54	23.54	7.85	15.9	70.6	928.13	31.38
12895	0.78	21.54	23.54	7.85	15.9	70.6	928.13	31.38
13243	0.78	21.54	23.54	7.85	15.9	70.6	928.13	31.38

3% volume fraction TiO$_2$ nanofluid

Volume flow Rate	Mass flow rate	Specific heat of nanofluid	Solar radiation	Inlet Temperature	Energy Efficiency	Q$_u$
1	0.0183	4077.3	500	300	8.9521	3485
1.1	0.0201	4077.3	500	300	9.8473	3833.5
1.2	0.0220	4077.3	500	300	10.7425	4182
1.3	0.0238	4077.3	500	300	11.6378	4530.5
1.4	0.0256	4077.3	500	300	12.5330	4879
1.5	0.0274	4077.3	500	300	13.4282	5227.5
1.6	0.0293	4077.3	500	300	14.3234	5576
1.7	0.0311	4077.3	500	300	15.2186	5924.5
1.8	0.0329	4077.3	500	300	16.1138	6273
1.9	0.0348	4077.3	500	300	17.0090	6621.5
2	0.0366	4077.3	500	300	17.9042	6970
2.1	0.0384	4077.3	500	300	18.7995	7318.5
2.2	0.0403	4077.3	500	300	19.6947	7667
2.3	0.0421	4077.3	500	300	20.5899	8015.5
2.4	0.0439	4077.3	500	300	21.4851	8364
2.5	0.0457	4077.3	500	300	22.3803	8712.5
2.6	0.0476	4077.3	500	300	23.2755	9061
2.7	0.0494	4077.3	500	300	24.1707	9409.5
2.8	0.0512	4077.3	500	300	25.0659	9758
2.9	0.0531	4077.3	500	300	25.9611	10106.5
3	0.0549	4077.3	500	300	26.8564	10455
3.1	0.0567	4077.3	500	300	27.7516	10803.5
3.2	0.0585	4077.3	500	300	28.6468	11152
3.3	0.0604	4077.3	500	300	29.5420	11500.5
3.4	0.0622	4077.3	500	300	30.4372	11849
3.5	0.0640	4077.3	500	300	31.3324	12197.5
3.6	0.0659	4077.3	500	300	32.2276	12546
3.7	0.0677	4077.3	500	300	33.1228	12894.5
3.8	0.0695	4077.3	500	300	34.0181	13243

3% volume fraction TiO$_2$ nanofluid

A	%	mass glass	mass copper	MJ/kg glass	MJ/kg copper	MJ total	mass total
0.78	22.14	23.36	7.79	15.9	70.6	921.07	31.14
0.78	22.14	23.36	7.79	15.9	70.6	921.07	31.14
0.78	22.14	23.36	7.79	15.9	70.6	921.07	31.14
0.78	22.14	23.36	7.79	15.9	70.6	921.07	31.14
0.78	22.14	23.36	7.79	15.9	70.6	921.07	31.14
0.78	22.14	23.36	7.79	15.9	70.6	921.07	31.14
0.78	22.14	23.36	7.79	15.9	70.6	921.07	31.14
0.78	22.14	23.36	7.79	15.9	70.6	921.07	31.14
0.78	22.14	23.36	7.79	15.9	70.6	921.07	31.14
0.78	22.14	23.36	7.79	15.9	70.6	921.07	31.14
0.78	22.14	23.36	7.79	15.9	70.6	921.07	31.14
0.78	22.14	23.36	7.79	15.9	70.6	921.07	31.14
0.78	22.14	23.36	7.79	15.9	70.6	921.07	31.14
0.78	22.14	23.36	7.79	15.9	70.6	921.07	31.14
0.78	22.14	23.36	7.79	15.9	70.6	921.07	31.14
0.78	22.14	23.36	7.79	15.9	70.6	921.07	31.14
0.78	22.14	23.36	7.79	15.9	70.6	921.07	31.14
0.78	22.14	23.36	7.79	15.9	70.6	921.07	31.14
0.78	22.14	23.36	7.79	15.9	70.6	921.07	31.14
0.78	22.14	23.36	7.79	15.9	70.6	921.07	31.14
0.78	22.14	23.36	7.79	15.9	70.6	921.07	31.14
0.78	22.14	23.36	7.79	15.9	70.6	921.07	31.14
0.78	22.14	23.36	7.79	15.9	70.6	921.07	31.14
0.78	22.14	23.36	7.79	15.9	70.6	921.07	31.14
0.78	22.14	23.36	7.79	15.9	70.6	921.07	31.14
0.78	22.14	23.36	7.79	15.9	70.6	921.07	31.14
0.78	22.14	23.36	7.79	15.9	70.6	921.07	31.14
0.78	22.14	23.36	7.79	15.9	70.6	921.07	31.14
0.78	22.14	23.36	7.79	15.9	70.6	921.07	31.14
0.78	22.14	23.36	7.79	15.9	70.6	921.07	31.14
0.78	22.14	23.36	7.79	15.9	70.6	921.07	31.14

3% volume fraction SiO_2 nanofluid

Volume flow Rate	Mass flow rate	Specific heat of nanofluid	Solar radiation	Inlet Temperature	Energy Efficiency	Qu
1	0.0182	4079.49	500	300	8.8859	3485
1.1	0.0200	4079.49	500	300	9.7745	3833.5
1.2	0.0218	4079.49	500	300	10.6631	4182
1.3	0.0236	4079.49	500	300	11.5517	4530.5
1.4	0.0254	4079.49	500	300	12.4403	4879
1.5	0.0272	4079.49	500	300	13.3289	5227.5
1.6	0.0290	4079.49	500	300	14.2175	5576
1.7	0.0309	4079.49	500	300	15.1061	5924.5
1.8	0.0327	4079.49	500	300	15.9947	6273
1.9	0.0345	4079.49	500	300	16.8833	6621.5
2	0.0363	4079.49	500	300	17.7719	6970
2.1	0.0381	4079.49	500	300	18.6605	7318.5
2.2	0.0399	4079.49	500	300	19.5491	7667
2.3	0.0417	4079.49	500	300	20.4377	8015.5
2.4	0.0436	4079.49	500	300	21.3263	8364
2.5	0.0454	4079.49	500	300	22.2149	8712.5
2.6	0.0472	4079.49	500	300	23.1035	9061
2.7	0.0490	4079.49	500	300	23.9921	9409.5
2.8	0.0508	4079.49	500	300	24.8806	9758
2.9	0.0526	4079.49	500	300	25.7692	10106.5
3	0.0545	4079.49	500	300	26.6578	10455
3.1	0.0563	4079.49	500	300	27.5464	10803.5
3.2	0.0581	4079.49	500	300	28.4350	11152
3.3	0.0599	4079.49	500	300	29.3236	11500.5
3.4	0.0617	4079.49	500	300	30.2122	11849
3.5	0.0635	4079.49	500	300	31.1008	12197.5
3.6	0.0653	4079.49	500	300	31.9894	12546
3.7	0.0672	4079.49	500	300	32.8780	12894.5
3.8	0.0690	4079.49	500	300	33.7666	13243

3% volume fraction SiO$_2$ nanofluid

A	%	mass glass	mass copper	MJ/kg glass	MJ/kg copper	MJ total	mass total
0.78	21.56	23.53	7.84	15.9	70.6	927.93	31.38
0.78	21.56	23.53	7.84	15.9	70.6	927.93	31.38
0.78	21.56	23.53	7.84	15.9	70.6	927.93	31.38
0.78	21.56	23.53	7.84	15.9	70.6	927.93	31.38
0.78	21.56	23.53	7.84	15.9	70.6	927.93	31.38
0.78	21.56	23.53	7.84	15.9	70.6	927.93	31.38
0.78	21.56	23.53	7.84	15.9	70.6	927.93	31.38
0.78	21.56	23.53	7.84	15.9	70.6	927.93	31.38
0.78	21.56	23.53	7.84	15.9	70.6	927.93	31.38
0.78	21.56	23.53	7.84	15.9	70.6	927.93	31.38
0.78	21.56	23.53	7.84	15.9	70.6	927.93	31.38
0.78	21.56	23.53	7.84	15.9	70.6	927.93	31.38
0.78	21.56	23.53	7.84	15.9	70.6	927.93	31.38
0.78	21.56	23.53	7.84	15.9	70.6	927.93	31.38
0.78	21.56	23.53	7.84	15.9	70.6	927.93	31.38
0.78	21.56	23.53	7.84	15.9	70.6	927.93	31.38
0.78	21.56	23.53	7.84	15.9	70.6	927.93	31.38
0.78	21.56	23.53	7.84	15.9	70.6	927.93	31.38
0.78	21.56	23.53	7.84	15.9	70.6	927.93	31.38
0.78	21.56	23.53	7.84	15.9	70.6	927.93	31.38
0.78	21.56	23.53	7.84	15.9	70.6	927.93	31.38
0.78	21.56	23.53	7.84	15.9	70.6	927.93	31.38
0.78	21.56	23.53	7.84	15.9	70.6	927.93	31.38
0.78	21.56	23.53	7.84	15.9	70.6	927.93	31.38
0.78	21.56	23.53	7.84	15.9	70.6	927.93	31.38
0.78	21.56	23.53	7.84	15.9	70.6	927.93	31.38
0.78	21.56	23.53	7.84	15.9	70.6	927.93	31.38
0.78	21.56	23.53	7.84	15.9	70.6	927.93	31.38
0.78	21.56	23.53	7.84	15.9	70.6	927.93	31.38
0.78	21.56	23.53	7.84	15.9	70.6	927.93	31.38

3% volume fraction CuO nanofluid

Volume flow Rate	Mass flow rate	Specific heat of nanofluid	Solar radiation	Inlet Temperature	Energy Efficiency	Qu
1	0.0192	4073.07	500	300	9.3681	3485
1.1	0.0211	4073.07	500	300	10.3049	3833.5
1.2	0.0230	4073.07	500	300	11.2417	4182
1.3	0.0249	4073.07	500	300	12.1785	4530.5
1.4	0.0268	4073.07	500	300	13.1153	4879
1.5	0.0288	4073.07	500	300	14.0521	5227.5
1.6	0.0307	4073.07	500	300	14.9889	5576
1.7	0.0326	4073.07	500	300	15.9257	5924.5
1.8	0.0345	4073.07	500	300	16.8625	6273
1.9	0.0364	4073.07	500	300	17.7993	6621.5
2	0.0383	4073.07	500	300	18.7361	6970
2.1	0.0403	4073.07	500	300	19.6729	7318.5
2.2	0.0422	4073.07	500	300	20.6097	7667
2.3	0.0441	4073.07	500	300	21.5465	8015.5
2.4	0.0460	4073.07	500	300	22.4833	8364
2.5	0.0479	4073.07	500	300	23.4202	8712.5
2.6	0.0498	4073.07	500	300	24.3570	9061
2.7	0.0518	4073.07	500	300	25.2938	9409.5
2.8	0.0537	4073.07	500	300	26.2306	9758
2.9	0.0556	4073.07	500	300	27.1674	10106.5
3	0.0575	4073.07	500	300	28.1042	10455
3.1	0.0594	4073.07	500	300	29.0410	10803.5
3.2	0.0613	4073.07	500	300	29.9778	11152
3.3	0.0633	4073.07	500	300	30.9146	11500.5
3.4	0.0652	4073.07	500	300	31.8514	11849
3.5	0.0671	4073.07	500	300	32.7882	12197.5
3.6	0.0690	4073.07	500	300	33.7250	12546
3.7	0.0709	4073.07	500	300	34.6618	12894.5
3.8	0.0728	4073.07	500	300	35.5986	13243

3% volume fraction CuO nanofluid

A	%	mass glass	mass copper	MJ/kg glass	MJ/kg copper	MJ total	mass total
0.74	25.60	22.32	7.44	15.9	70.6	880.17	29.76
0.74	25.60	22.32	7.44	15.9	70.6	880.17	29.76
0.74	25.60	22.32	7.44	15.9	70.6	880.17	29.76
0.74	25.60	22.32	7.44	15.9	70.6	880.17	29.76
0.74	25.60	22.32	7.44	15.9	70.6	880.17	29.76
0.74	25.60	22.32	7.44	15.9	70.6	880.17	29.76
0.74	25.60	22.32	7.44	15.9	70.6	880.17	29.76
0.74	25.60	22.32	7.44	15.9	70.6	880.17	29.76
0.74	25.60	22.32	7.44	15.9	70.6	880.17	29.76
0.74	25.60	22.32	7.44	15.9	70.6	880.17	29.76
0.74	25.60	22.32	7.44	15.9	70.6	880.17	29.76
0.74	25.60	22.32	7.44	15.9	70.6	880.17	29.76
0.74	25.60	22.32	7.44	15.9	70.6	880.17	29.76
0.74	25.60	22.32	7.44	15.9	70.6	880.17	29.76
0.74	25.60	22.32	7.44	15.9	70.6	880.17	29.76
0.74	25.60	22.32	7.44	15.9	70.6	880.17	29.76
0.74	25.60	22.32	7.44	15.9	70.6	880.17	29.76
0.74	25.60	22.32	7.44	15.9	70.6	880.17	29.76
0.74	25.60	22.32	7.44	15.9	70.6	880.17	29.76
0.74	25.60	22.32	7.44	15.9	70.6	880.17	29.76
0.74	25.60	22.32	7.44	15.9	70.6	880.17	29.76
0.74	25.60	22.32	7.44	15.9	70.6	880.17	29.76
0.74	25.60	22.32	7.44	15.9	70.6	880.17	29.76
0.74	25.60	22.32	7.44	15.9	70.6	880.17	29.76
0.74	25.60	22.32	7.44	15.9	70.6	880.17	29.76
0.74	25.60	22.32	7.44	15.9	70.6	880.17	29.76
0.74	25.60	22.32	7.44	15.9	70.6	880.17	29.76
0.74	25.60	22.32	7.44	15.9	70.6	880.17	29.76
0.74	25.60	22.32	7.44	15.9	70.6	880.17	29.76
0.74	25.60	22.32	7.44	15.9	70.6	880.17	29.76

Water

Volume flow Rate	Mass flow rate	Specific heat of nanofluid	Solar radiation	Inlet Temperature	Energy Efficiency	Qu
1	0.0167	4182	500	300	6.97	3485
1.1	0.0183	4182	500	300	7.67	3833.5
1.2	0.0200	4182	500	300	8.36	4182
1.3	0.0217	4182	500	300	9.06	4530.5
1.4	0.0233	4182	500	300	9.76	4879
1.5	0.0250	4182	500	300	10.46	5227.5
1.6	0.0267	4182	500	300	11.15	5576
1.7	0.0283	4182	500	300	11.85	5924.5
1.8	0.0300	4182	500	300	12.55	6273
1.9	0.0317	4182	500	300	13.24	6621.5
2	0.0333	4182	500	300	13.94	6970
2.1	0.0350	4182	500	300	14.64	7318.5
2.2	0.0367	4182	500	300	15.33	7667
2.3	0.0383	4182	500	300	16.03	8015.5
2.4	0.0400	4182	500	300	16.73	8364
2.5	0.0417	4182	500	300	17.43	8712.5
2.6	0.0433	4182	500	300	18.12	9061
2.7	0.0450	4182	500	300	18.82	9409.5
2.8	0.0467	4182	500	300	19.52	9758
2.9	0.0483	4182	500	300	20.21	10106.5
3	0.0500	4182	500	300	20.91	10455
3.1	0.0517	4182	500	300	21.61	10803.5
3.2	0.0533	4182	500	300	22.30	11152
3.3	0.0550	4182	500	300	23.00	11500.5
3.4	0.0567	4182	500	300	23.70	11849
3.5	0.0583	4182	500	300	24.40	12197.5
3.6	0.0600	4182	500	300	25.09	12546
3.7	0.0617	4182	500	300	25.79	12894.5
3.8	0.0633	4182	500	300	26.49	13243

Water

A	mass glass	mass copper	MJ/kg glass	MJ/kg copper	MJ total	mass total
1	30	10	15.9	70.6	1183	40
1	30	10	15.9	70.6	1183	40
1	30	10	15.9	70.6	1183	40
1	30	10	15.9	70.6	1183	40
1	30	10	15.9	70.6	1183	40
1	30	10	15.9	70.6	1183	40
1	30	10	15.9	70.6	1183	40
1	30	10	15.9	70.6	1183	40
1	30	10	15.9	70.6	1183	40
1	30	10	15.9	70.6	1183	40
1	30	10	15.9	70.6	1183	40
1	30	10	15.9	70.6	1183	40
1	30	10	15.9	70.6	1183	40
1	30	10	15.9	70.6	1183	40
1	30	10	15.9	70.6	1183	40
1	30	10	15.9	70.6	1183	40
1	30	10	15.9	70.6	1183	40
1	30	10	15.9	70.6	1183	40
1	30	10	15.9	70.6	1183	40
1	30	10	15.9	70.6	1183	40
1	30	10	15.9	70.6	1183	40
1	30	10	15.9	70.6	1183	40
1	30	10	15.9	70.6	1183	40
1	30	10	15.9	70.6	1183	40
1	30	10	15.9	70.6	1183	40
1	30	10	15.9	70.6	1183	40
1	30	10	15.9	70.6	1183	40
1	30	10	15.9	70.6	1183	40
1	30	10	15.9	70.6	1183	40
1	30	10	15.9	70.6	1183	40

Density data

Volume fraction	CuO Nanofluid	Al$_2$O$_3$ Nanofluid	TiO$_2$ Nanofluid	SiO$_2$ Nanofluid	Water
0.02	1100	1059.2	1065.2	1059.4	1000
0.0205	1102.5	1060.68	1066.83	1060.885	1000
0.021	1105	1062.16	1068.46	1062.37	1000
0.0215	1107.5	1063.64	1070.09	1063.855	1000
0.022	1110	1065.12	1071.72	1065.34	1000
0.0225	1112.5	1066.6	1073.35	1066.825	1000
0.023	1115	1068.08	1074.98	1068.31	1000
0.0235	1117.5	1069.56	1076.61	1069.795	1000
0.024	1120	1071.04	1078.24	1071.28	1000
0.0245	1122.5	1072.52	1079.87	1072.765	1000
0.025	1125	1074	1081.5	1074.25	1000
0.0255	1127.5	1075.48	1083.13	1075.735	1000
0.026	1130	1076.96	1084.76	1077.22	1000
0.0265	1132.5	1078.44	1086.39	1078.705	1000
0.027	1135	1079.92	1088.02	1080.19	1000
0.0275	1137.5	1081.4	1089.65	1081.675	1000
0.028	1140	1082.88	1091.28	1083.16	1000
0.0285	1142.5	1084.36	1092.91	1084.645	1000
0.029	1145	1085.84	1094.54	1086.13	1000
0.0295	1147.5	1087.32	1096.17	1087.615	1000
0.03	1150	1088.8	1097.8	1089.1	1000
0.0305	1152.5	1090.28	1099.43	1090.585	1000
0.031	1155	1091.76	1101.06	1092.07	1000
0.0315	1157.5	1093.24	1102.69	1093.555	1000
0.032	1160	1094.72	1104.32	1095.04	1000

Mass flow rate data

Volume Fraction	Al$_2$O$_3$ Nanofluid	TiO$_2$ Nanofluid	SiO$_2$ Nanofluid	CuO Nanofluid
0.0200	0.0177	0.0178	0.0177	0.0183
0.0205	0.0177	0.0178	0.0177	0.0184
0.0210	0.0177	0.0178	0.0177	0.0184
0.0215	0.0177	0.0178	0.0177	0.0185
0.0220	0.0178	0.0179	0.0178	0.0185
0.0225	0.0178	0.0179	0.0178	0.0185
0.0230	0.0178	0.0179	0.0178	0.0186
0.0235	0.0178	0.0179	0.0178	0.0186
0.0240	0.0179	0.0180	0.0179	0.0187
0.0245	0.0179	0.0180	0.0179	0.0187
0.0250	0.0179	0.0180	0.0179	0.0188
0.0255	0.0179	0.0181	0.0179	0.0188
0.0260	0.0179	0.0181	0.0180	0.0188
0.0265	0.0180	0.0181	0.0180	0.0189
0.0270	0.0180	0.0181	0.0180	0.0189
0.0275	0.0180	0.0182	0.0180	0.0190
0.0280	0.0180	0.0182	0.0181	0.0190
0.0285	0.0181	0.0182	0.0181	0.0190
0.0290	0.0181	0.0182	0.0181	0.0191
0.0295	0.0181	0.0183	0.0181	0.0191
0.0300	0.0181	0.0183	0.0182	0.0192
0.0305	0.0182	0.0183	0.0182	0.0192
0.0310	0.0182	0.0184	0.0182	0.0193
0.0315	0.0182	0.0184	0.0182	0.0193
0.0320	0.0182	0.0184	0.0183	0.0193

Specific heat data

Volume fraction	CuO Nanofluid	Al2O3 Nanofluid	TiO2 Nanofluid	SiO2 Nanofluid	Water
0.020	4109.380	4113.820	4112.200	4113.660	4182
0.021	4107.565	4112.116	4110.455	4111.952	4182
0.021	4105.749	4110.411	4108.710	4110.243	4182
0.022	4103.934	4108.707	4106.965	4108.535	4182
0.022	4102.118	4107.002	4105.220	4106.826	4182
0.023	4100.303	4105.298	4103.475	4105.118	4182
0.023	4098.487	4103.593	4101.730	4103.409	4182
0.024	4096.672	4101.889	4099.985	4101.701	4182
0.024	4094.856	4100.184	4098.240	4099.992	4182
0.025	4093.041	4098.480	4096.495	4098.284	4182
0.025	4091.225	4096.775	4094.750	4096.575	4182
0.026	4089.410	4095.071	4093.005	4094.867	4182
0.026	4087.594	4093.366	4091.260	4093.158	4182
0.027	4085.779	4091.662	4089.515	4091.450	4182
0.027	4083.963	4089.957	4087.770	4089.741	4182
0.028	4082.148	4088.253	4086.025	4088.033	4182
0.028	4080.332	4086.548	4084.280	4086.324	4182
0.029	4078.517	4084.844	4082.535	4084.616	4182
0.029	4076.701	4083.139	4080.790	4082.907	4182
0.030	4074.886	4081.435	4079.045	4081.199	4182
0.030	4073.070	4079.730	4077.300	4079.490	4182
0.031	4071.255	4078.026	4075.555	4077.782	4182
0.031	4069.439	4076.321	4073.810	4076.073	4182
0.032	4067.624	4074.617	4072.065	4074.365	4182
0.032	4065.808	4072.912	4070.320	4072.656	4182

Efficiency data

Volume fraction	Water	Al$_2$O$_3$ Nanofluid	TiO$_2$ Nanofluid	SiO$_2$ Nanofluid	CuO Nanofluid
1	6.97	8.8840	8.9521	8.8859	9.3681
1.1	7.667	9.7724	9.8473	9.7745	10.3049
1.2	8.364	10.6608	10.7425	10.6631	11.2417
1.3	9.061	11.5492	11.6378	11.5517	12.1785
1.4	9.758	12.4376	12.5330	12.4403	13.1153
1.5	10.455	13.3260	13.4282	13.3289	14.0521
1.6	11.152	14.2144	14.3234	14.2175	14.9889
1.7	11.849	15.1028	15.2186	15.1061	15.9257
1.8	12.546	15.9912	16.1138	15.9947	16.8625
1.9	13.243	16.8796	17.0090	16.8833	17.7993
2	13.94	17.7680	17.9042	17.7719	18.7361
2.1	14.637	18.6564	18.7995	18.6605	19.6729
2.2	15.334	19.5448	19.6947	19.5491	20.6097
2.3	16.031	20.4332	20.5899	20.4377	21.5465
2.4	16.728	21.3216	21.4851	21.3263	22.4833
2.5	17.425	22.2101	22.3803	22.2149	23.4202
2.6	18.122	23.0985	23.2755	23.1035	24.3570
2.7	18.819	23.9869	24.1707	23.9921	25.2938
2.8	19.516	24.8753	25.0659	24.8806	26.2306
2.9	20.213	25.7637	25.9611	25.7692	27.1674
3	20.91	26.6521	26.8564	26.6578	28.1042
3.1	21.607	27.5405	27.7516	27.5464	29.0410
3.2	22.304	28.4289	28.6468	28.4350	29.9778
3.3	23.001	29.3173	29.5420	29.3236	30.9146
3.4	23.698	30.2057	30.4372	30.2122	31.8514
3.5	24.395	31.0941	31.3324	31.1008	32.7882
3.6	25.092	31.9825	32.2276	31.9894	33.7250
3.7	25.789	32.8709	33.1228	32.8780	34.6618
3.8	26.486	33.7593	34.0181	33.7666	35.5986

Exergy efficiency data

Volume Fraction φ, (%)	Water	Al$_2$O$_3$	TiO$_2$	SiO$_2$	CuO
0.02	2.9747	3.0994	3.1158	3.0999	3.2153
0.0205	2.9747	3.1025	3.1192	3.1029	3.2212
0.021	2.9747	3.1055	3.1226	3.1060	3.2271
0.0215	2.9747	3.1085	3.1261	3.1090	3.2330
0.022	2.9747	3.1116	3.1295	3.1121	3.2388
0.0225	2.9747	3.1146	3.1329	3.1151	3.2447
0.023	2.9747	3.1176	3.1364	3.1182	3.2505
0.0235	2.9747	3.1207	3.1398	3.1212	3.2564
0.024	2.9747	3.1237	3.1432	3.1242	3.2622
0.0245	2.9747	3.1267	3.1466	3.1273	3.2681
0.025	2.9747	3.1297	3.1500	3.1303	3.2739
0.0255	2.9747	3.1327	3.1534	3.1333	3.2797
0.026	2.9747	3.1357	3.1568	3.1363	3.2855
0.0265	2.9747	3.1387	3.1602	3.1393	3.2913
0.027	2.9747	3.1417	3.1636	3.1423	3.2971
0.0275	2.9747	3.1447	3.1670	3.1453	3.3029
0.028	2.9747	3.1477	3.1704	3.1483	3.3087
0.0285	2.9747	3.1507	3.1737	3.1513	3.3145
0.029	2.9747	3.1537	3.1771	3.1543	3.3203
0.0295	2.9747	3.1567	3.1805	3.1573	3.3260
0.03	2.9747	3.1596	3.1839	3.1603	3.3318
0.0305	2.9747	3.1626	3.1872	3.1633	3.3375
0.031	2.9747	3.1656	3.1906	3.1663	3.3433
0.0315	2.9747	3.1685	3.1939	3.1693	3.3490
0.032	2.9747	3.1715	3.1973	3.1722	3.3548

<div align="center">**CURRICULUM VITAE**</div>

PERSONAL DETAIL

Name   **Mohd Faizal Fauzan**

Year of Birth   1987

ACADEMIC QUALIFICATION
(Qualification), (Institution)

1. PhD (ongoing) University of Malaya (2011-Present)
2. MEng Mechanical, University of Malaya (2009-2011)
3. BEng (Hons) Mechanical, University of Nottingham (2004-2008)

PROFESSIONAL AFFILIATION/MEMBERSHIP
(Organisation), (Role), (Year), (Level).

1. Institution of Mechanical Engineers, IMechE, Affiliate Member, 2005, (International)
2. Institution of Mechanical Engineers, IMechE, Associate Member, 2009, (International)
3. Board of Engineers Malaysia, BEM, Graduate Member, 2011, (National)
4. Institute of Engineers Malaysia, IEM, Graduate Member, 2011, (National)

CAREER HISTORY
(Post), (Organisation), (Period).

1. Jabatan Pengairan dan Saliran, JPS, Batu Pahat Johor, (May 2008-July 2008)
2. Assistant Lecturer, Faculty of Engineering UNISEL, (Nov 2008 – Jan 2012)
3. Lecturer, Faculty of Engineering INTI International University, (Jan 2012 – May 2012)
4. Lecturer, ADP Engineering Division Taylor's University Lakeside Campus, (May 2012 - Present)